N
P

JOURNAL

OF

FOOD

PROCESS

ENGINEERING

D.R. HELDMAN
and
R.P. SINGH
COEDITORS

FOOD & NUTRITION PRESS, INC.

JOURNAL OF FOOD PROCESS ENGINEERING

JOURNAL OF FOOD PROCESS ENGINEERING

Journal of
FOOD PROCESS
ENGINEERING

F
  N
    P
PUBLICATIONS IN
FOOD SCIENCE AND NUTRITION

Books

MULTIVARIATE DATA ANALYSIS, G.B. Dijksterhuis
NUTRACEUTICALS: DESIGNER FOODS III, P.A. Lachance
DESCRIPTIVE SENSORY ANALYSIS IN PRACTICE, M.C. Gacula, Jr.
APPETITE FOR LIFE: AN AUTOBIOGRAPHY, S.A. Goldblith
HACCP: MICROBIOLOGICAL SAFETY OF MEAT, J.J. Sheridan *et al.*
OF MICROBES AND MOLECULES: FOOD TECHNOLOGY AT M.I.T., S.A. Goldblith
MEAT PRESERVATION, R.G. Cassens
S.C. PRESCOTT, PIONEER FOOD TECHNOLOGIST, S.A. Goldblith
FOOD CONCEPTS AND PRODUCTS: JUST-IN-TIME DEVELOPMENT, H.R. Moskowitz
MICROWAVE FOODS: NEW PRODUCT DEVELOPMENT, R.V. Decareau
DESIGN AND ANALYSIS OF SENSORY OPTIMIZATION, M.C. Gacula, Jr.
NUTRIENT ADDITIONS TO FOOD, J.C. Bauernfeind and P.A. Lachance
NITRITE-CURED MEAT, R.G. Cassens
POTENTIAL FOR NUTRITIONAL MODULATION OF AGING, D.K. Ingram *et al.*
CONTROLLED/MODIFIED ATMOSPHERE/VACUUM PACKAGING, A.L. Brody
NUTRITIONAL STATUS ASSESSMENT OF THE INDIVIDUAL, G.E. Livingston
QUALITY ASSURANCE OF FOODS, J.E. Stauffer
SCIENCE OF MEAT & MEAT PRODUCTS, 3RD ED., J.F. Price and B.S. Schweigert
HANDBOOK OF FOOD COLORANT PATENTS, F.J. Francis
ROLE OF CHEMISTRY IN PROCESSED FOODS, O.R. Fennema *et al.*
NEW DIRECTIONS FOR PRODUCT TESTING OF FOODS, H.R. Moskowitz
ENVIRONMENTAL ASPECTS OF CANCER: ROLE OF FOODS, E.L. Wynder *et al.*
PRODUCT DEVELOPMENT & DIETARY GUIDELINES, G.E. Livingston, *et al.*
SHELF-LIFE DATING OF FOODS, T.P. Labuza
ANTINUTRIENTS AND NATURAL TOXICANTS IN FOOD, R.L. Ory
UTILIZATION OF PROTEIN RESOURCES, D.W. Stanley *et al.*
POSTHARVEST BIOLOGY AND BIOTECHNOLOGY, H.O. Hultin and M. Milner

Journals

JOURNAL OF FOOD LIPIDS, F. Shahidi
JOURNAL OF RAPID METHODS AND AUTOMATION IN MICROBIOLOGY,
   D.Y.C. Fung and M.C. Goldschmidt
JOURNAL OF MUSCLE FOODS, N.G. Marriott, G.J. Flick, Jr. and J.R. Claus
JOURNAL OF SENSORY STUDIES, M.C. Gacula, Jr.
JOURNAL OF FOODSERVICE SYSTEMS, C.A. Sawyer
JOURNAL OF FOOD BIOCHEMISTRY, N.F. Haard, H. Swaisgood and B. Wasserman
JOURNAL OF FOOD PROCESS ENGINEERING, D.R. Heldman and R.P. Singh
JOURNAL OF FOOD PROCESSING AND PRESERVATION, D.B. Lund
JOURNAL OF FOOD QUALITY, J.J. Powers
JOURNAL OF FOOD SAFETY, T.J. Montville and D.G. Hoover
JOURNAL OF TEXTURE STUDIES, M.C. Bourne and M.A. Rao

Newsletters

MICROWAVES AND FOOD, R.V. Decareau
FOOD INDUSTRY REPORT, G.C. Melson
FOOD, NUTRITION AND HEALTH, P.A. Lachance and M.C. Fisher

CONTENTS

TEXTURE DEGRADATION KINETICS OF GELS MADE FROM PACIFIC WHITING SURIMI

JIRAWAT YONGSAWATDIGUL, JAE W. PARK[1] and EDWARD KOLBE

Oregon State University
Seafood Laboratory
2001 Marine Dr. #253
Astoria, OR 97103-3427

ABSTRACT

Degradation kinetics of whiting surimi gel texture were examined over a temperature/time range (40-85C, 0.5-35 min). Changes in textural properties of whiting surimi gel were mainly affected by proteolytic activity of endogenous proteinase. A decrease of failure shear stress and shear strain followed first order kinetics. The kinetic parameters developed using either isothermal or nonisothermal principles were similar. Degradation rate of gel texture increased with temperature, reaching a maximum at 55C. It then decreased to a minimum at 70C. E_a values for the activation and inactivation temperature range were 138.6-162.6 and 13.5-35.0 kJ/mol, respectively.

INTRODUCTION

Pacific whiting (*Merluccius productus*) surimi without enzyme inhibitors normally undergoes texture degradation during slow heating (Chang-Lee *et al.* 1989; Morrissey *et al.* 1993; Yongsawatdigul *et al.* 1995). This is due to the presence of heat stable endogenous proteinase(s) that exhibit high hydrolytic activity on muscle myosin (Erickson *et al.* 1983; Patashnik *et al.* 1982). When surimi is heated in a 90C water bath, temperature at the geometric center of whiting surimi paste in stainless steel tubes (i.d. = 1.9 cm) increased from 10 to 80C within 8 min (Yongsawatdigul *et al.* 1995). Such a slow heating process allowed the proteinase(s) to be active for a relatively long period of time. As a result, substantial loss of myosin heavy chain (MHC) was evident, concomitant with very poor textural characteristics (Yongsawatdigul *et al.* 1995). Rapid heating methods, such as microwave and ohmic heating, have been reported to effectively minimize textural degradation of fish muscle caused by endogenous

heat stable proteinases (Greene and Babbitt 1990; Yongsawatdigul et al. 1995). For both heating methods, heat is internally generated, rather than externally transferred from the heating medium, therefore, temperature of the sample quickly increases. As a result, the proteinase is thermally inactivated in a rapid manner.

High quality of whiting surimi gel (shear stress and shear strain of 30 kPa and 2.8, respectively) was obtained when it was heated ohmically from 10 to 90C within 1 min (Yongsawatdigul et al. 1995). On the other hand, as the time of ohmic heating was prolonged to 80 min over the same temperature range, very soft and mushy gels were obtained, accompanying complete disappearance of MHC and a reduced actin band (Yongsawatdigul and Park 1996). It is clear that heating time and temperature are critical factors controlling textural properties of whiting surimi. This trend also extends to other fish species that exhibit similar problems with endogenous heat stable proteinase as shown for threadfin bream (Nemipterus bathybius) (Toyohara and Shimizu 1988), Atlantic menhaden (Brevoorti tyrannus) (Boye and Lanier 1988), and arrowtooth flounder (Atheresthes stomias) (Greene and Babbitt 1990). To obtain desired whiting surimi gel properties without the use of inhibitors, proper heating rates and temperature need to be determined. Therefore, the kinetics of gel weakening should be understood.

In systems where the sample size is so small that instantaneous heating and cooling can be assumed, kinetic parameters can be derived using isothermal approach. A reaction rate constant, k, is obtained from the relationship between a property or concentration and time at different temperatures. The temperature dependence of the rate constant is then modeled using either the Arrhenius equation or other function forms (Saguy and Karel 1980). However, the Arrhenius equation can be applied over a wide temperature range for foods, and often provides an accurate estimate (Lenz and Lund 1977a; Saguy and Karel 1980).

When instantaneous heating and cooling is not possible, i.e. when physico-chemical changes during heat-up and cool-down periods are significant, kinetic parameters cannot be accurately determined using an isothermal approach. In such cases, a thermal lag correction is required (Davies et al. 1977; Perkin et al. 1977; Wicker and Temelli 1988; Awuah et al. 1993). An equivalent isothermal process time can be calculated using the equations derived from the thermal death time (TDT) model (Davies et al. 1977; Perkin et al. 1977; Wicker and Temelli 1988; Palaniappan et al. 1992) or from the Arrhenius model (Lenz and Lund 1977a,b; Swartzel 1982).

Since the TDT method is only appropriate for first-order reactions (Ramaswamy and Abdelrahim 1992), it cannot be used to derive kinetic parameters for degradation of gel texture, a process for which reaction orders are unknown. The kinetic analysis in this study was also complicated by the fact

that both activation and inactivation of the endogenous proteinase took place as whiting surimi was heated to 90C. This was in contrast with degradation kinetics of microorganisms and nutrients during thermal processing in which the rate of degradation only increased with temperature. Therefore, the existing methodology developed for thermal processing could not be directly applied to this study. The objective of this research was to develop kinetic models describing the changes of gel texture when heated to 90C, using the Arrhenius model as a fundamental basis.

MATERIALS AND METHODS

Surimi Gel Preparation

Unfrozen Pacific whiting (*Merluccius productus*) surimi without enzyme inhibitors and cryoprotectants was obtained from Point Adams Packing Co. (Hammond, OR). Surimi was processed within 18 h after harvest. The surimi was mixed with cryoprotectants as described by Yongsawatdigul *et al.* (1995). The samples were stored at -30C throughout the experiment and used within 6 months.

Surimi pastes with 78% moisture content and 2% salt concentration were prepared as described by Yongsawatdigul *et al.* (1995). The paste was stuffed into chlorinated polyvinyl chloride (CPVC) tubes (1.9 cm i.d. × 20.5 cm long) and heated using an ohmic heating apparatus. This device, described in detail by Yongsawatdigul *et al.* (1995), was developed from two rhodium-coated stainless steel electrodes, a variable transformer, current and voltage transducers and a temperature controller (Model CN3201, OMEGA Engineering Inc., Stamford, CT) connected to a solid state on-off relay which enabled the control of temperature as a either constant or a ramp-increase function. To minimize electrical hazards, the sample tube and electrodes were housed inside a plexiglass enclosure equipped with an open-snap action switch, which was activated when the plexiglass box was closed. Temperatures at the geometric center of the sample were measured by a 30-gauge teflon-sealed thermocouple (Type-T) and were recorded on a datalogger (model 21X, Campbell Scientific, Inc., Logan, UT). Temperature variation during the constant-temperature holding period was ±0.5C.

Preliminary studies indicated no changes in shear stress and shear strain occurring in surimi gels held up to 1 h at 30C. Therefore, the samples were heated to temperatures ranging from 40 to 85C. Temperature increase was at the maximum allowable rate corresponding to a voltage gradient of 13.3 V/cm (Yongsawatdigul *et al.* 1995); the samples were held at set temperatures for various times. When the holding times were achieved, the samples were then

heated rapidly to 90C using the same voltage gradient applied for initial heating. Heating regimes at various temperatures are shown in Table 1. Control samples were prepared by heating surimi paste from 10C to 90C at 13.3 V/cm with no intermediate holding temperature. To obtain an adequate number of gel samples for torsion testing, three sample tubes were individually heated for each holding temperature and time. Once cooked, surimi gels were cooled in ice water and kept at 4C for torsion tests. One batch of surimi paste (1.5 kg) was used for each studied temperature and its control. The entire experiment was performed in duplicate.

TABLE 1.
HEATING REGIMES AT VARIOUS TEMPERATURES

Holding Temp. (˚C)	Initial Heat-up (s)	Holding Time (min)	Final Heat-up (s)
40	27	0,5,10,15,25,35	40
45	32	0,3,5,8,12,15	36
50	36	0,1,2,3,5,7	32
55	41	0,1,2,3,4,5	28
60	45	0,1,2,3,4,5	24
65	46	0,1,2,3,4,5	20
70	48	0,0.5,1,2,2.5,3	16
75	51	0,0.5,1,2,2.5,3	12
80	54	0,0.5,1,2,2.5,3	8
85	58	0,0.5,1,2,2.5,3	4

Torsion Test

Torsion failure tests were performed at room temperature, 18-24 h after gel preparation. The sample was milled to be an hour-glass shape with a diameter of 1 cm. The milled sample was twisted using a Brookfield viscometer (model DV-I, Brookfield Engineering Laboratories Inc., Stoughton, MA), as described by NFI (1991). Ten hourglass-shaped samples for each treatment were equilibrated to room temperature before torsion. Shear stress and shear strain at failure were calculated from equations described by Hamann (1983).

Kinetic Modeling of Textural Degradation

Changes of textural properties were initially assumed to follow first order reaction. The kinetic models were determined using two different approaches described as follows:

(1) The kinetic models for degradation of shear stress and shear strain were developed using the isothermal concept. The model can be expressed as:

$$\ln \left[\frac{P}{P_0}\right] = -kt \tag{1}$$

where P = textural property of surimi gel at time t
t = holding time (min)
k = apparent rate constant (min^{-1})
P_0 = textural property of the sample heated to 90C using voltage gradient of 13.3 V/cm (control).

This approach is based on the fact that temperature history of every sample during the heat-up periods would be identical to that of the control (Fig. 1). Therefore, the effect of any thermal lag on a sample would be equivalent to that on the control during the heat-up period. Thus, the ratio of P to P_0 would represent the effect of proteolysis during the holding time only. The effect of P reduction during the thermal lag period would be the same for samples and control and reflected in the value of P_0. Rate
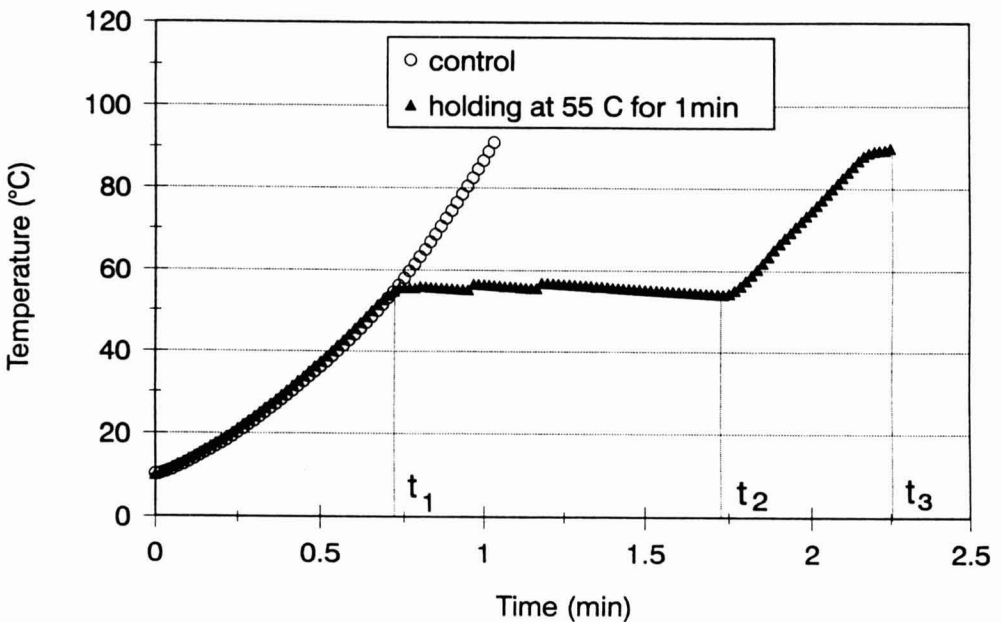
FIG. 1. REPRESENTATIVE TEMPERATURE PROFILES OF SURIMI PASTE HEATED
BY OHMIC MEANS

constants at each holding temperature were obtained using weighted least square regression between ln (P/P_0) and holding time. The inverse of the square of residuals from the unweighted regression was used as a weight factor (Hill and Grieger-Block 1980; Arabshahi and Lund 1985). Rate constant values were modeled as a function of temperature using the Arrhenius model, then kinetic parameters (activation energy, E_a) were calculated.

(2) The second approach applied nonisothermal principles to derive the kinetic models. P_{th} was theoretical value representing textural properties of the sample that could be heated instantaneously with no proteolysis. Even though the control was heated, using a maximum allowable voltage gradient (13.3 V/cm) within 1 min (Fig. 1), heat-up periods $(0 - t_1$ and $t_2 - t_3)$ was not instantaneous and inhibition of proteolytic activity was not completed. Thus, the second approach was to develop kinetic models which accounted for degradation during heat-up periods. For nonisothermal conditions, Eq. 1 was rewritten as:

$$\ln[\frac{P}{P_{th}}] = -\int_0^t k[T(t)] \, dt \qquad (2)$$

where the apparent rate constant was allowed to vary with temperature, and temperature was a function of time. If heating and cooling were instantaneous, Eq. 2 would become:

$$\ln[\frac{P}{P_{th}}] = -k_{Ti} \, t_{aTi} \qquad (3)$$

where k_{Ti} =   apparent rate constant at temperature Ti if there were no thermal lag

  t_{aTi} =   equivalent holding time at temperature Ti

For a nonisothermal process, t_{aTi} is the summation of the actual holding time at Ti and the equivalent holding time at Ti during those periods when temperature is raised from the initial temperature to Ti and from Ti to the final temperature (90C). To determine t_{aTi} for a nonisothermal process, Eq. 2 and 3 can be combined and rewritten in term of the Arrhenius model:

$$k_{Ti} \, t_{aTi} = k_0 \int_0^t e^{\frac{-E_a}{RT(t)}} \, dt \qquad (4)$$

where k_0 = a frequency factor (min^{-1})
E_a = activation energy (J/mol)
R = gas constant $(8.315\ J/mol\ K)$
T = absolute temperature (K)

Based on representative temperature profiles shown in Fig. 1, Eq. 4 can be rewritten as:

$$t_{aTi} = \frac{1}{k_{Ti}}[(k_0)_{ac,inc} \int_0^{t_1} e^{\frac{(-E_a)_{ac,inc}}{RT(t)}}\ dt + k_{Ti}(t_2-t_1)$$

$$+ (k_0)_{ac,inc} \int_{t_2}^{t_3} e^{\frac{(-E_a)_{ac,inc}}{RT(t)}}\ dt]$$

(5)

where t_1 is the time when the sample first reaches the holding temperature (Ti), t_2 the time when holding is completed, and t_3 the finished heating time. The subscripts "ac, inc" represent values of the kinetic parameters during activation and inactivation of the proteinase, respectively. When temperatures are in the range of activation, $(E_a)_{ac}$ and $(k_0)_{ac}$ are substituted in the integral terms, while $(E_a)_{inc}$ and $(k_0)_{inc}$ are applied in the inactivation range. The integral terms of Eq. 5 indicate degradation of textural property during heat-up periods, 0-t_1 and t_2-t_3. It can be seen that if the thermal lag effect is insignificant, equivalent holding time (t_{aTi}) will be the same as holding time $(t_2 - t_1)$.

Because the true values of P_{th}, t_{aTi}, k_{Ti}, $(E_a)_{ac,inc}$ and $(k_0)_{ac,inc}$ are unknown, an iterative procedure was adopted to determine these values. The results from the isothermal approach $(k_{Ti}$, $(E_a)_{ac,inc}$ and $(k_0)_{ac,inc})$ were used as starting values to calculate t_{aTi} , and P of control was used as the starting value of P_{th}. Temperature of sample was assumed to be uniformly distributed within a diameter of 1 cm $(r = \pm 0.5$ cm) where shear stress and shear strain of sample were measured. For this reason, the two integrals in Eq. 5 were numerically solved by Simpson's rule (Forsythe et al. 1977) using time-temperature data recorded during heat-up periods. Then, using calculated t_{aTi} from Eq. 5, new k_{Ti}'s were estimated from Eq. 3. When k_{Ti}'s at all studied temperatures were determined, $(E_a)_{ac,inc}$ and $(k_0)_{ac,inc}$ were calculated using an Arrhenius equation. Iterative calculation was performed over 3-5 cycles until the difference in k_{Ti} from the previous cycle was $\le 0.0001\ min^{-1}$ (or $< 0.02\%$).

The next iterative value of P_{th} was calculated using Eq. 2, rewritten as:

$$\ln P_{th} = \ln P_0 + \int_0^t k[T(t)]\ dt$$

(6)

where P_0 here represents textural properties of the control. The integral indicating the effect of a finite heating rate on the control was numerically solved by Simpson's rule using the current values of k_{Ti} and $(E_a)_{ac,inc}$. A P_{th} was

calculated for each individual run and was used to reestimate values of k_{Ti} and $(E_a)_{ac,inc}$ as shown in Eq. 3 and 5. Iterative calculation was performed until the difference in P_{th} for shear stress and shear strain within individual batch was less than 0.01 kPa ($< 0.025\%$) and 0.01 ($< 0.4\%$), respectively. The P_{th} values normally converged in 3 cycles of iteration.

RESULTS AND DISCUSSION

Changes in both shear stress and shear strain with respect to holding time are shown in Fig. 2 A, B and 3 A, B, respectively. Because there was no difference between 2 experimental runs ($P>0.05$), an average of 2 replications is presented. Failure shear stress and shear strain of the samples held at various times at any temperatures were normalized by those of the control. Textural breakdown of surimi gels occurred at 40C and the most severe deterioration was detected at 55-60C. Shear stress and shear strain of the samples held for 5 min at 55, 60, and 65C could not be evaluated because the samples were very soft and mushy. Textural properties of the samples held at 75 and 80C did not significantly change with holding times ($P>0.05$). This indicated that textural degradation of whiting surimi gel would be minimized if surimi was heated quickly to 75C.

Changes in shear stress and shear strain of whiting surimi did not reach equilibrium state at any recorded holding times and at temperatures below 75C (Fig. 2A-B and 3A-B). Shear stress and strain decreased with time and surimi gel became so mushy that textural properties could not be measured. When retention of shear stress and shear strain was less than 10% and 30%, respectively, the samples exhibited no gel properties. Changes in shear stress and shear strain of whiting gel were modeled using the ratio of textural properties as shown in Eq. 1. Apparent rate constants of textural degradation at each temperature, obtained from 2 different analyses, are shown in Table 2. The apparent rate constants of both shear stress and shear strain obtained from using either isothermal (P_0) or nonisothermal conditions (P_{th}) were not different ($P > 0.05$). Therefore, only the results calculated from the nonisothermal model are shown in the plots of $\ln(P/P_{th})$ versus equivalent holding time (Fig. 4A,B for shear stress and in 5A,B for shear strain). It is seen that assumption of a first order reaction sufficiently describes changes in textural properties of whiting surimi (Table 2 gives r^2 values for these models). Because heating rates of the control and samples were identical, textural degradation of the control was equivalent to that of the sample during heat-up periods. Kinetic analysis based on an isothermal condition was also reported by Lenz and Lund (1980a,b). The advantage of using the isothermal condition to derive the kinetic model is that apparent rate constants and other kinetic parameters can be readily determined

from the experimental data. The kinetic model is independent of heating rate during heat-up periods as long as the control and samples are subjected to the identical temperature history. However, in this case, P_0 depends on the conditions used for the control.
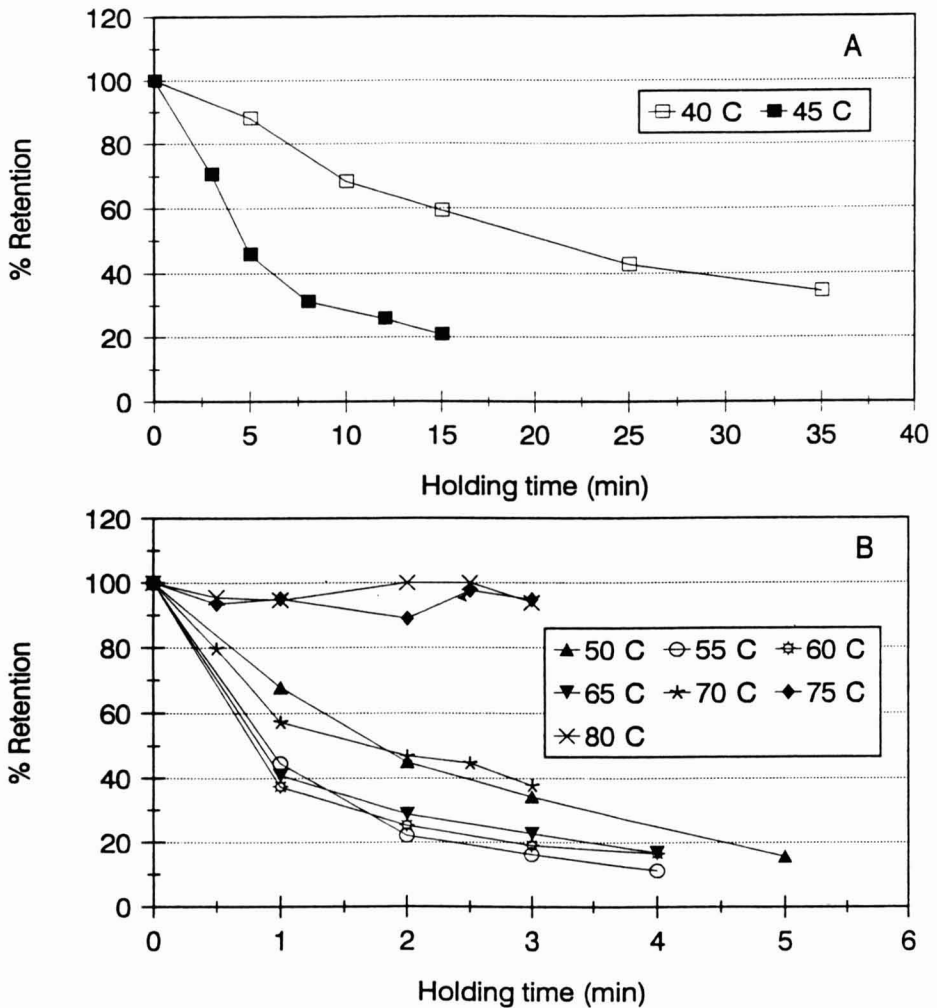
FIG. 2A-B. EFFECTS OF HOLDING TIME AND TEMPERATURE ON RETENTION OF SHEAR STRESS OF WHITING SURIMI
(A) at 40-45C; (B) at 50-80C
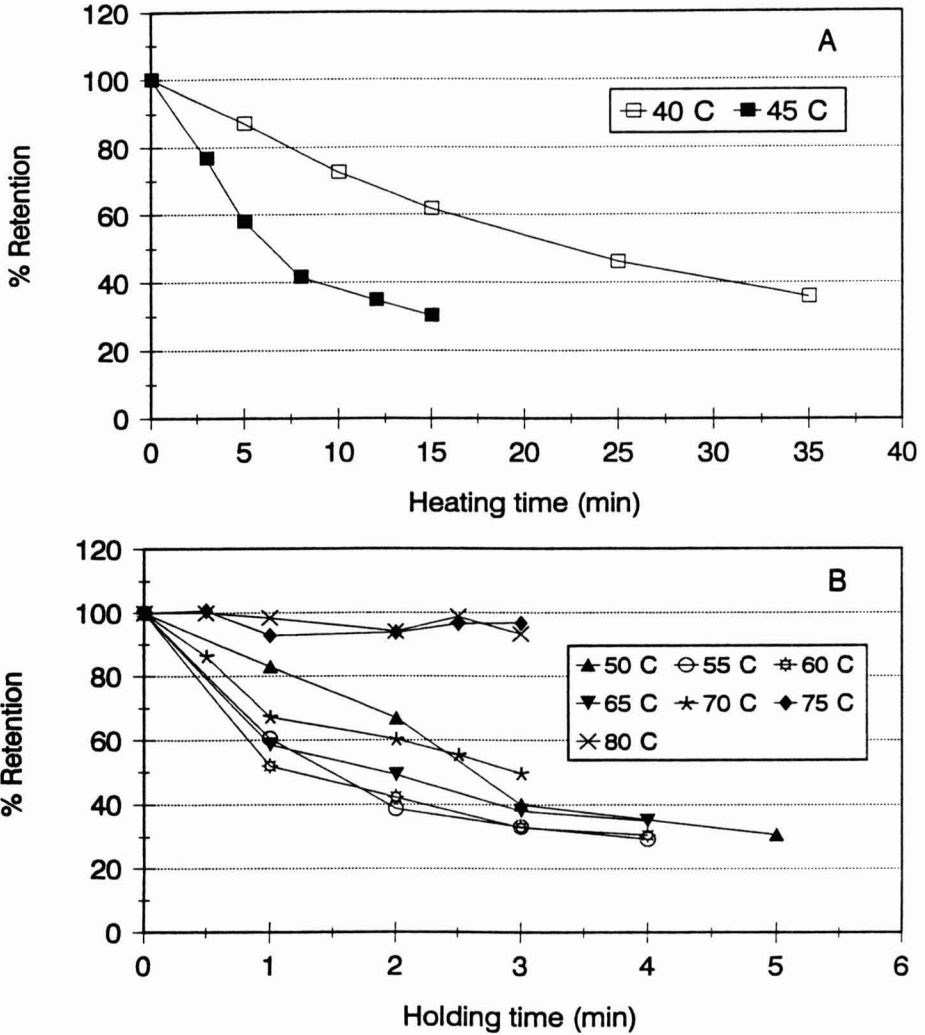
FIG. 3A-B. EFFECTS OF HOLDING TIME AND TEMPERATURE ON RETENTION OF
SHEAR STRAIN OF WHITING SURIMI
(A) at 40-45C; (D) at 50-80C

Shear stress and shear strain values obtained experimentally from the control
and those calculated from the nonisothermal approach are shown in Fig. 6A and
6B, respectively. The "P_{th}" indicates a theoretical maximum value of shear
stress and shear strain that could have been obtained if no textural degradation
had occurred. Shear stress and shear strain of whiting surimi decreased by ~ 10
and $\sim 7\%$, respectively, when it was heated from 10 to 90C at voltage gradient

TABLE 2.
APPARENT RATE CONSTANTS FOR KINETICS OF TEXTURAL DEGRADATION

Temp. (°C)	Shear stress				Shear strain			
	Isothermal		Nonisothermal		Isothermal		Nonisothermal	
	k (min^{-1}) (Std. dev.)	r^2	k_{Ti} (min^{-1}) (Std. dev.)	r^2	k (min^{-1}) (Std. dev.)	r^2	k_{Ti} (min^{-1}) (Std. dev.)	r^2
40	0.0370 (0.0012)	0.988	0.0366 (0.0012)	0.989	0.0292 (0.0005)	0.997	0.0292 (0.0005)	0.997
45	0.1077 (0.0050)	0.976	0.1092 (0.0048)	0.980	0.0821 (0.0046)	0.967	0.0828 (0.0044)	0.971
50	0.3560 (0.0067)	0.997	0.3659 (0.0022)	0.999	0.2269 (0.0038)	0.978	0.2044 (0.0144)	0.957
55	0.5376 (0.0185)	0.988	0.5419 (0.0193)	0.987	0.3046 (0.0144)	0.978	0.3152 (0.0134)	0.982
60	0.4267 (0.0576)	0.873	0.4341 (0.0548)	0.887	0.2840 (0.0386)	0.871	0.2886 (0.0368)	0.948
65	0.4157 (0.0075)	0.997	0.4175 (0.0066)	0.997	0.2582 (0.0213)	0.942	0.2614 (0.0129)	0.978
70	0.3046 (0.0160)	0.986	0.3088 (0.0164)	0.986	0.2462 (0.0424)	0.891	0.1997 (0.0227)	0.950
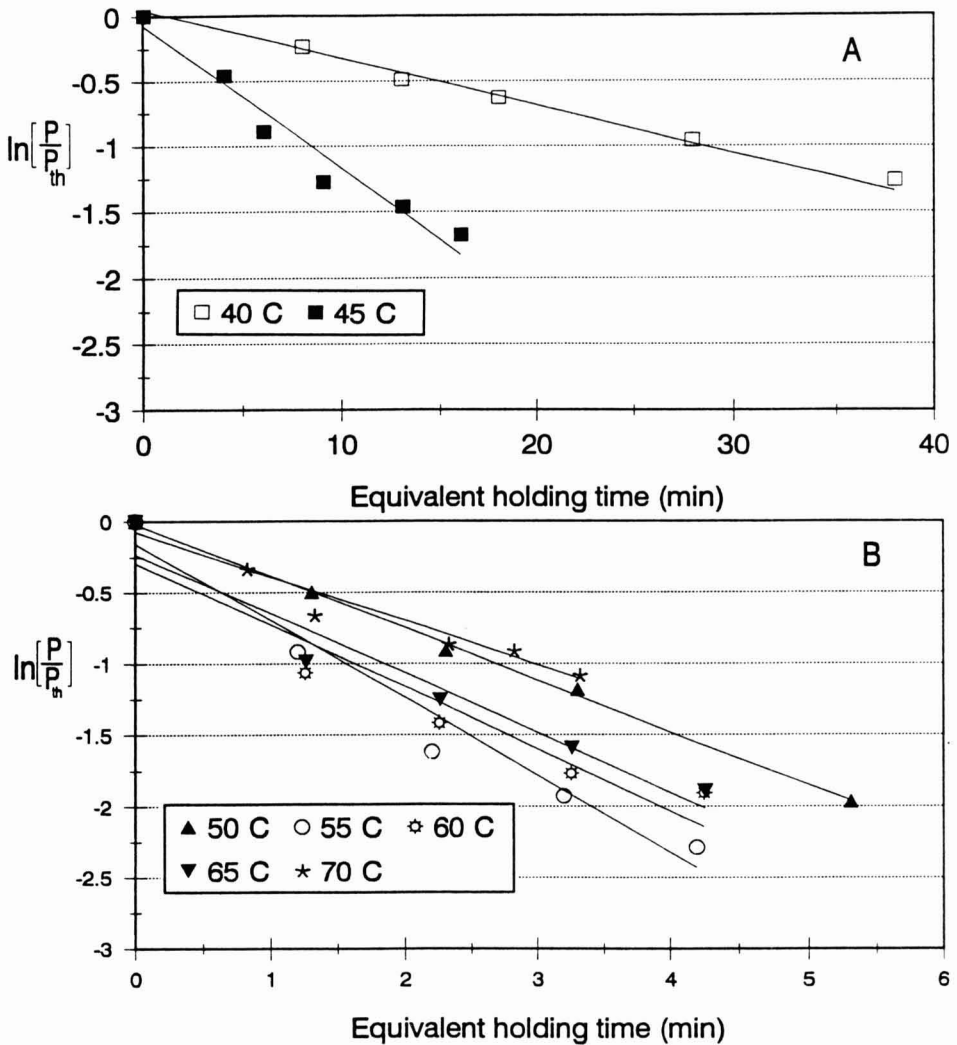
FIG. 4A-B. GRAPHICAL REPRESENTATION OF CHANGES IN SHEAR STRESS AS A
FIRST ORDER REACTION DETERMINED USING NONISOTHERMAL APPROACH
(A) at 40-45C; (B) at 50-70C

13.3 V/cm. This quantitative result illustrated the importance of rapid heating
in maximizing textural properties of whiting surimi. Shear stress and shear strain
could approach a theoretical value at higher applied voltage gradient, however,
it should be noted that whiting surimi still retained good gel quality despite the
approximate 10% textural degradation.
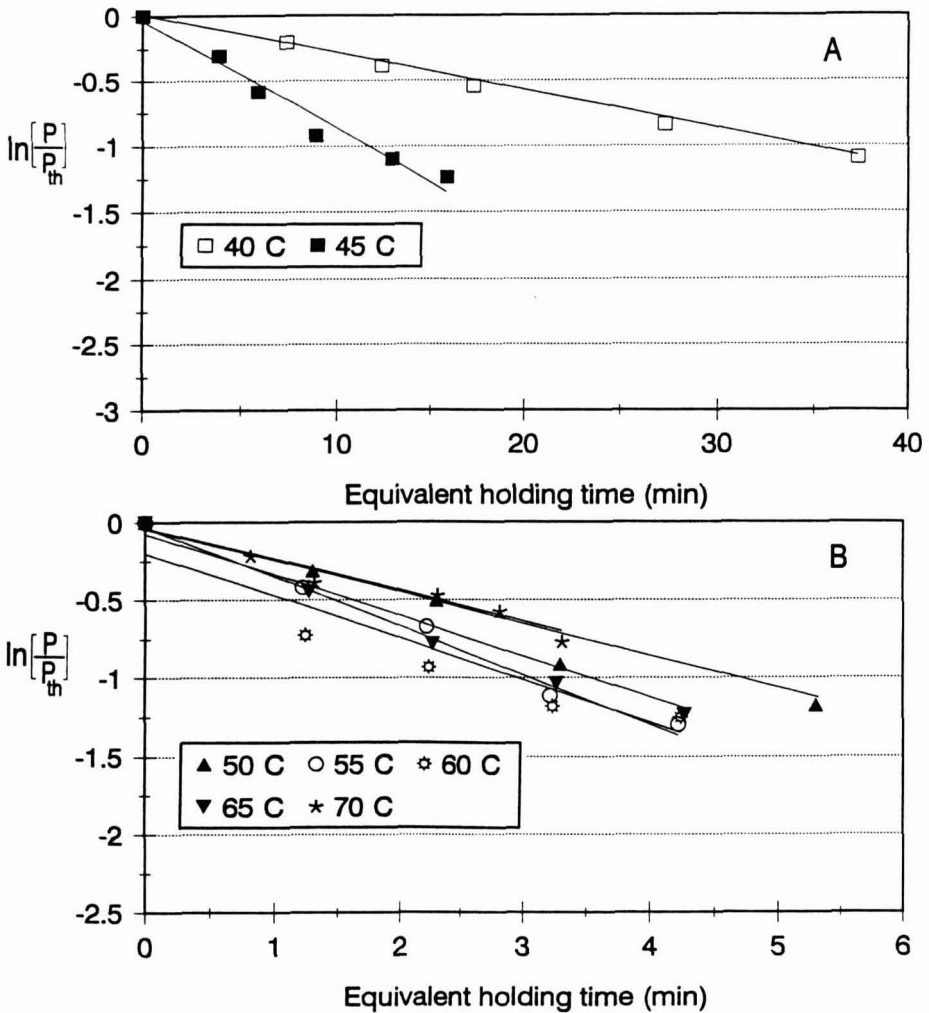
FIG. 5A-B. GRAPHICAL REPRESENTATION OF CHANGES IN SHEAR STRAIN AS A
FIRST ORDER REACTION DETERMINED USING NONISOTHERMAL APPROACH
(A) at 40-45C; (B) at 50-70C

Figures 7A,B illustrate Arrhenius plots of ln k_{Ti} of shear stress and shear
strain versus the reciprocal of the absolute temperature, respectively. The k_{Ti}'s
were calculated from the nonisothermal approach. It was evident that there were
two different temperature ranges in which the trends of apparent rate constant
(k_{Ti}) were markedly different. The break in straight line was at about 55C for
both shear stress and shear strain. Rate of textural degradation increased with
temperature and reached a maximum at 55C. Then, it gradually decreased until
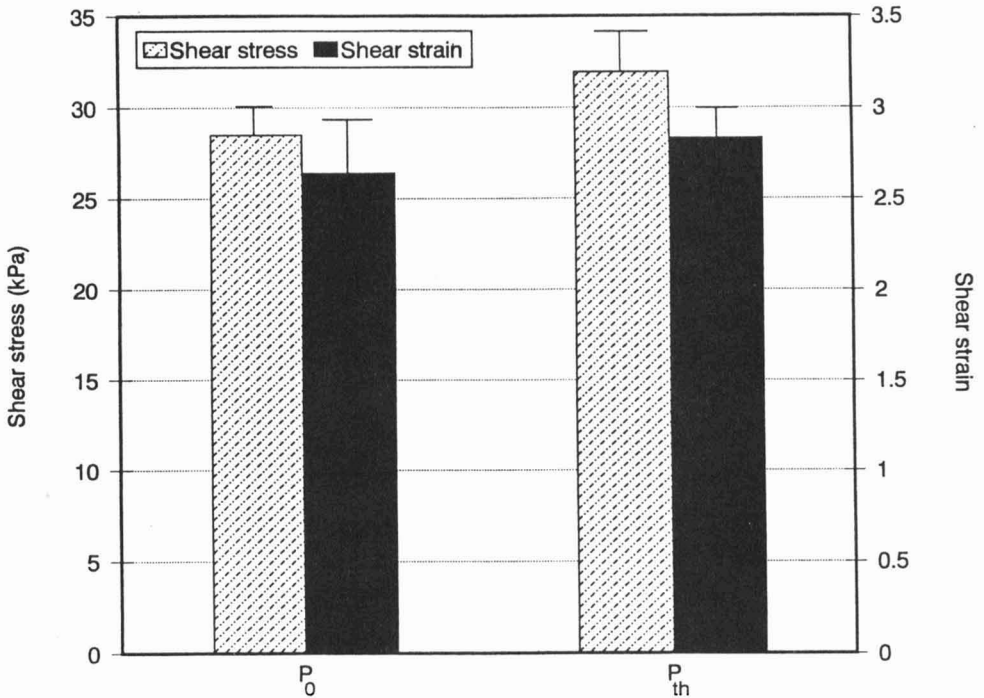
FIG. 6A-B. EXPERIMENTAL (P_0) AND THEORETICAL (P_{th}) VALUES OF SHEAR
STRESS AND SHEAR STRAIN OF THE SAMPLES HEATED OHMICALLY USING
13.3 V/CM
Values are means ± standard deviation (n = 20 batches).

70C. Rate of textural degradation could not be monitored at temperature ≥
75C. A plot of k_{Ti}'s vs 1/T resembled the temperature profile of purified
proteinase activity from Pacific whiting (Seymour et al. 1994) and the rate of
MHC proteolysis in whiting surimi (Yongsawatdigul et al. 1997). An increase
in the rate of textural degradation with temperature up to 55C was due to
enzyme activation, while a decrease in rate of degradation at higher temperature
was probably caused by thermal denaturation of the endogenous proteinase. This
indicated that proteolysis by the endogenous proteinase predominantly controlled
final gel texture.

Table 3 gives the values of E_a and r^2 determined from both isothermal and
nonisothermal approaches. At any given temperature range, E_a values of shear
stress and shear strain were comparable, implying that proteolysis affected these
two parameters to a similar extent. This was in agreement with Hamann and
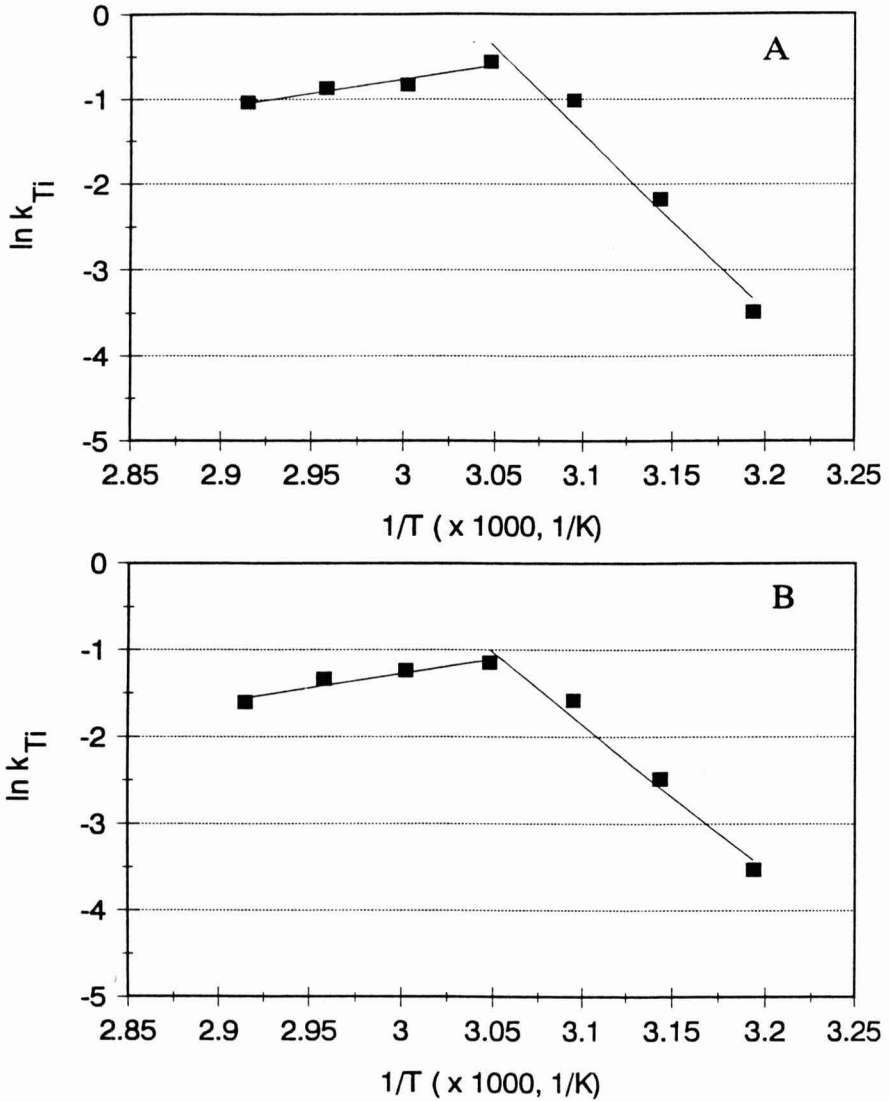
FIG. 7A-B. EFFECT OF TEMPERATURE ON THE APPARENT RATE CONSTANT, K_{ti}, OF TEXTURAL DEGRADATION

(A) shear stress; (B) shear strain

MacDonald (1992) who reported that proteolysis of surimi had profound effect on both shear stress and shear strain. E_a values in activation range (40-55C) of shear stress and strain were greater than those in inactivation range, regardless

TABLE 3.
REACTION RATE CONSTANTS FOR KINETICS OF GEL TEXTURE

Temp. (°C)	Shear Stress				Shear Strain			
	Isothermal		Nonisothermal		Isothermal		Nonisothermal	
	$E_a \pm$ Std. dev. (kJ/mol)	r^2	$E_a \pm$ Std. dev. (kJ/mol)	r^2	$E_a \pm$ Std. dev. (kJ/mol)	r^2	$E_a \pm$ Std. dev. (kJ/mol)	r^2
40-55	161.4±15.3	0.974	162.6±16.8	0.969	140.1±19.2	0.946	138.6±15.7	0.963
55-70	35.0±2.9	0.980	34.7±2.7	0.982	13.5±0.4	0.997	27.0±5.6	0.882

of modeling approach (Table 3). Therefore, degradation of textural properties was affected by temperature in activation range to a greater extent than that in inactivation range. These results suggested that Pacific whiting surimi should be rapidly heated to pass over activation temperature range (40-55C) so that severe textural deterioration could be avoided. Although 55-70C was considered as a inactivation range, degradation of surimi gel texture was noticed. Therefore, it is important to rapidly heat surimi > 70C to effectively minimized textural degradation. It should be mentioned that although E_a values were calculated from the log-transformed Arrhenius equation using weighted least square regression, standard deviation associated with those values were relatively small.

CONCLUSIONS

Kinetic models of textural degradation of whiting surimi gel were developed using the Arrhenius equation to account for thermal lag during heat-up periods. Kinetic models for textural properties were also readily obtained using an isothermal approach. Kinetic parameters obtained from either isothermal or nonisothermal approach were comparable. The models can be used to determine the optimum heating conditions that provide the desired textural properties of whiting surimi gel.

ACKNOWLEDGMENT

NOMENCLATURE

E_a Activation energy (J/mol)
$(E_a)_{ac}$ Activation energy in the activation temperature range (J/mol)
$(E_a)_{inc}$ Activation energy in the inactivation temperature range (J/mol)
k   Apparent rate constant obtained from isothermal approach (min^{-1})
k_0 Frequency factor (min^{-1})
k_{Ti} Apparent rate constant obtained from nonisothermal approach (min^{-1})
P   Textural property at time 't', failure shear stress (kPa), failure shear strain

P_0 Textural property of control, failure shear stress (kPa), failure shear strain

P_{th} Theoretical value of textural property at instantaneous heating, failure shear stress (kPa), failure shear strain

R   Gas constant, 8.315 J/mol ˚K

t   holding time (min)

t_{aTi} equivalent holding time at temperature Ti (min)

T   Temperature (˚K)

REFERENCES

ARABSHAHI, A. and LUND, D. 1985. Considerations in calculating kinetic parameters from experimental data. J. Food Process Engineering 7, 239–251.

AWUAH, G.B., RAMASWAMY, H.S., SIMPSON, B.K. and SMITH, J.P. 1993. Thermal inactivation kinetics of trypsin at aseptic processing temperature. J. Food Process Engineering 16, 315–328.

BOYE, S.M. and LANIER, T.C. 1988. Effect of heat stable alkaline proteinase activity of Atlantic menhaden (Brevoorti tyrannus) on surimi gels. J. Food Sci. 53, 1340–1342, 1398.

CHANG-LEE, M.V., PACHEO-AGUILAR, R., CRAWFORD, D.L. and LAMPILA, L. 1989. Proteolytic activity of surimi from Pacific whiting (Merluccius productus) and heat-set gel texture. J. Food Sci. 54, 1116–1119, 1124.

DAVIES, F.L., UNDERWOOD, H.M., PERKIN, A.G. and BURTON, H. 1977. Thermal death kinetics of Bacillus stearothermophilus spores at ultra high temperatures I. Laboratory determination of temperature determination of temperature coefficients. J. Food Technol. 12, 115–129.

ERICKSON, M.C., GORDON, D.T. and ANGLEMIER, A.F. 1983. Proteolytic activity in the sarcoplasmic fluid of parasitized Pacific whiting (Merluccius productus) and unparasitized true cod (Gadus macrocephalus). J. Food Sci. 48, 1315–1319.

FORSYTHE, G.E., MALCOLM, M.A. and MOLER, C.B. 1977. Computer Methods for Mathematical Computations. Prentice-Hall, Englewood Cliffs, NJ.

GREENE, D.H. and BABBITT, J. 1990. Control of muscle softening and proteinase parasite interactions in arrowtooth flounder (Atheresthes stomias). J. Food Sci. 55, 579–580.

HAMANN, D.D. 1983. Structural failure in solid foods. In Physical Properties of Foods, (M. Peleg and E.B. Bagely, eds.) pp. 351–383, Chapman & Hall, New York.

HAMANN, D.D. and MACDONALD, G.A. 1992. Rheology and texture properties of surimi and surimi-based foods. In *Surimi Technology*. (T.C. Lanier and C.M. Lee, eds.) pp. 429–501. Marcel Dekker, New York.

HILL, JR., C.G. and GRIEGER-BLOCK, R.A. 1980. Kinetic data: generation, interpretation and use. Food Technol. *94*, 56–66.

LENZ, M.K. and LUND, D.B. 1977a. The lethality-Fourier number method. Experimental verification of a model for calculating temperature profiles and lethality in conduction-heating canned foods. J. Food Sci. *42*, 989–996.

LENZ, M.K. and LUND, D.B. 1977b. The lethality-Fourier number method. Experimental verification of a model for calculating average quality factor retention in conduction-heating canned foods. J. Food Sci. *42*, 997–1001.

LENZ, M.K. and LUND, D.B. 1980. Experimental procedures for determining destruction kinetics of food components. Food Technol. *34*(2), 51–55.

MORRISSEY, M.T., WU, J.W., LIN, D. and AN, H. 1993. Proteinase inhibitor effects on torsion measurements and autolysis of Pacific whiting surimi. J. Food Sci. *58*, 1050–1054.

NFI. 1991. *A Manual of Standard Methods for Measuring and Specifying the Properties of Surimi,* (T.C. Lanier, K. Hart, and R.E. Martin, eds.) Univ. of North Carolina Sea Grant College Program, Raleigh, NC.

PALANIAPPAN, S., SASTRY, S.K. and RICHTER, E.R. 1992. Effect of electroconductive heat treatment and electrical pretreatment on thermal death kinetics of selected microorganisms. Biotech. Bioeng. *39*, 225–232.

PATASHNIK, M., GRONINGER, JR., H.S., BARNETT, H., KUDO, G. and KOURY, B. 1982. Pacific whiting (*Merluccius productus*): I. Abnormal muscle texture caused by myxosporidian-induced proteolysis. Mar. Fish. Rev. *44*(5), 1–12.

PERKIN, A.G., BURTON, H., UNDERWOOD, H.M. and DAVIES, F.L. 1977. Thermal death kinetics of *Bacillus stearothermophilus* spores at ultra high temperatures II. Effect of heating period on experimental results. J. Food Technol. *12*, 131–148.

RAMASWAMY, H. and ABDELRAHIM, K. 1992. Thermal processing and computer modeling. In *Encyclopedia of Food Science and Technology*, Vol. 4. (Y.H. Hui, ed.) pp. 2538–2561, John Wiley & Sons, New York.

SAGUY, I. and KAREL, M. 1980. Modeling of quality deterioration during food processing and storage. Food Technol. *34*(2), 78–85.

SEYMOUR, T.A., MORRISSEY, M.T., PETERS, M.Y. and AN, H. 1994. Purification and characterization of Pacific whiting proteinases. J. Agri. and Food Chem. *42*, 2421–2427.

SWARTZEL, K.R. 1982. Arrhenius kinetics as applied to product constituent losses in ultra high temperature processing. J. Food Sci. *47*, 1886–1891.

TOYOHARA, H. and SHIMIZU, Y. 1988. Relation between modori phenome-
non and myosin heavy chain breakdown in threadfin-bream gel. Agric.
Biol. Chem. *52*, 255–257.

WICKER, L. and TEMELLI, F. 1988. Heat inactivation of pectinesterase in
orange juice pulp. J. Food Sci. *53*, 162–164.

YONGSAWATDIGUL, J. and PARK, J.W. 1996. Linear heating rate affects
gelation of Alaska pollock and Pacific whiting. J. Food Sci. *61*, 149–153.

YONGSAWATDIGUL, J., PARK, J.W. and KOLBE, E. 1997. Degradation
kinetics of myosin heavy chain of Pacific whiting surimi. J. Food Sci. *62*,
724–728.

YONGSAWATDIGUL, J., PARK, J.W., KOLBE, E., ABUDAGGA, Y. and
MORRISSEY, M.T. 1995. Ohmic heating maximizes gel functionality of
Pacific whiting surimi. J. Food Sci. *60*, 10–14.

A NEW TECHNIQUE FOR EVALUATING FLUID-TO-PARTICLE HEAT TRANSFER COEFFICIENTS UNDER TUBE-FLOW CONDITIONS INVOLVING PARTICLE OSCILLATORY MOTION

M.R. ZAREIFARD and H.S. RAMASWAMY[1]

Department of Food Science and Agricultural Chemistry
Macdonald Campus of McGill University
21,111 Lakeshore, P.O.B. 187
Ste. Anne de Bellevue, P.Q.
H9X 3V9, Canada

ABSTRACT

One of the critical parameters for the modelling of particle temperature profiles in continuous processing of particulate foods in a carrier liquid is the fluid-to-particle heat transfer coefficient between the fluid and the particles (h_{fp}). A laboratory scale apparatus was fabricated to evaluate h_{fp} under conditions imparting particle oscillatory motion while being heated in a model holding tube. Spherical particles ($d = 12.7 \times 10^{3}$ m) with centrally located fine-wire flexible thermocouples ($d = 7.62 \times 10^{5}$ m) were suspended from the upper mid-section of a curved glass tube ($ID = 50.8 \times 10^{3}$ m) to provide lateral movement of the particle as the tube was subjected to an oscillatory motion. A variable speed reversible motor, in conjunction with an electronic circuit board, was used to control the frequency and amplitude of the tube thereby keeping the particle in continuous motion. Time-temperature data were gathered continuously from the time the particle-mounted oscillatory unit, set at room temperature for the desired amplitude and frequency, was transferred to a heated sucrose solution (0, 30 and 50% w/w) at 70 or 90C. The h_{fp} values were calculated from the evaluated heat rate index, f_h, at three particle velocities (0.09, 0.16 and 0.26 m/s) under three oscillatory amplitudes (90, 180 and 270°). The h_{fp} values increased with amplitude of oscillation and particle velocity, and decreased with the sucrose concentration. The h_{fp} values associated with the fixed particles were higher than those for particles which were free to move.

[1]Corresponding Author

INTRODUCTION

Aseptic processing has been used commercially for liquid products and acid foods containing particulate matters but its use for low-acid and particulate food is still under investigation. Conventional thermal processes are established based on the temperature response of the food which can be easily evaluated during heating and cooling. However, in continuous flow aseptic processing situations, with discrete particles suspended in a continuously moving fluid, particle temperature can not be easily measured. Since implementing traditional routines for process calculations becomes questionable under such situations, mathematical modeling has been used as an alternative. A major obstacle for modelling particle temperature history in an aseptic processing unit is lack of adequate information on heat transfer coefficient between the carrier fluid and suspended particles (Heldman 1989). Considerable effort has gone into finding suitable models for estimation of lethality of low-acid food containing particulate (Sastry 1986; Chandarana et al. 1989; Chang and Toledo 1990; Larkin 1990; Sablani and Ramaswamy 1995; Kelly et al. 1995; Balasubramaniam and Sastry 1996a). Dignan et al. (1989) listed critical factors needed in modelling heat transfer and lethality distribution in continuously processed low-acid particulate foods as: particle size/distribution, convective heat transfer coefficient and residence time distribution both in the heat exchanger and holding tube.

In process evaluation through simulations, the fluid-to-particle heat transfer coefficients in both heat exchanger and holding tube probably are the most important but difficult parameters to be determined experimentally (Dignan et al. 1989; Heldman 1989). For continuous sterilization of food particulate, de Ruyter and Brunet (1973), and Manson and Cullen (1974) assumed the heat transfer coefficient to be infinite. However, several researchers demonstrated a finite convective heat transfer coefficient at the fluid-particle interface (Sastry 1986; Chandarana and Gavin 1989a,b; Chang and Toledo 1990; Chandarana et al. 1990; Zitoun and Sastry 1994a,b; Bhamidipati and Singh 1995; Awuah and Ramaswamy 1996).

Determining of (h_{fp}) poses a unique challenge to the investigators because of the difficulty in monitoring the temperature of moving particles without interfering with particle motion. Chau and Synder (1988), Chandarana et al. (1989 and 1990), Chang and Toledo (1990), Zuritz et al. (1990) and Awuah et al. (1995) determined h_{fp} by recording the time-temperature data of a stationary particle while the fluid pass over it. Researchers have also attempted to simulate more realistic situation, putting the particle in moving condition, and evaluate h_{fp}. Sastry et al. (1989) suggested a moving thermocouple method in which the temperature of a particle attached to a thermocouple could be monitored while the thermocouple wire is withdrawn from the downstream end at the same speed as that of the particle. Using this method, Zitoun and Sastry (1994b) studied the

heat transfer coefficient for cube shaped particles in continuous tube flow. More recently, a liquid crystal, which changes with temperature, has been used to get the surface temperature history of a moving particle in studying of heat transfer coefficient under continuous flow conditions. This method involves coating the moving particle with a specific liquid crystal and recording the color changes on the particle surface as a function of temperature. Stoforos and Merson (1991) were the first to use the liquid crystal material to evaluate overall and liquid-to-particle heat transfer coefficient for model food particles in a rotating liquid/particulate canned food system. Balasubramaniam and Sastry (1994a,b and 1995) applied the same technique to measure the heat transfer coefficient but in a continuous flow system. They observed that the liquid crystal method resulted in higher values of h_{fp} compared to the moving thermocouple method under the same experimental condition. Other methods, like measuring the relative velocity between fluid and particle, and back-calculation of h_{fp} using the existing dimensionless correlations (Zitoun and Sastry 1994a; Balasubramaniam and Sastry 1994b); or indirect methods of h_{fp} determination which are based on locating heat-labile substances such as enzymes or microbial spores at the center of simulated food particles (Weng *et al.* 1992), and more recently use of remote temperature sensor in a moving particle (Balasubramaniam and Sastry 1996b) have also been proposed.

Although various techniques employed for evaluating the fluid-to-particle heat transfer coefficient have contributed to understanding of the heat transfer phenomena, they all have limitations and partially simulate the commercial processing situation. Some studies have used aseptic processing conditions, but are limited to a stationary particle. Some others involve particle motion, but are limited to a transparent carrier medium in glass holding tubes. The objective of this study was to develop a new technique which, to some extent, overcomes these problems. An oscillatory approach was used for imparting particle motion in a model holding tube while using the conventional thermocouple approach for measuring h_{fp} in continuous flow systems. The particle was held in a continuous oscillatory motion within a section of a circular tube which was subjected to an oscillatory motion while immersed in a constant temperature water bath. The particle velocity in a relatively stationary fluid could thus be defined by controlling the amplitude and frequency of oscillations.

GOVERNING EQUATIONS FOR THE HEAT TRANSFER

The unsteady state heat conduction differential equation governing heat transfer to an isotropic spherical particle, suddenly transferred into a constant temperature medium is expressed as:

$$\frac{\partial U}{\partial t} = \alpha \ (\frac{\partial^2 U}{\partial r^2} + \frac{2}{r} \cdot \frac{\partial U}{\partial r}) \tag{1}$$

The analytical solution to Eq. (1) is given below as detailed in Carslaw and Jaeger (1959) and Luikov (1968):

$$U = 2Bi \sum_{n=1}^{n=\infty} \frac{[\delta_n^2 + (Bi-1)^2]\sin(\delta_n)}{\delta_n^2(\delta_n^2 + Bi(Bi-1))} \cdot \frac{\sin(\delta_n r/a)}{(r/a)} \exp(-\delta_n^2 Fo) \tag{2}$$

where δ_n is the nth positive root of

$$Bi = 1 - \delta \cot(\delta) \tag{3}$$

The series solution converges to the first term beyond an Fo value of 0.2 (Heisler 1947). Using δ as the first root of Eq. (3), and abbreviating all parameters behind the exponential term as A, Eq. (2) can be rewritten as:

$$U = A \ \exp \ (-\delta^2 \ Fo) \tag{4}$$

By taking the logarithm on both sides of the above equation, transforming to logarithm to base 10, and expanding Fo as $\alpha t/a^2$, Eq.(4) can be written as:

$$\log U = \log A - (\frac{\delta^2 \alpha t}{2.303 \ a^2}) \tag{5}$$

This equation represents the straight line portion of the heating or cooling curve obtained by a plot of log U vs t. The slope index of such a curve is called heating rate index, f_h, which is related to δ in the following form:

$$f_h = \frac{2.303 \ a^2}{\alpha \delta^2} \tag{6}$$

The slope index, f_h, is dependent on δ, particle size and thermal diffusivity (α), but independent of the location. Therefore, using this method, it is not necessary to know the exact location of the thermocouple within the sample. Knowing a, α and f_h, which can be evaluated from experimental data, δ can be calculated using Eq.(6). Using δ in Eq.(3), the corresponding Bi and hence, the heat transfer coefficient, h, can be calculated [h = Bi (k/a)].

MATERIALS AND METHODS

Experimental Setup

Two transparent glass tubes (ID = 50.8×10^{-3} m) were bent into the radii of curvatures of 0.15 and 0.25 m and an arc was cut to a length representing about one quarter of a full circle. On the upper midpoint of each tube a hole was cut to pass thermocouples through a connector. Two such units were nested together facing each other in diametrically opposite locations. The four bent tubes were secured on an aluminum cross bar to form two diametrically opposite open ended quarters of a circular tubing.

Nylon spheres (d = 12.7×10^{-3} m) were used as test particles and thermophysical properties of the particles were experimentally evaluated using procedures described elsewhere (Sablani and Ramaswamy 1996): density = 1128 Kg/m^3, thermal diffusivity = 1.58×10^{-7} m^2/s, and heat capacity = 2073 J/Kg°C. The thermal conductivity was calculated as 0.369 W/m°C ($k = C_p \rho \alpha$).

The spherical particles were carefully drilled to the geometric center using a one millimeter drill bit. A very fine and flexible Teflon coated type-T copper-constantan thermocouple of 7.62×10^{-5} m diameter (Omega Engineering Inc., Stamford, CT) was made and inserted to the center of each Nylon sphere. The gap between the thermocouple wire and the particle was filled with glue (epoxy resin and hardener 50/50). Then, one of the particles was located inside the tube with some extra lead of thermocouple wire to let the particle move inside the tube during oscillation. In the parallel assembly, on the other side, a thicker gage thermocouple of 25.4×10^{-5} m diameter was used in order to hold the particle rigidly at the center or bottom surface of the tube. All thermocouples were calibrated against an ASTM standard mercury-in-glass thermometer with a temperature resolution of ±0.05C. Thus, there were two fixed particles at 0.15 and 0.25 m radial distances from the center and two other particles which were free to move inside the tube at the same radial distance but on the other side. During the oscillations, the fixed particle would move along with the tube thus experiencing a programmed velocity in a relatively stationary liquid phase. On the other hand, the particle that was actually "free" to move remained partly stationary, while the tube slid below it during the oscillations.

The whole assembly was supported by a shaft connected to the output of a 100W electric DC motor. An electronic circuit in conjunction with two micro-switches which reversed the direction of rotation was designed in such a way that the shaft could be rotated at different speeds (rpm) and amplitudes (the distance between the two micro-switches could be adjusted to give different amplitudes). Therefore, changing the position of micro-switches provided different amplitudes of the oscillation and changing the power level provided different revolutions per minute and hence frequency. The assembly of particle equipped glass tubes could thus be subjected to controlled oscillations. A schematic diagram of the experimental setup is shown in Fig. 1.

The whole assembly was kept in a cooling tank at room temperature for equilibration of temperatures in test particles and an appropriate oscillatory motion was designed with a specified frequency and amplitude. While the tubes were in a steady oscillatory condition, the assembly was transferred to a stainless steel insulated tank containing a heating medium at the desired temperature. The heating tank was previously heated using steam injection and controlled to a constant set-point temperature $\pm$ 1C. Time-temperature data were gathered at 5 s time intervals using a data logger (Dash-8, Metra-Byte Corp, Taunton, Ma) connected to a personal computer.

Experimental Procedure

Several experiments were carried out using water and Nylon particles of different sizes to evaluate the experimental set-up. To work in the lower range of Biot numbers, it was necessary to restrict the particle size to d = 12.7×10^{-3} m. Sucrose solutions were used as additional heating media providing a higher viscosity. Sucrose solution was prepared in a $0.6 \times 0.6 \times 0.9$ m stainless steel tank and heated to the desired temperature (70 or 90C). The temperature of the medium was continuously monitored and was found to be stable within $\pm$ 1C during a given test run. The concentration of the solution was monitored using a refractometer and kept constant during the experiment by addition of small amounts of a higher concentration syrup or water as needed.

Experiments were carried out in water as well as 30 and 50% (w/w) sucrose solutions, three different amplitudes 90, 180 and 270° (angle of oscillation), two temperatures (70 and 90C). The rotation speed of 6 and 10 rpm provided three linear velocities for the particle 0.09, 0.16 and 0.26 m/s with respect to their position from the center of rotation (V = $R\omega$ = $2\pi Rn$). The number of replications was at least three for each experimental condition. In a majority of experiments, the fixed particle was positioned at the central axis of the tube while in some it was located along the bottom surface for comparative purposes.

Top View

Glass Tubes
ID=50.8x10^{-3}m

Cross bars
to support the tubes.
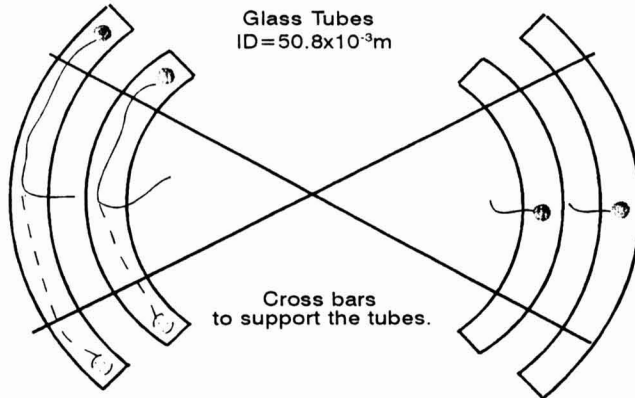
Left: sphere particles (d=12.7x10^{-3}m) attached to the
flexible thermocouple (d=7.62x10^{-5}m). Free to move
back and forth during oscillation.
Right: the same particles fixed at the center of the
tube using thicker thermocouple (d=25.4x10^{-5}m).

Side View

| P C | Data Logger | Motor | Controller |

Free Particles

Fixed Particles

0.15 m

0.25 m
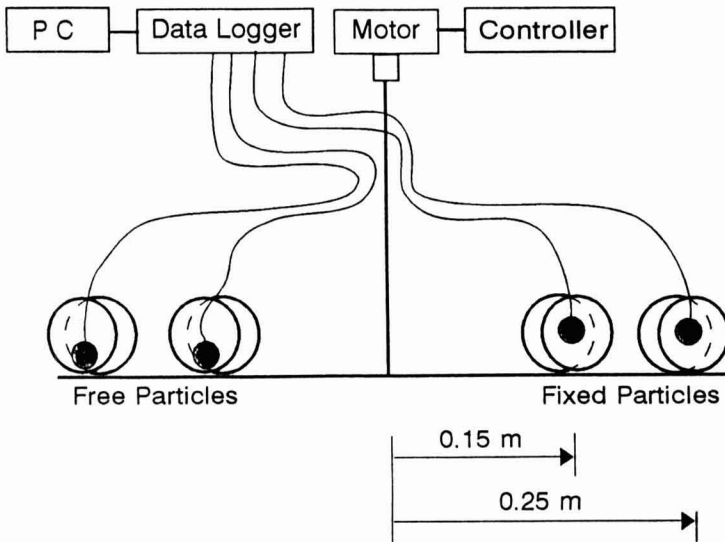
FIG. 1. SCHEMATIC DIAGRAM OF EXPERIMENTAL SETUP

RESULTS AND DISCUSSION

Typical time-temperature curves for all of four particles at the same run are shown in Fig. 2 which illustrates the slightly rapid heating behavior of the fixed particles as compared to the free particles in both radial locations (0.15 and 0.25 m from the central axis). Semi-logarithmic plots of temperature difference (medium temperature minus center point temperature of the particle) versus time are shown in Fig. 3, from which the heating rate indexes (f_h) were calculated as negative reciprocal slopes of the straight portion of the heating curves. Generally, a Fo value greater than 0.2 is taken to assure convergence of the
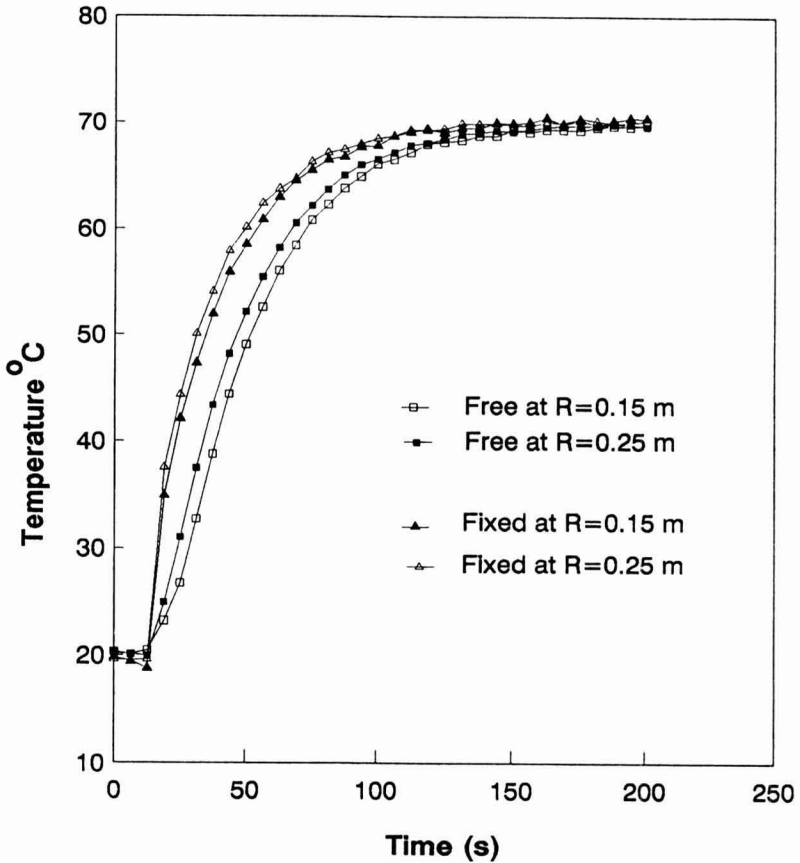
FIG. 2. TYPICAL TIME-TEMPERATURE CURVES FOR FREE AND FIXED PARTICLES
AT TWO RADIAL DISTANCES FROM THE CENTER OF ROTATION
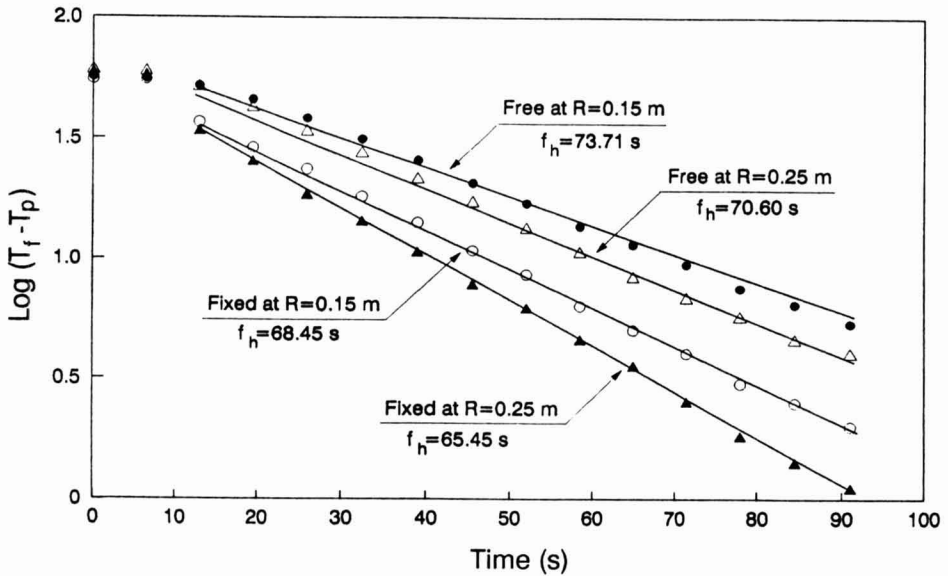
FIG. 3. SEMI-LOGARITHMIC PLOTS OF TEMPERATURE DIFFERENCE VERSUS TIME
FOR FREE AND FIXED PARTICLES (NEGATIVE RECIPROCAL SLOPE OF THE LINEAR
PORTION OF THE CURVE WAS CALCULATED AS f_h)

series solution for the heat conduction differential equation (Eq. 2) to the first
term. However, the actual number depends on particle shape and associated Biot
numbers. It was observed that for the spherical particles used under the
experimental conditions employed in this study, convergence (linearization of the
semi-logarithmic plot) was generally observed from Fo value as low as 0.1 as
can be seen from Fig. 3 (Fo = 0.1 at t ~ 25 s). Typical data shown in Table 1
indicates almost identical values of the calculated slope index (f_h) between Fo
values of 0.1-0.4 and 0.2-0.4 (maximum difference was about 1.5%). The
evaluated f_h is used as input for calculating the associated heat transfer
coefficients. Average values of the fluid to particle heat transfer coefficients and
their associated coefficients of variations are presented in Tables 2 and 3 for the
free and fixed particles under various conditions.

Effect of Oscillation Amplitude on h_{fp}

An initial set of experiments was performed with the purpose of evaluating
the effect of the degree of amplitude of oscillation at different levels on the h_{fp}.
At any given rotation speed (rpm), the frequency of oscillation (cycles per min)

TABLE 1.
TYPICAL DATA FOR COMPARISON OF f_h FOR Fo < 0.2 AND Fo > 0.2 FOR
A SPHERICAL GEOMETRY

Fo	f_h (s)	R^2	Difference %	f_h (s)	R^2	Difference %
0.12 - 0.39	73.21	0.998		72.13	0.999	
0.20 - 0.39	72.32	0.999	1.2	71.22	0.999	1.3
0.13 - 0.40	73.16	0.996		72.47	0.997	
0.21 - 0.40	73.59	0.998	0.6	73.40	0.998	1.3
0.12 - 0.38	70.07	0.995		71.95	0.998	
0.20 - 0.38	69.71	0.988	0.5	72.90	0.997	1.3
0.12 - 0.40	69.19	0.999		70.09	0.999	
0.20 - 0.40	69.67	0.998	0.7	71.05	0.998	1.3
0.15 - 0.42	67.32	0.997		70.22	0.999	
0.20 - 0.42	67.09	0.996	0.3	71.28	0.999	1.5

would be different at each of the three selected degrees of oscillations. For example, at 6 rpm rotation speed, the number of oscillations per min is 24, 12 and 8, respectively, at amplitudes of 90, 180 and 270°. Therefore, the lower the angle of amplitude, the higher the frequency of oscillation. Results of these experiments are shown in Fig. 4 for both the "free" and "fixed" particles at different velocities for experiments carried out in a 30% sucrose solution. Similar results were observed for experiments conducted in water. The linear velocity of 0.09 m/s for the "fixed" particle is the result of 6 rpm at 0.15 m radius of rotation, while 10 rpm at 0.25 m radius of rotation gives 0.26 m/s; the

TABLE 2.
ASSOCIATED FLUID-TO-PARTICLE HEAT TRANSFER COEFFICIENTS FOR FREE PARTICLES UNDER DIFFERENT TUBE-FLOW CONDITIONS

Heating Medium (°Brix)	Temp (°C)	Rotation Speed (n) (rpm)	Radial Location (R) (m)	Linear Velocity (V) (m/s)	Amp. (deg)	Rep.	h_{fp} (W/m^2 K)	CV (%)	Bi	Nu
0	70	10	0.15	0.16	270	3	750	8.4	13.0	14.3
0	70	10	0.25	0.26	270	3	790	8.7	13.7	15.1
0	70	10	0.15	0.16	180	3	520	14.9	9.0	9.9
0	70	10	0.25	0.26	180	4	570	8.8	9.8	10.8
0	70	10	0.15	0.16	90	6	560	9.5	9.6	10.6
0	70	10	0.25	0.26	90	6	590	7.1	10.2	11.2
30	70	6	0.15	0.09	270	3	610	9.9	10.5	14.0
30	70	6, 10	0.25, 0.15	0.16	270	9	670	14.6	11.6	15.4
30	70	10	0.25	0.26	270	8	840	7.4	14.5	19.3
30	70	6	0.15	0.09	180	5	480	14	8.2	10.9
30	70	6, 10	0.25, 0.15	0.16	180	10	520	9	8.9	11.9
30	70	10	0.25	0.26	180	11	590	10	10.1	13.5
30	70	6	0.15	0.09	90	8	450	11.5	7.7	10.2
30	70	6, 10	0.25, 0.15	0.16	90	9	470	6.5	8.0	10.7
30	70	10	0.25	0.26	90	8	530	7	9.1	12.2
50	70	10	0.15	0.16	90	6	430	8.3	7.3	11.2
50	70	10	0.25	0.26	90	6	440	7.6	7.6	11.5
30	90	10	0.15	0.16	90	4	460	2.3	7.9	10.2
30	90	10	0.25	0.26	90	4	510	3.9	8.8	11.4
50	90	10	0.15	0.16	90	5	460	4.3	7.9	11.7
50	90	10	0.25	0.26	90	5	480	4.7	8.2	12.1

Amp. : Amplitude. Rep. : Replicates

TABLE 3.
ASSOCIATED FLUID-TO-PARTICLE HEAT TRANSFER COEFFICIENTS FOR FIXED PARTICLES UNDER DIFFERENT TUBE-FLOW CONDITIONS

Particle Position	Heating Medium (°Brix)	Temp (°C)	Rotation Speed (n) (rpm)	Radial Location (R) (m)	Linear Velocity* (V) (m/s)	Amp. (deg)	Rep.	h_{fp} (W/m^{2}K)	CV (%)	Bi	Nu	Re
FS	0	70	10	0.15	0.16	270	3	1240	6.4	21.3	23.6	4900
FS	0	70	10	0.25	0.26	270	3	1370	6.9	23.5	26.0	8000
FS	0	70	10	0.15	0.16	180	3	1000	19.6	17.3	19.1	4900
FS	0	70	10	0.25	0.26	180	3	1200	7.2	20.5	22.7	8000
FS	0	70	10	0.15	0.16	90	3	840	16	14.5	16.0	4900
FS	0	70	10	0.25	0.26	90	3	1060	17	18.2	20.1	8000
FC	0	70	10	0.15	0.16	90	3	660	15	11.4	12.6	4900
FC	0	70	10	0.25	0.26	90	3	850	3.6	14.6	16.2	8000
FC	30	70	6	0.15	0.09	270	3	890	7	15.3	20.4	1250
FC	30	70	6 , 10	0.25 , 0.15	0.16	270	7	1140	5	19.6	26.0	2250
FC	30	70	10	0.25	0.26	270	3	1260	3	21.6	28.7	3650
FS	30	70	10	0.15	0.16	270	4	1250	6.1	21.6	28.7	2250
FS	30	70	10	0.25	0.26	270	3	1440	12	24.8	33.0	3650
FC	30	70	6	0.15	0.09	180	3	750	6.8	12.9	17.1	1250
FC	30	70	6 , 10	0.25 , 0.15	0.16	180	4	890	5.3	15.4	20.4	2250
FC	30	70	10	0.25	0.26	180	3	960	4	16.6	22.1	3650
FS	30	70	10	0.15	0.16	180	4	950	3	16.4	21.8	2250
FS	30	70	10	0.25	0.26	180	4	1100	8.2	19.0	25.3	3650
FS	30	70	6	0.15	0.09	90	3	630	12	10.8	14.4	1250
FS	30	70	6 , 10	0.25 , 0.15	0.16	90	3	820	16	14.0	18.6	2250
FS	30	70	10	0.25	0.26	90	3	1090	15	18.7	24.9	3650
FC	30	70	6	0.15	0.09	90	4	580	10	10.0	13.3	1250
FC	30	70	10	0.25	0.26	90	4	690	6	11.9	15.9	3650
FC	30	70	6 , 10	0.25 , 0.15	0.16	90	5	640	7	11.1	14.7	2250
FC	50	70	10	0.15	0.16	90	4	560	6.4	9.7	14.8	850
FC	50	70	10	0.25	0.26	90	4	600	9.5	10.4	15.9	1350
FC	30	90	10	0.15	0.16	90	5	710	10	12.1	15.7	3150
FC	30	90	10	0.25	0.26	90	4	820	4.1	14.1	18.2	5150
FC	30	90	10	0.15	0.16	90	3	770	1.1	13.3	19.7	1400
FC	50	90	10	0.25	0.26	90	3	810	1.6	13.9	20.5	2250

FS: Particle fixed at surface. FC: Particle fixed at center. *V=2πRn. Amp: Amplitude. Rep: Replicates
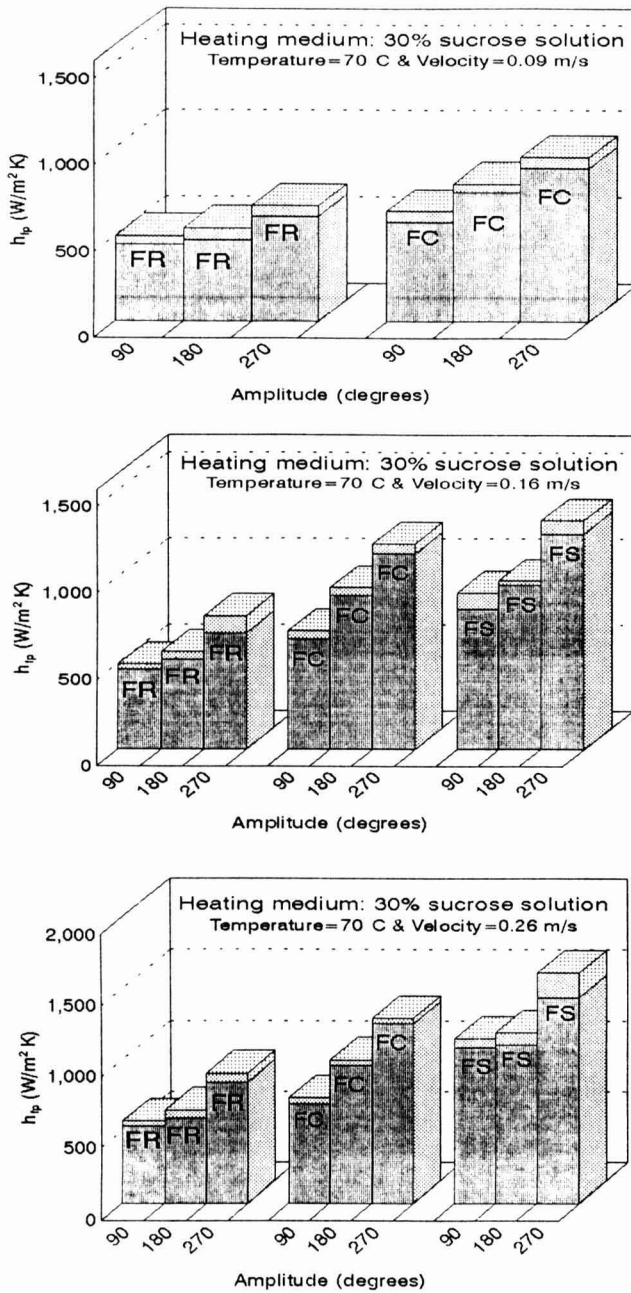
FIG. 4. EFFECT OF OSCILLATION AMPLITUDE ON h_{fp} VALUES IN 30% SUCROSE SOLUTION AT 70C FOR FREE PARTICLE (FR), FIXED AT THE CENTER (FC) AND FIXED AT THE SURFACE (FS) FOR DIFFERENT AMPLITUDE AND VELOCITIES

intermediate value of 0.16 m/s is for 6 rpm at 0.25 m or 10 rpm at 0.15 m. For the "free" particle, these should be taken as "nominal" values because it was observed that the particle remained "stationary" for a portion of the oscillatory motion as the tube changed the direction of oscillation. During this "stationary phase", the tube actually slid below the particle until the free-lead distance of the thermocouple wire (about one half of the tube length) is covered by the oscillation. As can be seen from Fig. 4, the values of h_{fp} consistently increased with the amplitude of oscillation at each condition (with a steeper change at 270°). With the free particle, the increase in h_{fp} was about 40% and with the fixed particle the increase was 50 to 100%. With the fixed particle, this increase in h_{fp} is ascribed to a longer exposure of the particle to steady flow conditions at higher amplitudes. With the free particles, this is consistent with the shift of the particle flow behavior from "stationary" toward "moving" (dragging situation) as the amplitude of oscillation is increased. With the 90° amplitude the particle remained "stationary" for about 50% of the oscillation time, while at 180° and 270° amplitudes the stationary phase accounted for 30% and 20%, respectively.

Effect of Temperature and Viscosity on h_{fp}

The effect of temperature on the associated h_{fp} in 30 and 50% sucrose solutions at an oscillation velocity of 0.26 m/s are shown in Fig. 5. A similar plot was also obtained at the other velocity of 0.16 m/s. With the fixed particle, the associated h_{fp} values at 90C were clearly higher than at 70C. Although a similar trend also existed with the free particles, the difference in h_{fp} between the two temperatures was much smaller. As will be further evident from the discussion of viscosity effects detailed below, this higher value of h_{fp} could be due to lower viscosities associated with the heating medium at higher temperatures.

The average values of h_{fp} and their standard deviations as influenced by the sucrose concentration (0, 30 and 50%) are shown in Fig. 6 at two velocities (0.16 and 0.26 m/s) while the medium temperature was maintained at 70C and the amplitude of the oscillation was fixed at 90°. Values of h_{fp} for the free particle varied from 590 ± 35 W/m²K in water to 440 ± 33 W/m²K in 50% sucrose solution with 30% sucrose giving intermediate values. For the particle fixed along the central axis, the values were 850 ± 53 W/m²K in water and 560 ± 57 W/m²K in 50% sucrose solution, again with intermediate values with 30% sucrose solution. The values of h_{fp} decreased with sucrose concentration for both fixed and free particles. This was expected because of increasing the viscosity of the medium at higher sucrose concentration. A lower value of h_{fp} has been reported by several of researchers for the more viscous fluid. Lenz and Lund (1978) found significantly lower h_{fp} for particle processed in a 60%

aqueous sucrose solution than for solids processed in water. Chandarana *et al.* (1989) noticed that heat transfer coefficient values were larger in water when it passed over solid particles than in high viscous fluid under the same condition.
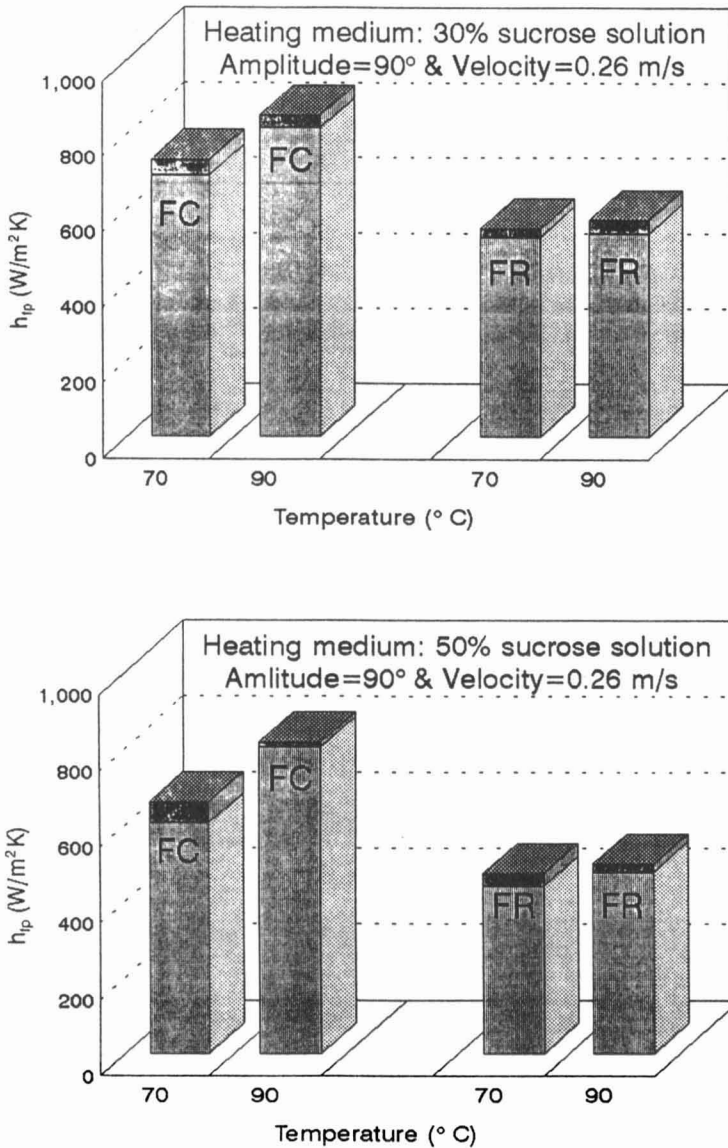
FIG. 5. EFFECT OF TEMPERATURE ON h_{fp} VALUES IN 30% SUCROSE SOLUTION FOR FREE PARTICLE (FR) AND PARTICLE FIXED AT THE CENTER (FC)
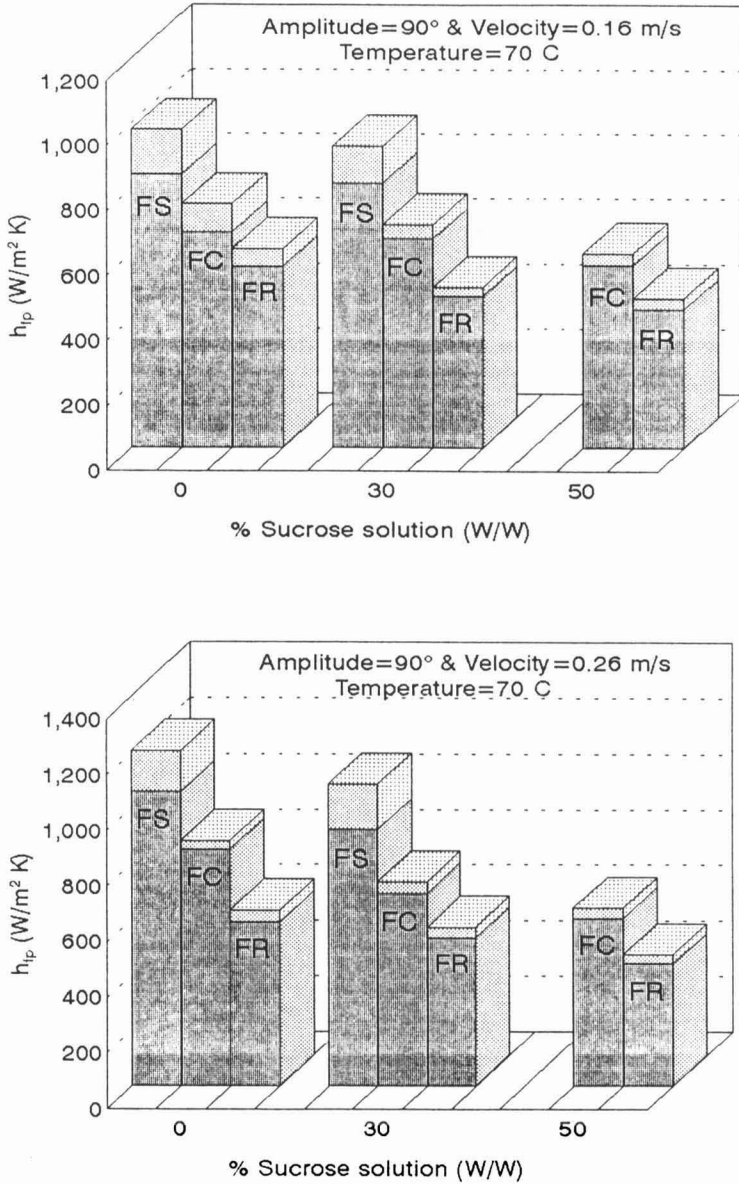
FIG. 6. EFFECT OF THE VISCOSITY ON h_{fp} VALUES FOR FREE PARTICLE (FR), AND
PARTICLE FIXED AT THE CENTER (FC) AND AT THE SURFACE (FS) AT 70C AND
DIFFERENT VELOCITIES

Also Zuritz *et al.* (1990), Gaze *et al.* (1990) as well as Dutta and Sastry (1990) confirmed the same trend. The higher viscosity of the fluid in which the particulate is immersed, hampers heat transfer, at least where the lower turbulence decreases the effective relative particle-to-fluid velocity at the interface.

Effect of Velocity (Particle Oscillation Frequency) on h_{fp}

To evaluate the effect of the particle velocity on h_{fp}, experiments were carried out at two rotation speeds (6 and 10 rpm) and different radial distances (0.15 and 0.25 m) giving three different linear velocities for the particles depending on their position (0.09, 0.16 and 0.26 m/s; the combination of 10 rpm at 0.15 m radial distance giving the same linear velocity of 0.16 m/s as 6 rpm at 0.25 m). As noted before, these values apply mainly to the relative velocity of the fixed particle. Since the free particles remain stationary for periods ranging from 20 to 50% of the oscillation time, the velocities indicated should only be considered as "nominal". A detailed analysis will be performed while quantifying the effect of the "velocity" component of the "free" particle. In this study, the free particles would have a relative velocity 20 to 50% lower than their fixed counterparts. In Fig. 7, data on means and standard deviations of heat transfer coefficient values are shown as influenced by linear velocity of the particles in water (0% sucrose) and 30% sucrose solution, respectively. Medium temperature was kept constant at 70C and the amplitude of oscillation was again fixed at 90°. The h_{fp} values were found to increase by increasing the particle velocity. Overall, a three fold increase in velocity (from 0.09 to 0.26 m/s) increased the h_{fp} value by a factor of 1.15 for the free particle, 1.25 for the particle fixed in the center and 1.75 for the particle fixed at the surface. The increase in h_{fp} for the "free" particle are in the range of values observed by Sastry *et al.* (1989 and 1990) in study of h_{fp} using the moving thermocouple method. Up to 150% increase in h_{fp} values were also reported for stationary particle by increasing the relative velocity almost three times (Maesmans *et al.* 1992).

Comparison of h_{fp} for "Fixed" Versus "Free" Particle

The difference in associated h_{fp} values between free and fixed particles can be seen in Fig. 4-7 (also Tables 2 and 3) under various conditions. Overall, it was observed that the fluid to particle convective heat transfer coefficient was always higher for the fixed particles than that for the free particles. The differences in h_{fp} values between free and fixed particles were about 20% on the lower side and 100% on the higher side probably because of the higher fluid-to-particle relative velocity associated with fixed particle situations. This is an important observation which needs further investigation and may have
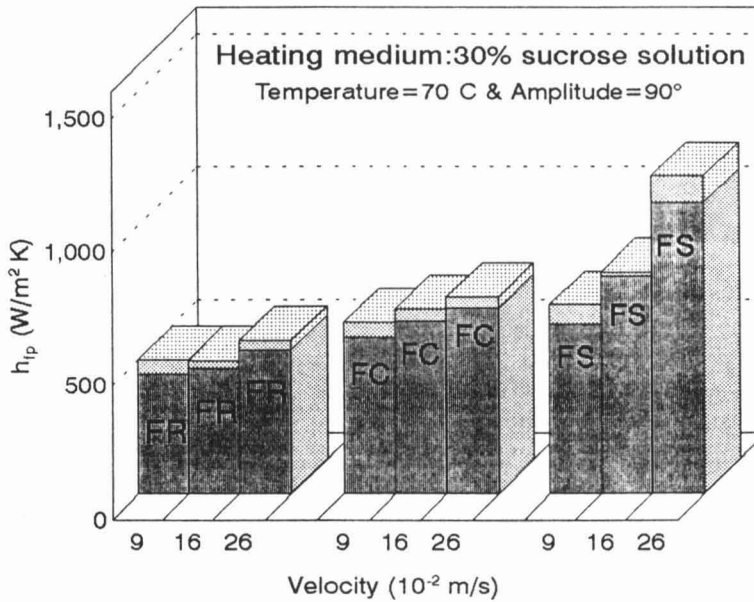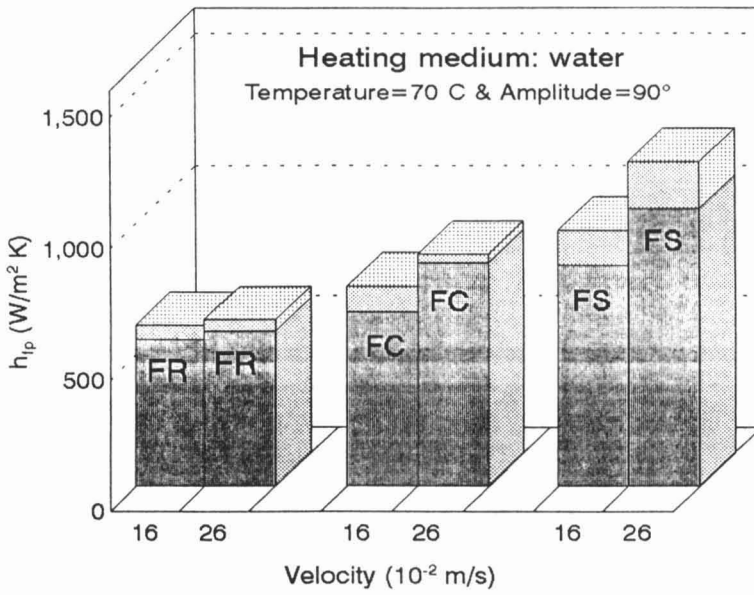
FIG. 7. EFFECT OF THE PARTICLE VELOCITY ON h_{fp} VALUES FOR THE FREE
PARTICLE (FR), AND PARTICLE FIXED AT THE CENTER (FC) AND AT THE
SURFACE (FS) IN WATER AS WELL AS 30% SUCROSE SOLUTION AT 70C

implications with respect to studies involving heat transfer coefficients evaluated with fixed particles which would overestimate the h_{fp} values although carried at comparable fluid-to-particle relative velocities.

Comparison of h_{fp} of Fixed Particle: Center Versus Surface Location

The differences in the associated h_{fp} values between a particle fixed at the central axis versus that at the bottom surface can be observed in Fig. 4-7. In general, the h_{fp} values associated with the particle at the surface are relatively higher than that at the center. Although this may appear, at first, to be contradictory to common knowledge, it can be explained. The fixed particle at the center will have symmetrical fluid flow behavior around the particle, and hence would face a fluid of relatively "smooth" or less "turbulent" flow regime. The particle fixed along the surface would face a fluid stream of considerably varying velocity profiles trying to pass through the narrow clearance between the spherical particle and the tube surface thereby creating "rough" or more "turbulent" flow conditions which would result in an enhanced heat transfer. Free particles under such conditions would also tend to roll (which is somewhat restricted in the present set-up because of attachment of thermocouples) which could also result in an enhanced heat transfer.

CONCLUSIONS

Interest in the aseptic processing of particulate foods demands measurement of fluid-to-particle heat transfer coefficient (h_{fp}). An oscillatory approach was used to impart motion to particles in a model holding tube immersed in an appropriate heating medium while allowing time-temperature data gathering and evaluation of heat transfer coefficient using conventional techniques. Evaluated heat transfer coefficients under different conditions confirmed the conventional trends of increasing with velocity and temperature, and decreasing with fluid viscosity. Further, it was observed that the h_{fp} values for the fixed particle could be about 20-100% higher than that for the free particles depending on the experimental condition. This implies that the h_{fp} values determined using a stationary particle in a moving fluid as employed in several studies situation may not be conservative.

The experimental set-up designed permits easier investigation of the effect of several parameters affecting h_{fp} because of the better control on factors such as particle velocity and particle location inside the tube. Easy maintenance of a stable medium temperature and ability of using opaque medium/tube are added advantages of oscillatory method. Use of conventional thermocouple approach to obtain the temperature history makes the gathered data more authentic than from other indirect methods.

NOMENCLATURE

a   Radius of sphere (m)
Bi   Biot number (h_{fp} a/k)
C_p Heat capacity (J/kg °K)
d   Particle diameter (m)
D   Inside tube diameter (m)
f_h Negative reciprocal slope of the straight line portion of the heating curve on semi-log coordinate (heating rate index) (s)
Fo   Fourier number ($\alpha t/a^2$)
h_{fp} Fluid-to-particle heat transfer coefficient (W/m² K)
ID   Inside tube diameter (m)
k   Thermal conductivity (W/m K)
k_f Thermal conductivity of the fluid (W/m K)
Nu   Nusselt number (h_{fp} d/k_f)
n   Number of revolution per minute (rpm)
r   Position along radius of a sphere ($0 \leq r \leq a$) (m)
R   Position of the particle from the center of rotation (m)
Re   Reynold number (ρVd / μ)
t   Heating or cooling time (s)
T_a Ambient temperature (°C)
T_i Initial temperature (°C)
T_f Fluid or medium temperature
T_p Particle temperature
U   Dimensionless temperature ratio ((T_a -T)/(T_a -T_i))
V   Linear particle velocity (m/s)
α Thermal diffusivity (m²/s)
δ Root of the characteristic equation
ρ Density (kg/m³)
μ Viscosity (kg/m.s)
ω Angular velocity (2πn)

REFERENCES

AWUAH, G.B. and RAMASWAMY, H.S. 1996. Dimensionless correlations for mixed and forced convection heat transfer to spherical and finite cylindrical particles in an aseptic processing holding tube simulator. J. Food Process Engineering, *19*(3), 269–287.

AWUAH, G.B., RAMASWAMY, H.S. and SIMPSON, B.K. 1995. Comparison of two methods for evaluating fluid-to-surface heat transfer coefficients. Food Res. Int. *28*(3), 261–271.

BALASUBRAMANIAM, V.M. and SASTRY, S.K. 1994a. Convective heat transfer at particle-liquid interface in continuous tube flow at elevated fluid temperatures. J. Food Sci. 59(3), 675–681.

BALASUBRAMANIAM, V.M. and SASTRY, S.K. 1994b. Liquid-to-particle convective heat transfer in non-newtonian carrier medium during continuous tube flow. J. Food Eng. 23, 169–187.

BALASUBRAMANIAM, V.M. and SASTRY, S.K. 1995. Use of liquid crystal as temperature sensors in food processing research. J. Food Eng. 26, 219–230.

BALASUBRAMANIAM, V.M. and SASTRY, S.K. 1996a. Fluid to particle convective heat transfer coefficient in a horizontal scraped surface heat exchanger determined from relative velocity measurement. J. Food Process Engineering 19, 75–95.

BALASUBRAMANIAM, V.M. and SASTRY, S.K. 1996b. Estimation of convective heat transfer between fluid and particle in continuous flow using remote temperature sensor. J. Food Process Engineering 19, 223–240.

BHAMIDIPATI, S. and SINGH, R.K. 1995. Determination of fluid-particle convective heat transfer coefficient. Trans. ASAE 38 (3), 857–862.

CARSLAW, H.S. and JAEGER, J.C. 1959. Conduction of Heat in Solids. 2nd Ed. Oxford University. Press. London, England.

CHANDARANA, D.I. and GAVIN, A. III. 1989a. Modeling and heat transfer studies of heterogeneous foods processed aseptically. In Innovations in Aseptic Processing of Particulate. (J.V. Chambers, ed.) 1st Int. congress on aseptic processing technologies. March 19-21, Indianapolis, IN.

CHANDARANA, D.I. and GAVIN, A. III. 1989b. Establishing thermal process for heterogenous foods to be processed aseptically: a theoretical comparison of process development methods. J. Food Sci. 54, 198–204.

CHANDARANA, D.I., GAVIN, A. III and WHEATON, F.W. 1989. Simulation of parameters for modelling of aseptic processing of food containing particulate. Food Technol. 43 (3), 137–143.

CHANDARANA, D.I., GAVIN, A. III and WHEATON, F.W. 1990. Particle/fluid interface heat transfer under UHT conditions at low particle/fluid relative velocity. J. Food Process Engineering 13, 191–206.

CHANG, S.Y. and TOLEDO, R.T. 1990. Simultaneous determination of thermal diffusivity and heat transfer coefficient during sterilization of carrot dices in a packed bed. J. Food Sci. 55, 199–205.

CHAU, K.V. and SYNDER, G.V. 1988. Mathematical model for temperature distribution of thermally processed shrimp. Trans. ASAE. 31, 608–612.

DE RUYTER, P.W. and BRUNET, R. 1973. Estimation of process conditions for continuous sterilization of foods containing particles. Food Technol. 27(7), 44–51.

DIGNAN, D.M., BERRY, M.R., PFLUG, I.J. and GARDINE, T.D. 1989. Safety considerations in establishing aseptic processing for low-acid foods containing particulate. Food Technol. *43* (3), 118–121, 131.

DUTTA, B. and SASTRY, S.K. 1990. Velocity distribution of food particle suspensions in holding tube flow: Distribution characteristics of and fastest-particle velocities. J. Food Sci. *55*, 1703–1710.

GAZE, J.E., SEENCE, L.E., BROWN, C.D. and HOLDSWORTH, S.D. 1990. Microbiological assessment of process lethality using food alginate particles. pp. 1–47, Tech. Memo. No. 580. Camden Food and Drink Research Assoc. Chipping Campend.

HEISLER, M.P. 1947. Temperature charts for induction and constant temperature heating. Trans. ASME. *69*, 227–236.

HELDMAN, D.R. 1989. Establishing aseptic processing for low-acid foods containing particulate. Food Technol. *43*(3), 122–125.

KELLY, B.P., MAGEE, T.R.A. and AHMAD, M.N. 1995. Convective heat transfer in open channel flow: effect of geometric shape and flow characteristics. Trans IChem. *73*, part C.

LARKIN, J.W. 1990. Mathematical analysis of critical parameters in aseptic particulate processing systems. J. Food Process Engineering *13*, 155–167.

LENZ, M.K. and LUND, D.B. 1978. The lethality-Fourier number method. Heating rate variations and lethality confidence intervals for forced-convection heated foods in containers. J. Food Process Engineering *2*, 227–271.

LUIKOV, A.V. 1968. Analytical heat diffusion theory. Academic Press, New York.

MAESMANS, G., HENDRICKX, M., DECORDT, S., FRANSIS, A. and TOBBACK, P. 1992. Fluid-to-particle heat transfer coefficient determination of heterogeneous foods: A review. J. Food Processing and Preservation *16*, 29–69.

MANSON, J.E. and CULLEN, J.F. 1974. Thermal process simulation for aseptic processing of food containing discrete particulate matter. J. Food Sci. *39*, 1084–1089.

SABLANI, S.S. and RAMASWAMY, H.S. 1995. Fluid-to-particle heat transfer coefficients in cans during end-over-end processing. Lebensm-Wiss. u.-Technol. *28*, 56–61.

SABLANI, S.S. and RAMASWAMY, H.S. 1996. Particle heat transfer coefficients under various retort operating conditions with end-over-end rotation. J. Food Process Engineering *19*, 403–424.

SASTRY, S.K. 1986. Mathematical evaluation of process schedules for aseptic processing of low-acid foods containing discrete particulate. J. Food Sci. *51*, 1323–1328, 1332.

SASTRY, S.K., HESKITT, B.F and BLASIDEL, J.L. 1989. Convective heat transfer at particle-liquid interface in aseptic processing system. Food Technol. *43* (3), 132–136, 143.

SASTRY, S.K., LIMA, M., BRIM, J., BRUNN, T. and HESKITT, B.F. 1990. Liquid-to-particle heat transfer during continuous tube flow: influence of flow rate and particle to tube diameter ratio. J. Food Process Engineering *13*, 239–253.

STOFOROS, N.G. and MERSON, R.L. 1991. Measurement of heat transfer coefficient in rotating liquid/particulate system. Biotechnol. Prog. *7*, 267–271.

WENG, Z., HENDRICKX, M., MAESMANS, G. and TOBBACK, P. 1992. The use of time-temperature integrator in conjunction with mathematical modeling for determining liquid/particle heat transfer coefficients. J. Food Eng. *16*, 197–214.

ZITOUN, K.B. and SASTRY, S.K. 1994a. Determination of convective heat transfer coefficient between fluid and cubic particles in continuous tube flow using noninvasive experimental techniques. J. Food Process Engineering *17*, 209–228.

ZITOUN, K.B. and SASTRY, S.K. 1994b. Convection heat transfer coefficient for cubic particles in continuous tube flow using the moving thermocouple method. J. Food Process Engineering *17*, 229–241.

ZURITZ, C.A., MCCOY, S. and SASTRY, S.K. 1990. Convection heat transfer coefficients for irregular particles immersed in non-newtonian fluids during tube flow. J. Food Eng. *11*, 159–174.

MEASUREMENT AND PREDICTION OF THE PRESSURE DROP INSIDE A PIPE: THE CASE OF A MODEL FOOD SUSPENSION WITH A NEWTONIAN PHASE

L.P. MARTÍNEZ-PADILLA[1], A.C. ARZATE-LÓPEZ and
V.A. DELGADO-REYES

Laboratorio de Propiedades Reológicas y Funcionales en Alimentos
Universidad Nacional Autónoma de México. FES-Cuautitlán

AND

G.V. BARBOSA-CÁNOVAS

Biological Systems Engineering Department
Washington State University

ABSTRACT

The aim of this study was to measure the pressure drops of a solid-liquid food model and to compare pressure drop estimations obtained from proposed correlations for asymmetric distributed suspensions in a horizontal pipe. The model food suspension consisted of alginate spheres suspended in a Newtonian sugar syrup of medium viscosity. The suspension was pumped into a horizontal pipe and measurements for three different sphere diameters and solid-phase concentrations were carried out. Particle velocity, necessary for pressure drop estimations, was predicted using the Eulerian approach, which assumed solid and liquid phases as continuous. Considerations taken were: one dimensional flow of fluid and particles, drag force acting on the particles and constant pressure drop. The momentum equations were solved by the fourth order Runge-Kutta method. Predicted particle velocities showed a retarded parabolic profile compared to the fluid. Drag expressions used, considerably influenced the predicted particle velocities. Estimated pressure drops for the suspensions using the predicted particle velocities agreed with the experimental pressure drops when the tube-particle diameter ratio was higher than 5.8.

[1] To whom correspondence should be addressed, FES- Cuautitlán, UNAM, Departamento de Ingeniería y Tecnología, Lapryfal, Av. Primero de mayo s.n., 54740 Cuautitlán Izcalli. Edo. de México. México, e-mail: lpmp@servidor.unam.mx

INTRODUCTION

Knowledge of the flow behavior of foods with large particles in horizontal pipes is important in the food industry to estimate frictional pressure drop during the pumping process, as well as to offer consumers good products with uniform solid-fluid ratios. The literature on solid-liquid flow in pipes concerning the transport of slurries, suspensions, and isolated particles in chemical engineering applications is extensive. There are many studies which apply to the turbulent flow regime; nonorganic particles such as sand, clay, magnetite, lime, bentonite, and glass; Newtonian fluids and small particles ($d_p < 4 \times 10^{-3}$ m) (Turian *et al.* 1971; Zandi 1971; Govier and Aziz 1972; Jinescu 1974).

In the food industry, a number of commercial products consists of large size particles in a Newtonian or non-Newtonian carrier fluid. According to the physical properties of commercial suspensions these solid-fluid mixtures can be classified into three groups (Table 1). Considerations taken for this grouping are the flow behavior of the carrier fluid, and particle size and shape. Group I and III have the same shape, but different behavior of the carrier fluid. Group II and III have the same non-Newtonian carrier fluid; however, the number of particles in Group II is higher than in Group III, due to the small particle volume fraction. In operating processes, such mixtures generally exhibit viscous laminar flow. Suspensions corresponding to these groups are usually pumped with the coarse particles before the canning or packaging process. However, a calculation method for pressure drop estimations when these suspensions are flowing in a straight pipe is not available in food engineering literature.

One method of pressure drop estimation in horizontal pipes is the evaluation of rheological parameters of the whole suspension. Conventional viscometer techniques can be employed to obtain shear viscosity, power law parameters or shear time dependence when the solid-liquid mixtures are homogeneous, including fine particles, and no electrostatic effects. These rheological parameters allow calculation of the Reynolds number or generalized Reynolds number and the Fanning friction factor, needed for the pressure drop estimations.

Numerous studies concerning the rheological behavior of juices, purees and sauces with small particles have been reviewed (maximum size about 4×10^{-4} m) (Holdsworth 1971; Rao 1986). Nevertheless, few studies including large particles have been reported. The large diameter tube viscometers can be utilized in obtaining rheological parameters of food mixtures containing coarse particles (Bhamidipati and Singh 1990; Tucker and Withers 1994). In this case, it is important to know the velocity conditions, as well as the length when considering the laminar flow as pseudo-homogeneous. Symmetric concentration of the suspensions with particles is required (Skelland 1967; Govier and Aziz 1972). In the case of the Newtonian carrier fluid (Group I, Table 1), it is not evident

that the symmetric distributed concentration can be observed; therefore, the use of tube viscometer principles is not recommended. However, the principles of fluid flow are still applicable.

TABLE 1.

CLASSIFICATION AND EXAMPLES OF SOLID FOOD- FLUID MIXTURES

GROUP	FLUID	SOLID	TYPICAL FOODS
I	Newtonian $0.002<\eta<0.025$ Pa.s	spheres cubes $0.001<d_p<0.008m$	Fruit preserves: blueberry, raspberry, cherry. pineapple. peach. mango, grape.
II	Thixotropic and Power law $0.15<n<0.8$ $0.2<K<15$ Pa.s^n	discs spheres $0.001<d_p<0.005m$	Mexican sauces with seeds. Mustard with seeds. Preserves with seeds.
III	Thixotropic and Power law $0.15<n<0.8$ $0.2<K<15$ Pa.s^n	spheres cubes $0.001<d_p<0.008m$	Concentrated cream soups: pea, carrot, potato.

If asymmetric concentration is present, empirical adimensional equations can be applied to fully describe suspended liquid-solid systems behavior. Some chemical engineering pressure drop correlations can be used to make such predictions, but they have not proven to be useful for conditions present in the food industry. Durand (1953) proposed a series of correlations obtained by a variety of sands and gravel in horizontal pipes utilized to estimate the pressure gradient of coarse solid-liquid mixtures. In order to make such estimates, particle and fluid velocities (slip velocity) are necessary. The fluid velocity can be taken as the measured velocity for the whole suspension (Govier and Aziz 1972). The velocity of coarse particles has been studied by several authors in thermal treatment applications (Sastry and Zuritz 1987). The maximum velocity along the center line (particle or fluid) of the tube is necessary to determine the minimum fluid residence time.

Some residence time determinations in fluid with coarse particles have been reported. The use of visual detectors, video-recorders, and magnetic photosensors has been suggested to measure particle velocity. Nevertheless, there is no standard technique employed and contradictory results were reported. For example, experimental results obtained by videorecording, showed that the fastest particles of polystyrene were below the theoretical centerline velocities

for non-Newtonian fluids (CMC dispersions, $D/d_p = 4.9$), but were above the average fluid velocity (Dutta and Sastry 1990). Similar results were observed for cubes (0.008 m diced carrot, 3.25-11.85% w/w, $D/l = 5.9$) in non-Newtonian fluids. It was also found that the velocity of the fastest moving particle was less than the mean flow velocity. In contrast, using a higher particle diameter (0.015 m $D/l = 3.1$), it was observed in some trials that particles traveled faster than the fluid velocity (Tucker and Withers 1994). In addition, the volumetric flow rate cannot be accurately metered using conventional flowmeters (Tucker and Withers 1994).

Mathematical modeling could be regarded as an option to predict the velocity of the particles. Some works, based in Eulerian and Lagrangian methods (Durts *et al.* 1984), have been proposed. In the Eulerian approach, solid and liquid phases are considered to be continuous. In the Lagrangian approach, the particle velocities are predicted as a result of forces acting on them, and the fluid is considered a continuous phase. In both cases the buoyancy and drag forces are taken into account. The buoyancy force is considered in vertical flow, while the drag force is included due to the movement of solids in a liquid medium. The drag on a falling sphere has been considered, and the drag coefficient was estimated in the transition from laminar to turbulent regime flow. Both approaches predicted the same back-influence on the particles in the fluid, compared to fluid velocity. However, only turbulent flow examples were simulated (Durts *et al.* 1984).

Sastry *et al.* (1989), applying the Lagrangian approach, added Magnus (sphere spinning with an angular velocity) and Saffman (inertial effects near the sphere) lift forces acting on the particles. Linear and angular momentum equations were solved for three dimensions. Recently, Liu and Zuritz (1995) using the same approach for a Newtonian fluid (0.10 Pa.s, $D/dp = 5.1$, $Re_f = 150$, 10% v/v), predicted particle velocities in a conventional holding tube for continuous sterilization. They proposed one dimensional flow (axial) in the first straight tube where the particle had a negligible influence on the velocity profile. In this case, the calculated particle velocity was the same as the fluid velocity in axial direction. This suggested that the drag force is the only force acting on the particle in a straight tube, but these results did not agree with reported experimental particle velocities in Newtonian carrier fluids (Durts *et al.* 1984) and non-Newtonian carrier fluids (Dutta and Sastry 1990; Tucker and Withers 1994).

The objective of this study was to measure the pressure drop of a model food suspension with a Newtonian carrier fluid and to compare the pressure drop estimated from proposed correlations for the flow of solid-fluid mixtures with asymmetric distributed concentration. Particle velocity, necessary for pressure drop estimations, was obtained solving the momentum equations applying the Eulerian approach.

This approach includes the momentum equations for each phase, considering the drag force acting on the particle in the respective equation; one dimensional flow of the fluid and particles, and constant pressure drop of the suspension. In the mathematical solution, two expressions of drag coefficient in unsteady state flow were used (Allen 1900; Clift and Gauvin 1971). A slip velocity was obtained for each expression, and it was introduced in Durand (1953) relationships to compute predictions of pressure drop in a horizontal pipe. Values of experimental gradient of pressure were compared to the pressure drop estimated in the suspensions under evaluation.

Mathematical Model

Particle velocity was predicted using the Eulerian approach, considering particles and fluid phases as continuous (Durts *et al.* 1984). The momentum equations were solved assuming the following conditions: (1) the fluid flow was fully developed and moving in one dimension; (2) the particles moved in axial flow; (3) a constant suspension pressure drop was considered; and (4) only drag force acted on the particles (Sastry *et al.* 1989).

The momentum balance equations for each phase (particle and fluid respectively) are:

$$\alpha \rho_p \frac{dV_{pz}}{dt} = -\alpha \frac{dP_s}{dz} - \alpha \left(\frac{1}{r} \frac{d}{dr}(r\tau_{rz}) \right) + \alpha \sum \frac{F}{m_p} \tag{1}$$

$$\beta \rho_f \frac{dV_{fz}}{dt} = -\beta \frac{dP_s}{dz} - \beta \left(\frac{1}{r} \frac{d}{dr}(r\tau_{rz}) \right) \tag{2}$$

Equation (1), refers to the dispersed phase, and includes drag force acting on the particle. The algebraic sum of Eq. (1) and (2) gives the velocity of the suspension as a whole. For steady state and laminar flow, the shear stress or momentum flux (τ_{rz}) is defined in the classical expression given by Bird *et al.* (1960):

$$\tau_{rz} = \frac{r\Delta P_s}{2L} \tag{3}$$

This expression is valid in both equations because particle acceleration is not taken into account in systems at steady state. Therefore, the resultant force acting on the particle must be zero. Substituting Eq. (3) into the algebraic sum of Eq. (1) and (2), and solving for dV_{pz}/dt:

$$\frac{dV_{pz}}{dt} = -\frac{3\Delta P_s}{2\alpha \rho_p L} - \frac{\beta \rho_f}{\alpha \rho_p} \left(\frac{dV_{fz}}{dt} \right) + \frac{F_D}{v_p \rho_p} \tag{4}$$

It was assumed that the fluid phase would reach steady state before the solid-phase steady state, and for Newtonian fluids the term dV_{fz}/dt can be expressed as (Bird *et al.* 1960):

$$\left(\frac{dV_{fz}}{dt}\right) = 2\bar{V}f\left(1-\frac{r}{R}\right)^2 \tag{5}$$

Suspension pressure drops, needed for the solution, can be experimentally evaluated or estimated if the suspension viscosity is known, using the Fanning friction factor (f):

$$\frac{\Delta P_s}{L} = \frac{4f\rho_s\bar{V}s}{2D} \tag{6}$$

which in laminar flow is:

$$f = \frac{16}{Re_s} = \frac{16\eta_s}{D\rho_s\bar{V}s} \tag{7}$$

The drag force per unit mass is given by Newton's law of motion for a particle in a fluid (Eq. (8)). In this case, the drag force is acting in the opposite direction of the particle motion. In order to calculate the drag force, a drag coefficient (C_D) is needed.

$$\frac{F_D}{v_p\rho_p} = \frac{3}{4}C_D\frac{\rho_f}{\rho_p d_p}|V_{pz}-V_{fz}|(V_{fz}-V_{pz}) \tag{8}$$

Measurements of fluid drag, or particle motion have often been confusing and sometimes contradictory (Clift and Gauvin 1971). Several expressions for C_D, based on the motion of a simple sphere in a uniform flow, have been proposed for the transitional flow (Allen 1900; Dallavalle 1948; Lawler and Lu 1971; Clift and Gauvin 1971). Equation (9), as proposed by Clift and Gauvin (1971), and Eq. (10), presented by Allen (1900) are shown below. The first one includes C_D derived from the theoretical analysis of Stokes ($C_D = 24/Re_p$) and predicts the lowest C_D coefficients in the range of interest of this study. The second equation gives a linear approximation in the logarithmic plot and predicts the highest C_D coefficients.

$$C_D = \frac{24}{Re_p}(1+0.15Re_p^{0.687}) \tag{9}$$

$$C_D = 30Re_p^{-0.625} \tag{10}$$

All of these relationships are a function of the particle Reynolds number that is defined as:

$$Re_p = \frac{\rho_f d_p |V_f - V_p|}{\eta_f} \tag{11}$$

Both C_D relationships were used in the mathematical model proposed. The fourth order Runge-Kutta method was applied to solve Eq. (4), and two predicted particle velocities were obtained. Figure 1 shows the sequence of computation for the method proposed. When results of particle velocity were obtained, the average velocity was evaluated by:

$$\bar{V}_p = \frac{1}{\pi R^2} \int_0^R 2\pi V_{pz} r dr \tag{12}$$

where:

$$V_{pz} = a + b\frac{r}{R} + c\left(\frac{r}{R}\right)^2 \tag{13}$$

Finally, the prediction of pressure drops for the heterogeneous flow of coarse particles suspended in a Newtonian fluid was calculated using the relationship proposed by Durand (1953) (Eq. (14)). The tube diameter and physical properties, fluid and particle densities and particle diameter, are the values needed for such estimations. The fluid pressure drops (without particles) was also required and can be evaluated using the viscosity and density of the fluid (Eq. (6) and (7)). It was assumed that the fluid velocity was the same than the measured suspension velocity, and the average particle velocity was evaluated from the resulting particle profile velocity obtained by simulation (Eq. (12) and (13)). There has been considerable discussion regarding the value of the two constants K and m in Eq. (14). In this study, parameters of the Durand (1953) modified equation corresponding to proportionally constant $K = 100$ and exponent $m = 1.3$ were taken from Hayden and Stelson (1968) since they gave the best predictions.

$$\frac{\Delta P_s - \Delta P_f}{\alpha \Delta P_f} = K\left[\frac{gD(\rho_f / \rho_p - 1)}{\bar{V}_f^2}\right]\left[\frac{\bar{V}_f - \bar{V}_p}{\sqrt{gd_p(\rho_f/\rho_p - 1)}}\right]^m \tag{14}$$
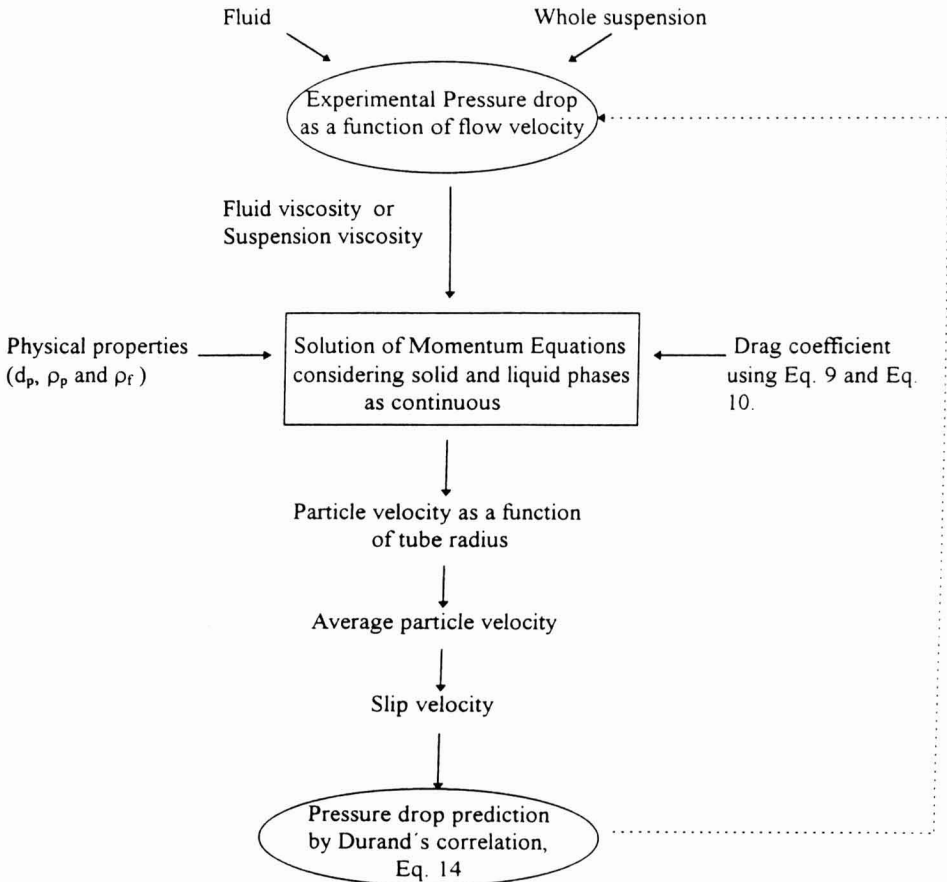
FIG. 1. SEQUENCE OF COMPUTATION FOR THE METHOD PROPOSED

MATERIALS AND METHODS

Physical properties of several commercial food suspensions were evaluated. A suspension of sodium alginate spheres in a sugar syrup (37°Bx) was used to imitate blueberry fruit preserves, which is a typical food suspension with a Newtonian carrier fluid (Group I, Table 1). The physical properties taken into account to prepare the model food were: fluid and particle density, fluid viscosity, and particle size and shape.

Spheres were prepared by extrusion of a sodium alginate mixture in acid media (Davidson 1980), and the particles were colored red and dark blue to ease the observations. The selected diameters were 0.004, 0.006 and 0.008 m, and volume fractions studied were 0.118, 0.169 and 0.218. The alginate spheres were chosen because they have a similar consistency to blueberry particles, and through a transparent tube it was easy to observe if they were destroyed by the system at different handled speeds.

Coarse suspensions need a large pipe diameter to avoid particle damage. A concentration near 38% w/w, found in commercial samples, could not be handled in the 0.035 m pipe diameter in the pilot plant flow system because the number of particles was larger than the 100% maximum allowed. The maximum number of particles flowing in the tube was calculated, adding 50% of the diameter of each particle studied.

Density of the continuous phase was measured by picnometry, while the particle densities were determined by liquid displacement techniques (Koichi et al. 1991). Shear viscosity of the fluid was measured in a rotational viscometer (Contraves-Mettler Rheomat 115; Mettler-Toledo A.G., Switzerland) in the shear range of 1 to 1008 1/s, using the Couette geometry with conical bottom cylinders; bob and cup radius of 0.0446 m and 0.0485 m (MS DIN 145), respectively.

A pilot plant pumping system, including a progressive cavity positive displacement pump (Sine pump model SPS-20, Div. Kontro Co., Orange, MA), and stainless steel pipe, 0.035 m internal diameter (1½ in.), was used (Fig. 2). The velocity was changed from 0.1 to 0.6 m/s with an electronic frequency driven speed control. An ultrasonic flowmeter was unsuccessful because a calibration for each suspension was needed, so the suspension flow was measured using a test tube (0.002 m³) and a stopwatch (0.01s accuracy). The suspensions (0.045 m³) were pumped at different flow rates at room temperature (21 ± 1C) and atmospheric pressure (548 mm Hg). The flow system was equipped with two transparent tubes to facilitate recording the suspension motion. Particle velocity in the center of the largest tube was measured through a length of 1.5 m using a stopwatch.

Because laminar and steady state flow conditions have to be assured, a long straight pipe is necessary before and after pressure drop sensors. The pressure drop of 4.5 m of horizontal tube (L/D = 128) was measured with two U-tube open manometers. The measurement points were located 2.1 m after a sudden contraction (L/D = 60) and 4.5 m (L/D = 128) before a 90° elbow. The flow was maintained laminar ($203 < Re_f < 1323$), and for each suspension ten different flow rates were tested using three replicates or more. Measurements of the continuous phase were carried out for comparison purposes. The main inconvenience of this kind of experiment was the use of considerably large samples.

SIMBOLOGY
PR-01 Piezometric ring
PR-02 Piezometric ring
PUM-01 SINE pump
TT-01 Transparent Pipe (Particle velocity meassures)
TT-02 Transparent Pipe (Videotaping)
TAN-01 Deposit Tank
TUB-01 Tube Viscometer
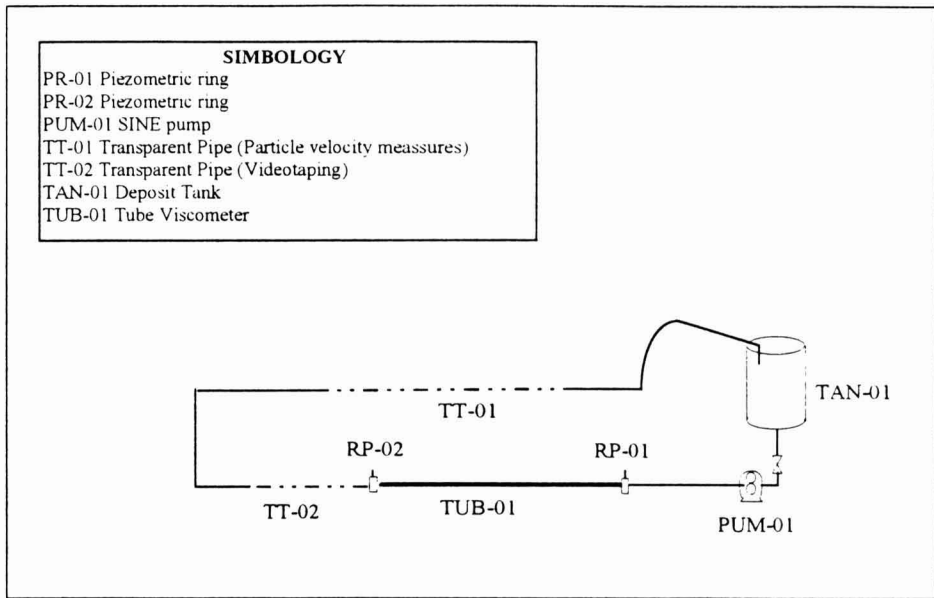
FIG. 2. SCHEMATIC DIAGRAM OF THE PILOT PLANT PUMPING SYSTEM

RESULTS AND DISCUSSION

The model was prepared based on the physical properties of the suspensions group I (Table 1) which had a Newtonian carrier fluid of intermediate viscosity, particle diameter of a few millimeters and similar relative density (particle/fluid). The average physical properties of commercial blueberry fruit preserves were: fluid density of 1082 kg/m^3 and fluid viscosity of 0.015 Pa.s. Blueberry densities were 1129, 1078 and 1074 kg/m^3 for the 0.004, 0.006 and 0.008 m diameters, respectively. These properties were used to select the characteristics of the proposed model food.

Fluid and particle properties of the model food suspension which are summarized below, were used in simulation of the particle velocity. The fluid density was 1158 kg/m^3, while the particle densities were 1091, 1111 and 1113 kg/m^3, for the 0.004, 0.006 and 0.008 m diameters, respectively. The syrup viscosity was 0.0153 Pa.s. The viscosity was enough to keep the laminar flow, but it was unable to maintain the particles in suspension; nevertheless, the particle density and the fluid density were very close.

In Fig. 3 the experimental average velocities of suspensions ($\bar{V}_f$), fluid (without particles) and particles are presented as a function of controlled pump velocity (V_c) for each diameter. The V_c was increased linearly. The volume pump discharge was decreased because the presence of the particles caused an increase of viscosity of solid-liquid mixtures. As expected the fluid alone showed the largest velocities, whereas the smallest velocity was obtained for the largest particle size. Particle velocities measured for the 0.004, 0.006 and 0.008m diameters did not show significant differences compared with the average suspension velocity. Hence, the experimental slip velocity could not be evaluated.

V (m/s)
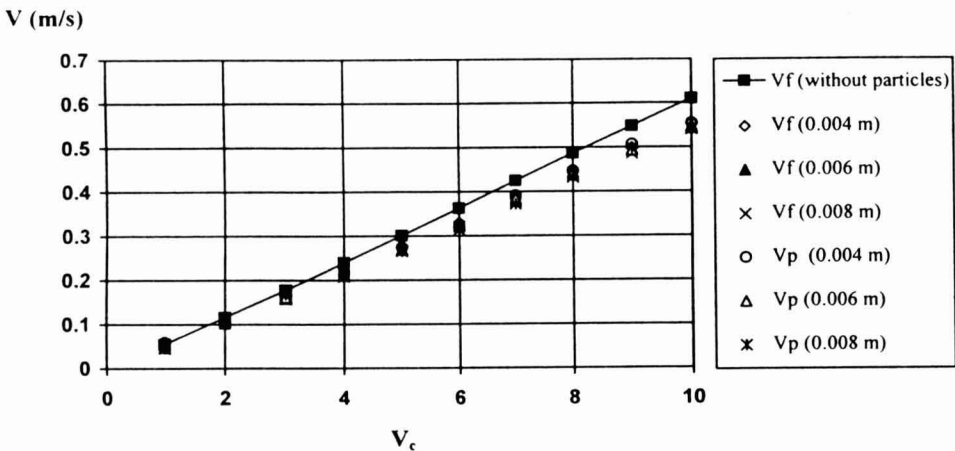
FIG. 3. AVERAGE FLUID ($\bar{V}_f$) AND PARTICLE ($\bar{V}_p$) VELOCITIES AS A FUNCTION OF CONTROLLED VELOCITY (V_c) FOR DIFFERENT SUSPENSION PARTICLE DIAMETER

In order to validate the measurements, fluid pressure drops evaluated in the pilot plant pumping system were compared with pressure drops estimates corresponding to viscosity measured in the rotational rheometer. In Fig. 4 experimental values for the suspension and fluid pressure drops are plotted as a function of V_f in logarithmic coordinates. These curves allow the identification of characteristic flow patterns encountered in the horizontal flow of liquid-solid and gas-solid mixtures (Govier and Aziz 1972). The moving bed pattern and the nonsymmetric suspension flow component were detected (dispersed values) in the studied velocity range. The classical parallel straight lines for the symmetric flow compared with the fluid pressure drops were not observed. However, an increase from 40% to 140% in the suspension pressure drops respect to the fluid pressure drops was observed. Critical velocities, where transition takes place

from one flow pattern to another, were unclear (Fig. 4), between 0.2 to 0.3 m/s
for all the studied suspensions. Videorecorded flows showed a laying bed
existing on the bottom of the pipe before reaching these critical velocities.
Nonrotation and nonsettling of particles were detected after reaching those
velocities.

ΔP/L (Pa/m)
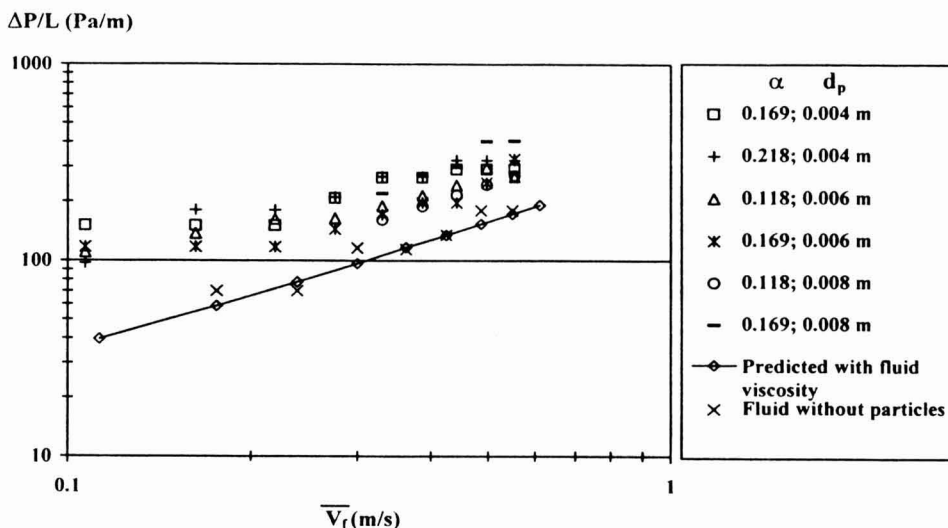
FIG. 4. EXPERIMENTAL VALUES OF SUSPENSION PRESSURE DROPS (ΔP/L) FOR
DIFFERENT SUSPENSION PARTICLE DIAMETERS (d_p) AND VOLUME FRACTIONS
(α) AS A FUNCTION OF AVERAGE FLUID VELOCITY ($\overline{V}_f$)

According to the proposed equations (Eq. 4, 6 and 7) the viscosity of the
suspensions is needed for the simulation of particle velocity. Pressure drop and
volumetric flow of the suspensions allowed the calculation of the apparent shear
viscosity using the Hagen-Poiseuille relationship ($27 < \dot{\gamma} < 130$ 1/s) at each
controlled velocity. Experimental apparent viscosity of suspensions ranged from
0.023 to 0.033 Pa.s, and they were considered as the average of the viscosity
at each velocity after passing the critical velocities. Standard deviation between
replicates ranged from 0.0025 to 0.0047 (Table 2).

These suspensions showed the same Newtonian behavior as the liquid
phase. This is due to the low interactions between particles. A change in the
rheological behavior (from Newtonian to non-Newtonian) was reported when the
number of particles exceeded a given value (critical concentration). Newtonian
behavior can be changed to shear thinning behavior when the particle concentra-

tion is increased, and shear thinning might be changed to thixotropic behavior. These flow behaviors have been justified as a result of particle interactions due to a hydrodynamic or an electrostatic nature of particles (Jinescu 1974).

TABLE 2.

SUSPENSION APPARENT VISCOSITY CALCULATED IN THE PIPE USING THE HAGEN-POISEUILLE LAW, AS A FUNCTION OF PARTICLE DIAMETER (d_p) AND VOLUME FRACTION (α). PREDICTED VISCOSITY ESTIMATE BY EINSTEIN'S OR HAPPEL'S THEORETICAL EQUATIONS

	d_p	0.004 m	0.004 m	0.006 m	0.006 m	0.008 m	0.008 m
Viscosity	α	0.169	0.218	0.118	0.169	0.118	0.169
Mean (Pa.s)		0.029	0.031	0.023	0.027	0.030	0.033
Standard deviation		0.0047	0.0038	0.0025	0.0026	0.0037	0.0029
Einstein prediction		0.024	0.026	0.022	0.024	0.022	0.024
Happel prediction		0.037	0.048	0.028	0.037	0.028	0.037

The well-known Einstein formula to predict viscosity in very diluted suspensions gave values of viscosity which varied from 0.020 to 0.024 Pa.s. The Happel (1957) relationship for concentrated systems predicted values from 0.028 to 0.047 Pa.s. Both predictions are summarized in Table 2. There is not a theoretical expression which can give a good estimate of suspension viscosity for the flow conditions presented in this study, probably due to asymmetrical distribution of the particles.

Regarding the simulation of particle velocity, the average velocities as a function of fluid velocity (average suspension velocity), particle diameter, fluid viscosity and drag coefficient relationship are summarized in Table 3. It was observed that if the viscosity or pressure drop of the continuous phase was used instead of the experimental viscosity or pressure drop of the suspension in Eq. (7) through (9), similar average particle velocity was obtained. As an example, the average particle velocity predicted for a fluid viscosity of 0.015 Pa.s was 0.526 m/s and the particle velocity predicted for a suspension viscosity of 0.032 Pa.s was 0.516 m/s (Table 3). Therefore, experimental pressure drops of the whole suspension are not needed for particle velocity predictions.

In reported work using the Lagrangian approach (Sastry et al. 1989; Liu and Zuritz 1995), the pressure drops of the suspension were not included. Using

TABLE 3.

PREDICTED AVERAGE PARTICLE VELOCITY OBTAINED IN THE SIMULATION PROPOSED
AS A FUNCTION OF PARTICLE DIAMETER. FLUID VISCOSITY AND DRAG COEFFICIENT(C_D)
USING EQ. (9) (CLIFT AND GAUVIN 1971) AND EQ. (10) (ALLEN 1900)

FLUID VELOCITY (m/s)	PARTICLE DIAMETER (m)	FLUID VISCOSITY (Pa.s)	C_D	PARTICLE VELOCITY (m/s)
0.555	0.004	0.0153	Eq. 9	0.476
0.331	0.004	0.0153	Eq. 9	0.276
0.555	0.004	0.0153	Eq. 10	0.506
0.331	0.004	0.0153	Eq. 10	0.296
0.610	0.004	0.015	Eq. 9	0.526
0.610	0.004	0.032	Eq. 9	0.516
0.555	0.004	0.0153	Eq. 9	0.474
0.555	0.006	0.0153	Eq. 9	0.466
0.555	0.008	0.0153	Eq. 9	0.458
0.331	0.004	0.0153	Eq. 9	0.276
0.331	0.006	0.0153	Eq. 9	0.270
0.331	0.008	0.0153	Eq. 9	0.262

the same approach for the flow conditions of this study, identical particle-fluid velocity was obtained, implying homogenous flow and symmetric distribution. Nevertheless, the viscosity of these suspensions could not be predicted using theoretical expressions.

Some of the results of the predicted particle velocities are shown in Fig. 5. Particle velocities applying Clift and Gauvin (1971) (Eq. 8) were plotted. The Eulerian approach allowed retarded profiles for the particles under these conditions. The continuous line shows the classical parabolic profile of a Newtonian fluid. The effect of particle diameter was plotted (Fig. 5), where no apparent differences were detected. Particle velocities were 0.474, 0.466 and 0.458 m/s for 0.004, 0.006 and 0.008 m diameter, when the fluid velocity was 0.555 m/s (See Table 3). However, drag relationships had an effect on the predicted particle velocities; the slip velocity was different for each drag coefficient expression used. The Allen relationship (Eq. 10) gave an average particle velocity of 0.506 m/s while the Clift and Gauvin relationship (Eq. 9) gave an average particle velocity of 0.476 m/s for a fluid velocity of 0.555 m/s (See Table 3). The average slip velocities (V_f-V_p), using the two expressions

selected, are given in Fig. 6. The Clift and Gauvin-C_D relationship provided bigger slip velocities than the Allen-C_D relationship.
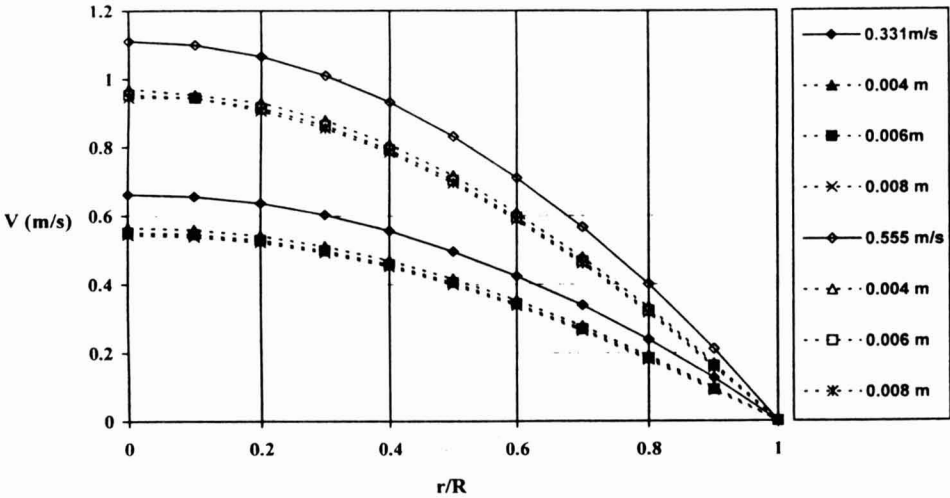
FIG. 5. PREDICTED VALUES OF PARTICLE VELOCITY ($\overline{V}_p$), USING CLIFT AND GAUVIN (1971) RELATIONSHIP, AT TWO DIFFERENT FLUID VELOCITIES AND THREE SUSPENDED SPHERE DIAMETERS
Volume fraction = 0.118. (r/R) dimensionless radius. ------ Predicted particle velocity.
_____ Experimental fluid velocity.

Liu and Zuritz (1995), applying the Lagrangian approach, for a higher fluid viscosity (0.10 Pa.s), reported no differences between fluid velocity and particle velocity, as found in preliminary studies using the Eulerian approach with non-Newtonian fluids (shear-thinning) of the same or higher apparent viscosities. In those cases the viscosity forces are predominant, thus the viscosity of the carrier fluid represents an additional resistance to the particle flotation or sedimentation.

The pressure drop was estimated with values for each slip velocity. A small magnitude of slip velocity had an important influence on the pressure drop calculations. The slip velocity obtained from Allen (1900) underestimated pressure drop predictions by 35% when they were compared to the experimental suspensions pressure drops, while those obtained from Clift and Gauvin (1971) equation for C_D disagreed in about 5%. The particle velocities obtained by the Clift and Gauvin (1971) relationship were used for computations. A comparison of the predicted and experimental suspension pressure drops is given in Table 4.
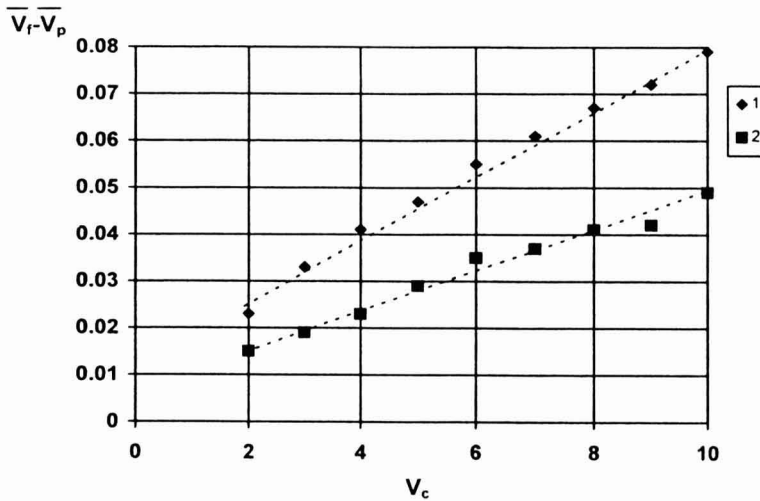
FIG. 6. AVERAGE SLIP VELOCITIES PREDICTED $(\bar{V}_f - \bar{V}_p)$ AS A FUNCTION OF
CONTROLLED VELOCITY $(\bar{V}_c)$ USING C_D RELATIONSHIPS PROPOSED BY
(1) CLIFT AND GAUVIN (1971) AND (2) ALLEN (1900)

The case of the food mixture model with particles of 0.004 m (D/d_p = 8.8)
showed the best agreement with the method proposed (error <5%), except for
the velocity of 0.331 m/s. This exception was also observed in the suspensions
with particles of 0.006 m (D/d_p = 5.8). These results might indicate that the
critical velocity was 0.331 m/s, instead of the observed value of 0.30 m/s in the
logarithmic plot. The suspensions with particles of d_p = 0.004 m and d_p =
0.006 m were flowing as an asymmetric distributed suspension. Suspensions
with particles of d_p = 0.008 m gave the poorer agreements at the velocity range
of 0.498-0.555 m/s. These coarse particles showed an additional resistance to
motion at those velocities because the experimental pressure drop was higher
than the predicted pressure drop.

Tube-particle diameter ratio seems to be an important relationship to predict
if wall effects may be neglected. Differences found in pressure drops for
particles of 8 mm may be caused by contact (wall effect) with the pipe (D/d_p =
4.4). Most of the recent studies of particulate suspensions have been carried out
in a tube-particle diameter ratio < 5.8 where the interferences with the wall
seem to be significant, as seen by the results of this work. Only one particle
reported by Tucker and Withers (1994) had a ratio > 5.8, but, they did not
report power-law parameters for the fluid (without particles) which would allow
calculations of the fluid apparent viscosity in order to make some comparisons.

TABLE 4.

PREDICTION AND EXPERIMENTAL RESULTS OF PRESSURE DROP
PER METER OF STRAIGHT TUBE AS A FUNCTION OF PARTICLE DIAMETER (d_p) AND
VOLUME FRACTION (α)

$\Delta P/L$ (Pa/m)	d_p α	0.004 m 0.169	0.004 m 0.218	0.006 m 0.118	0.006 m 0.169	0.008 m 0.118	0.008 m 0.169	$\overline{V_t}$ (m/s)
PREDICTED		276.54	323.66	232.19	283.46	208.78	246.0	0.331
EXPERIMENTAL		207.91	267.19	189.73	144.43	226.32	219.3	
DIFFERENCE		24.8%	17.4 %	18.3 %	48.9 %	8.4 %	10.9%	
PREDICTED		267.08	307.39	229.15	273.13	209.54	240.92	0.387
EXPERIMENTAL		264.67	267.19	214.72	171.3	226.32	271.63	
DIFFERENCE		0.9 %	13.1 %	6.3 %	37.3 %	8.0%	12.7 %	
PREDICTED		289.67	328.69	253.15	295.27	232.9	264.3	0.443
EXPERIMENTAL		291.79	323.9	242.01	196.7	251.3	298.93	
DIFFERENCE		0.7 %	1.5 %	4.4 %	33.4 %	7.9 %	13.1%	
PREDICTED		282.03	315.69	250.82	287.64	233.95	260.8	0.498
EXPERIMENTAL		291.79	323.9	296.31	248.98	376.2	403.5	
DIFFERENCE		3.5 %	2.6 %	18.1 %	13.4 %	60.8 %	54.7 %	
PREDICTED		299.07	331.35	269.19	304.46	253.72	278.62	0.555
EXPERIMENTAL		291.79	323.9	266.99	328.55	353.52	405.8	
DIFFERENCE		2.4 %	2.2 %	0.8 %	7.9 %	39.3 %	45.6 %	

The effect of interaction between particles seems to be less important, because the number of particles in suspensions with $d_p = 0.008$ m was less than the number of particles in suspensions with $d_p = 0.004$ and $d_p = 0.006$ m. The studied suspensions flowed at 40% and 57% of the maximum number of particles allowed in the tube, except for the particles of $d_p = 0.004$ m that flowed at 73.5% (0.218 v/v).

The results obtained in this study can be extrapolated to the suspensions with intermediate Newtonian fluid viscosity, including sphere shaped particles and a diameter of a few millimeters if the tube-particle diameter ratio is > 5.8. In these conditions, the particles tend to settle or to float; this is why the asymmetric concentration is present. If a shear thinning carrier fluid is used instead of a Newtonian carrier fluid, similar results can be expected if the fluid has an equivalent apparent viscosity when flowing at a constant shear rate. If the particles are replaced with those which can truly interact with each other or with the carrier fluid, the results reported here cannot be applied.

This work shows that the flow behavior of coarse food particles carried in a Newtonian fluid of intermediate viscosity flow as asymmetric distributed suspensions. Hence, their pressure drops may be predicted using correlations applied to sands and gravels. This kind of behavior cannot be successfully evaluated by means of the tube viscometer principle applying Hagen-Poiseuille relationship. Physical properties such as fluid and particle densities, particle diameter, suspension velocity, and pressure drop of the fluid are the only parameters necessary to estimate the pressure drops of the coarse suspensions.

The C_D relationship for the transitional flow, caused by intermediate viscosity of the carrier fluid, had the most important effect in the predicted particle velocities. Unfortunately, there are many C_D expressions reported in the literature for transitional flow. The particle diameter in the simulation did not significantly affect the predicted particle velocity; however, in experimental conditions, the tube-particle diameter ratio had a strong influence on the flow behavior of the suspensions studied.

The calculations proposed in this study allowed determination of the retarded particle velocity. It is expected that in canned or packed commercial products a nonuniform final solid-fluid ratio is to be attained. To avoid this technological problem, the concentration of syrup can be increased to achieve a high viscosity carrier fluid, but it implies an increase in the final product cost. The addition of a thickener may be an alternative, but might not be allowed for these types of products.

CONCLUSION

Particle velocities in a model food suspension were predicted by the Eulerian approach, obtaining retarded profiles of particle velocity compared to fluid velocity. Particle diameter and suspension viscosity did not considerably modify the predicted particle velocity; however, the drag coefficient relationship did. Physical properties like density and viscosity of continuous fluid, and diameter and density of particles were the only parameters needed for computation of pressure drops in horizontal pipes.

The best estimates of pressure drop were obtained using the Durand (1953) modified correlation and particle velocity predicted by the relationship proposed by Clift and Gauvin (1971). This study presented an effective methodology to calculate pressure drop of food suspensions with medium viscosity (0.015 Pa.s) and large particles (1×10^{-3} m) when the tube-particle diameter ratio is higher than 5.8.

ACKNOWLEDGMENTS

NOMENCLATURE

a, b, c	Constants in Eq. 13
C_D	Drag coefficient
d_p	Particle diameter (m)
D	Tube diameter (m)
f	Friction factor
F	Force (N)
F_D	Drag Force (N)
g	Gravitational acceleration (m/s^2)
K, m	Constants in Eq. 14
L	Tube length (m)
l	Cube length (m)
m	Particle mass (kg)
P	Pressure (Pa)
r	Radius position (m)
R	Tube radius (m)
Re	Reynolds number
t	Time (s)
ν	Particle volume (m^3)
V	Velocity (m/s)
$\underline{V}_c$	Controlled velocity
$\overline{V}$	Average velocity (m/s)

Greek Letters

α	Particle volume fraction
β	Fluid volume fraction
ρ	Density (kg/m^3)
η	Viscosity (Pa.s)
$\dot{\gamma}$	Shear rate (1/s)
τ	Shear stress (Pa)

Subscripts

f	Fluid
p	Particle
s	Suspension
r, z	Direction

REFERENCES

ALLEN, H.S. 1900. Phil. Mag. *50*, 323. Cited in Govier, G.W. and Aziz, K. 1972. *The Flow of Complex in Pipes*. Robert E. Krieger Publishing Co. Florida.

BHAMIDIPATI, S. and SINGH, R.K. 1990. Flow behavior of tomato sauce with or without particulates in tube flow. J. Food Process Engineering *12*, 275–293.

BIRD, R.B., STEWART, W.E. and LIGHTFOOT, E.N. 1960. *Transport phenomena*. John Wiley & Sons. New York.

CLIFT, R. and GAUVIN, W. 1971. Motion of entrained particles in gas streams. Can. J. Chem. Eng. *49*, 439–450.

DALLAVALLE, J.M. 1948. *Micromeritics: The Technology of Fine Particles*. 2nd Ed., Pitman, London.

DAVIDSON, R.L. 1980. *Handbook of Water Soluble Gums and Resins*. McGraw Hill, New York.

DURAND, R. 1953. Basic relationships of the transportation of solids in pipes. Proc. Minn. Int. Hydraulic Conv. pp 89–103. Int. Assoc. for Hydraulic Res.

DURST, F., MILOJEVIC, D. and SCHOUNG, B. 1984. Eulerian and Lagrangian predictions of particulate two-phase flows, a numerical study. Appl. Math. Modelling *8*, 101–115.

DUTTA, B. and SASTRY, S.K. 1990. Velocity distributions of food particle suspensions in holding tube flow: distribution characteristics and fastest-particle velocities. J. Food Sci. *55* (6), 1703–1710.

GOVIER, G.W. and AZIZ, K. 1972. *The Flow of Complex in Pipes*. Robert E. Krieger Publishing Co. Florida.

HAPPEL, J. 1957. Viscosity of suspensions of uniform spheres. J. Appl. Phys. *28* (11), 1288–1292.

HAYDEN, J.W. and STELSON, T.E. 1968. Hydraulic conveyance of solids in pipes. Int. symposium on solid-flow in pipes. University of Pennsylvania, Philadelphia, PA.

HOLDSWORTH, S.D. 1971. Applicability of rheological models to the interpretation of flow and processing behaviour of fluid food products. J. Texture Studies *2*, 393–418.

JINESCU, V.V. 1974. The rheology of suspensions. Int. Chem. Eng. *14* (3), 397–420.

KOICHI, L., KEISHI, G. and KO, H. 1991. *Power Technology Handbook*. Marcel Dekker, New York.

LAWLER, M.T. and LU, P.C. 1971. The role of lift in the radial migration of particles in a pipe flow. In *Advances of Solid-liquid Flow in Pipes and Its Application*. (I. Zandi, ed.) pp. 39–57, Pergamon Press Ltd. Oxford, New York.

LIU, Y. and ZURITZ, C.A. 1995. Mathematical modeling of solid-liquid two phase tube flow, an application to aseptic processing. J. Food Process Engineering *18*, 135–163.

RAO, M.A. 1986. Rheological properties of fluid foods. In *Engineering Properties of Foods*. (M.A. Rao and S.S.H. Rizvi, eds.) pp. 1–42, Marcel Dekker, New York.

SASTRY, S.K., HESKITT, B.F. and BLAISDELL, J.L. 1989. Experimental and modeling studies on convective heat transfer at the particle-liquid interface in aseptic processing systems. Food Technol. *43* (3), 132–136, 143.

SASTRY, S.K. and ZURITZ, C.A. 1987. A review of particle behavior in tube flow: Applications to aseptic processing. J. Food Process Engineering *10*, 27–52.

SKELLAND, A.H.P. 1967. *Non Newtonian Flow and Heat Transfer*. John Wiley & Sons, New York.

TUCKER, G.S. and WITHERS, P.M. 1994. Determination of residence time distribution of nonsettling food particles in viscous food carrier fluid using hall effect sensors. J. Food Process Engineering *17*, 401–422.

TURIAN, R.M., YUAN, T. and MAURI, G. 1971. Pressure drop correlation for pipeline flow of solid-liquid suspensions. AIChE J. *17* (4), 809–817.

ZANDI, I. 1971. Hydraulic transport of bulk materials. *Advances in Solid-liquid Flow in Pipes and Its Application*. (I. Zandi, ed.) pp. 1–34, Pergamon Press, Ltd. Oxford.

CHANGES IN ELECTRICAL CONDUCTIVITY OF SELECTED VEGETABLES DURING MULTIPLE THERMAL TREATMENTS[1]

WEI-CHI WANG[2] and SUDHIR K. SASTRY[3]

The Ohio State University
Department of Food, Agricultural, and Biological Engineering
590 Woody Hayes Drive
Columbus, OH 43210

ABSTRACT

Electrical conductivity (σ) is the most important parameter in ohmic heating. Although data exist on its changes during ohmic heating, limited information is available about preheated foods. In this study, the conductivity changes of raw vegetable samples (potato, carrot, and yam) in cyclic ohmic heating and samples preheated by conventional heating prior to ohmic heating were investigated. In cyclic ohmic heating, cylindrical vegetable samples were subjected to three repeated cycles of ohmic heating (40 V/cm, 60Hz) to 80C, and cooling to 25C. Fresh samples were also preheated by conventional heating to 80C, then subjected to ohmic heating for comparison. Specific heats changed by cycles, although moisture content remained constant in all cases. The results show that in cyclic ohmic heating, the heating rate increased by cycles. Samples preheated by either conventional or ohmic heating showed a higher heating rate than raw materials. Electrical conductivity data during ohmic heating showed that preheated vegetables have higher conductivities than fresh ones, and a tendency of increase by cycles was found.

INTRODUCTION

Ohmic heating of particulate foods for continuous aseptic processing has the potential to ensure food safety without compromising quality. To ensure food

---

safety, accurate measurement of the particle temperature is required. Several methods were developed to detect the temperature of moving particles (Balasubramaniam 1993) but more investigations are required to apply them to industrial scale processes. An alternative is to predict the particle temperature by mathematical modeling; a few models have been developed for prediction of moving particle temperature (Sastry 1986; Chandarana and Gavin 1989; Lee *et al.* 1990). In modeling of the continuous ohmic heating process, the critical parameter which significantly affects temperature is electrical conductivity (σ). The basic relationship for heat generation rate in ohmic heating is:

$$\dot{u} = |\nabla V|^2 \sigma \tag{1}$$

Palaniappan and Sastry (1991a) reported that electrical conductivity is a linear function for temperature, and the σ-T relationship can be expressed as:

$$\sigma_T = \sigma_{ref} [1 + m(T - T_{ref})] \tag{2}$$

Halden *et al.* (1990) studied the electrical conductivity of foods during ohmic heating and compared the changes with data from conventional heating. Palaniappan and Sastry (1991b) studied factors which may affect electrical conductivity of selected juices. Wang and Sastry (1993) investigated the effect of electrolyte concentration on conductivity by infusing vegetable tissue with sodium chloride solution. However, none of the above studies involved preheated foods. Like other factors, thermal processing itself can affect electrical conductivity by causing irreversible changes in cellular structure. In industrial practice, most products sterilized by ohmic heating will have been thermally pretreated for cooking, enzyme inactivation, or to raise the initial temperature. Limited information exists on the effects of processing on σ. Since ohmic heating rate is sensitive to σ, a small error in the value can significantly affect food quality or safety. The objectives of this research were to (1) determine changes in electrical conductivity during multiple heat treatments, and (2) measure the change in electrical conductivities of preheated vegetables due to different thermal treatments.

MATERIALS AND METHODS

Fresh carrot, potato and yam purchased from local grocery stores were used. All samples were peeled and cut into cylindrical pieces of 2cm length and 2.35cm diameter; the shape and dimensions being chosen to fit precisely within the ohmic heater. Pretreatment by conventional heating was performed by sealing samples in a plastic bag, and immersing in a boiling water bath to protect samples from moisture gain or loss. For ohmic heating, samples were placed in a cylindrical glass chamber, and sandwiched between two coated

titanium electrodes (with slight pressure to ensure good contact without damage). Alternating current at 60Hz, 80V (voltage gradient of 40V/cm) were used to heat samples ohmically. A thermocouple was inserted into the geometric center of the sample to monitor temperature for both operations.

All three vegetable samples were first heated up to an average temperature of 80C by either conventional or ohmic heating. After heating, samples were cooled to a center temperature of 25C by immersing the heating systems (the plastic bag or the glass ohmic heater) in ice. Samples were then subjected to ohmic heating up to 80C and cooling for two additional cycles. The current, voltage, and temperature were recorded by a data-logger every second during ohmic heating, and σ was determined by the following formula:

$$\sigma = \frac{L}{AR} \tag{3}$$

The temperature coefficient (m in Eq. (2)) and the reference conductivity (σ_{ref}) of samples in each ohmic heating cycle were determined from σ-T curves. Also, the heat capacities (C_p) of raw and ohmically preheated samples (after one and two cycles) were determined by differential scanning calorimetry (DSC). Moisture contents were determined by drying samples in an oven at 120C for 24 h. All operations in this study were conducted in triplicate.

Average-Temperature Determination for Conventional Heating

Preliminary experiments had indicated that ohmically heated samples typically show nearly uniform heating; however, samples that were heated conventionally would be expected to have spatial thermal gradients. Since the purpose was to heat both sets of samples to an average temperature of 80C, and only center temperatures were available, it was necessary to determine the average temperature corresponding to a given center temperature. This was accomplished by the following procedure.

Assuming thermal properties are constant (this is not strictly true, but a sufficiently good assumption to provide a reasonable approximation of average temperatures), the governing equation for the temperature profile of a cylindrical sample can be described by Fourier's law:

$$\frac{1}{r}(\frac{\partial T}{\partial r} + r\frac{\partial^2 T}{\partial r^2}) + \frac{\partial^2 T}{\partial z^2} = \frac{1}{\alpha}\frac{\partial T}{\partial t} \tag{4}$$

where $r = z = 0$ at the center, and $r = \pm r_0$, $z = \pm L/2$ at the surface. The initial and boundary conditions are:

$$T = T_i \quad \text{at } t = 0, \tag{5}$$

$$\frac{\partial T}{\partial z} = \frac{\partial T}{\partial r} = 0 \qquad at \ z=0, \ r=0, \tag{6}$$

$$\frac{\partial T}{\partial z} = \frac{h}{k}(T-T_{\infty}) \qquad at \ -r_o \leq r \leq r_o, \ z = \pm\frac{L}{2}, \tag{7}$$

$$\frac{\partial T}{\partial r} = \frac{h}{k}(T-T_{\infty}) \qquad at \ -\frac{L}{2} \leq z \leq \frac{L}{2}, \ r = \pm r_o, \tag{8}$$

The analytical solutions of an infinite plate and cylinder were provided by Schneider (1955). By superposition, the center temperature (T_c) of a finite cylindrical sample can be determined as:

$$T_c = T_{\infty} + 8(T_i - T_{\infty})\sum_{n=1}^{\infty}\sum_{m=1}^{\infty}(\frac{sinM_n}{2M_n + sin2M_n}) \cdot$$

$$\frac{1}{R_m}\frac{J_1(R_m)}{J_0^2(R_m) + J_1^2(R_m)}e^{(-M_n^2F_o - R_m^2F_o)} \tag{9}$$

where M_n and R_m are given by:

$$M_n tanM_n = Bi \tag{10}$$

and

$$R_m\frac{J_1(R_m)}{J_0(R_m)} = Bi \tag{11}$$

respectively. Since the sample temperature was detected by a thermocouple at the geometric center, the experimental data on temperature history were used in Eq. (9) to determine M_n, R_m and Bi, thereby yielding h.

The sample average temperature $(\bar{T})$ can be analytically solved by volumetrically integrating Eq. (9), and dividing by the volume, yielding:

$$\bar{T} = \frac{\int TdV}{V} \tag{12}$$

or:

$$\bar{T} = T_\infty + 8(T_i - T_\infty)\sum_{n=1}^{\infty}\sum_{m=1}^{\infty}\frac{1}{M_n}\frac{1}{R_m^2}[\frac{\sin M_n^2}{M_n + \sin M_n \cos M_n}]\cdot$$
$$[\frac{1}{1 + J_0^2(R_m)/J_1^2(R_m)}]e^{(-M_n^2 F_o - R_m^2 F_o)}$$
(13)

Thus the average sample temperature can be determined by monitoring the center temperature, determining M_n, R_m, and using Eq. (12).

This approach was performed for all three vegetables in three replications. Table 1 provides the thermal property data of vegetables, while Table 2 shows the calculated center temperatures required to attain specific average temperatures.

TABLE 1.
THERMAL PROPERTY DATA OF VEGETABLES[1]

Product	k (w/m^{o}K)	α (m^2/s)x10^7	ρ (kg/m^3)
Carrot	0.57	1.73	980
Potato	0.52	1.68	1050
Yam	0.56	1.89	1010

[1] k determined by modified Fitch method, ρ by measurement of mass and volume, and α ($=k/\rho C_p$) by measurement of C_p by differential scanning calorimetry.

TABLE 2.
CENTER TEMPERATURES REQUIRED TO ATTAIN SPECIFIC AVERAGE
TEMPERATURES IN CONVENTIONAL HEATING (T_i=20C, T_∞=100C)

Product	$\bar{T}$=70C	$\bar{T}$=75C	$\bar{T}$=80C	$\bar{T}$=85C
Carrot	T_c=26C	T_c=30.5C	T_c=40C	T_c=52C
Potato	T_c=31.5C	T_c=38C	T_c=47C	T_c=57.5C
Yam	T_c=30.5C	T_c=36.5C	T_c=45.5C	T_c=57C

RESULTS AND DISCUSSION

Cyclic Ohmic Heating

The typical heating rate curves of carrot, potato and yam in cyclic ohmic heating are shown on Fig. 1, 2 and 3, respectively, and the corresponding data on electrical conductivity versus temperature are shown on Fig. 4, 5, and 6, respectively. A tendency of increasing heating rate by cycles were found in all materials. Data also show that samples after one or two cycles of ohmic heating
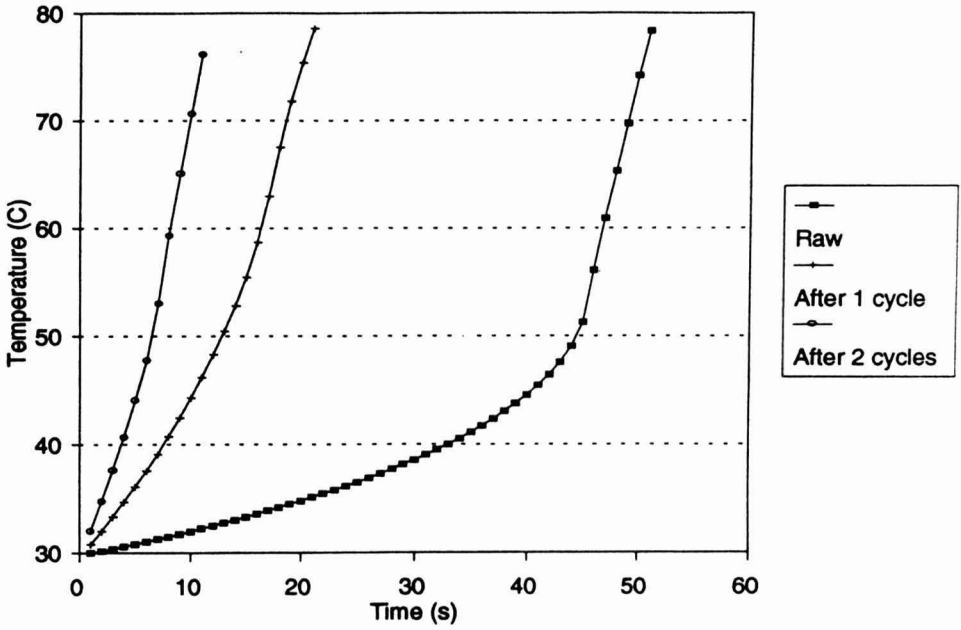
FIG. 1. HEATING CURVES IN CYCLIC OHMIC HEATING (CARROT)
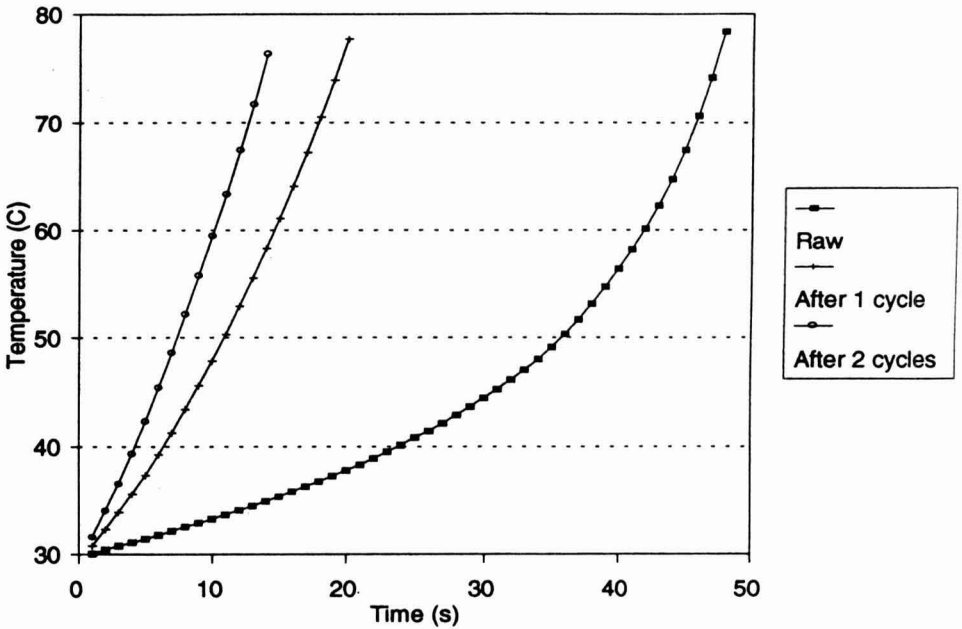
FIG. 2. HEATING CURVES IN CYCLIC OHMIC HEATING (POTATO)
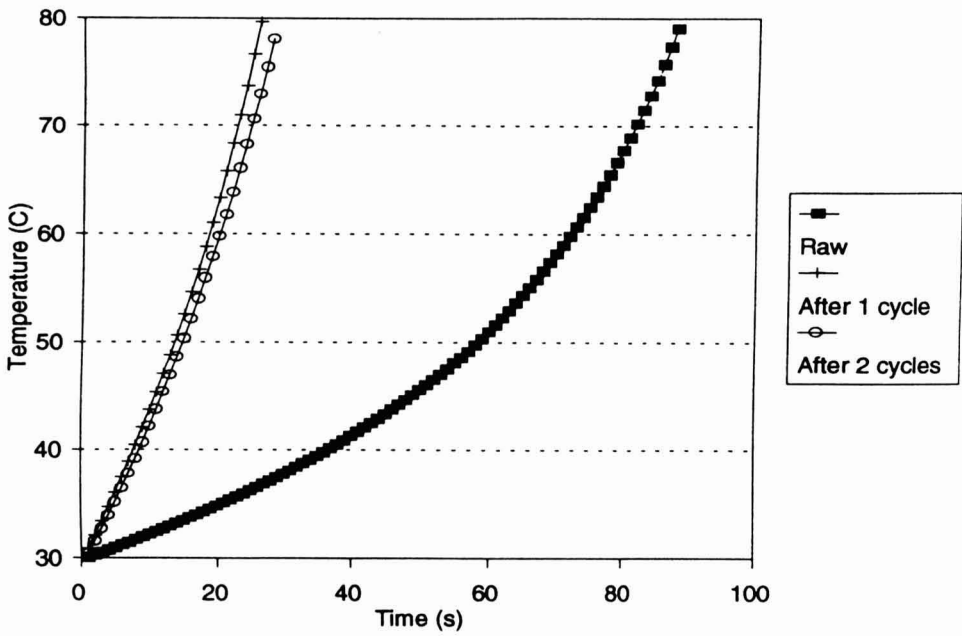
FIG. 3. HEATING CURVES IN CYCLIC OHMIC HEATING (YAM)
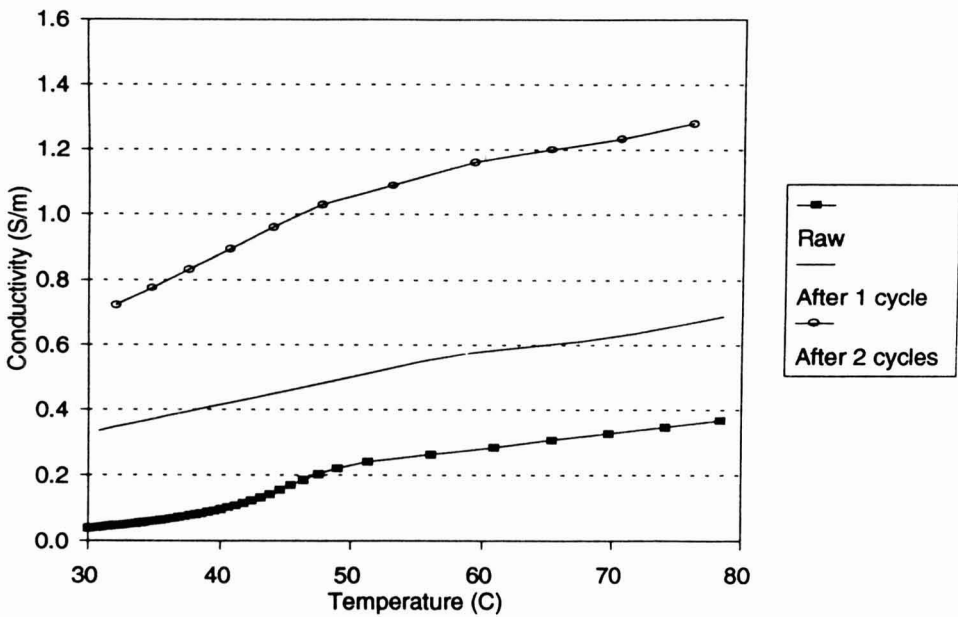
FIG. 4. ELECTRICAL CONDUCTIVITY CURVES IN CYCLIC OHMIC HEATING
(CARROT)

W.-C. WANG and S.K. SASTRY
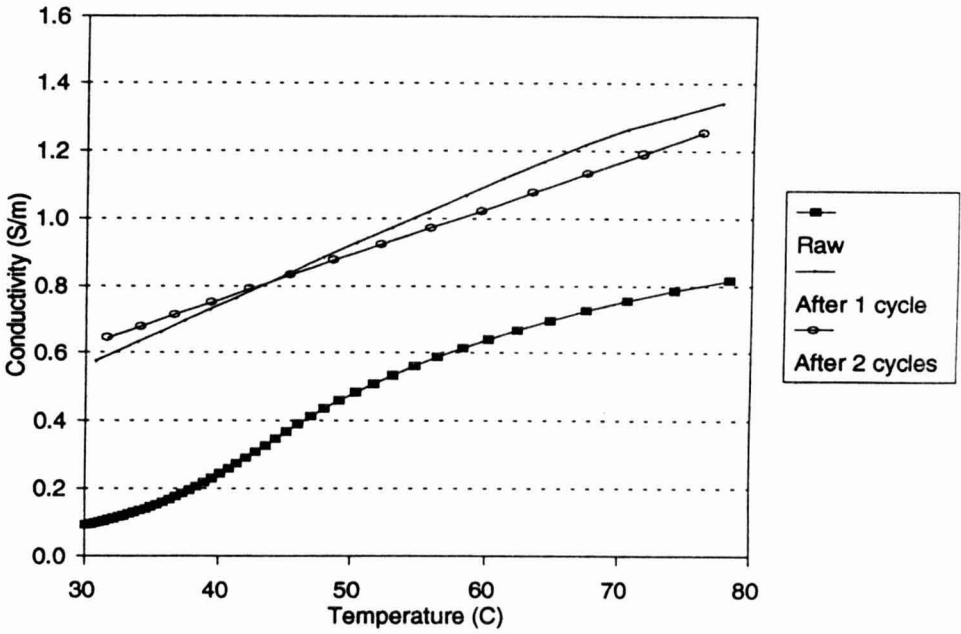
FIG. 5. ELECTRICAL CONDUCTIVITY CURVES IN CYCLIC OHMIC HEATING
(POTATO)
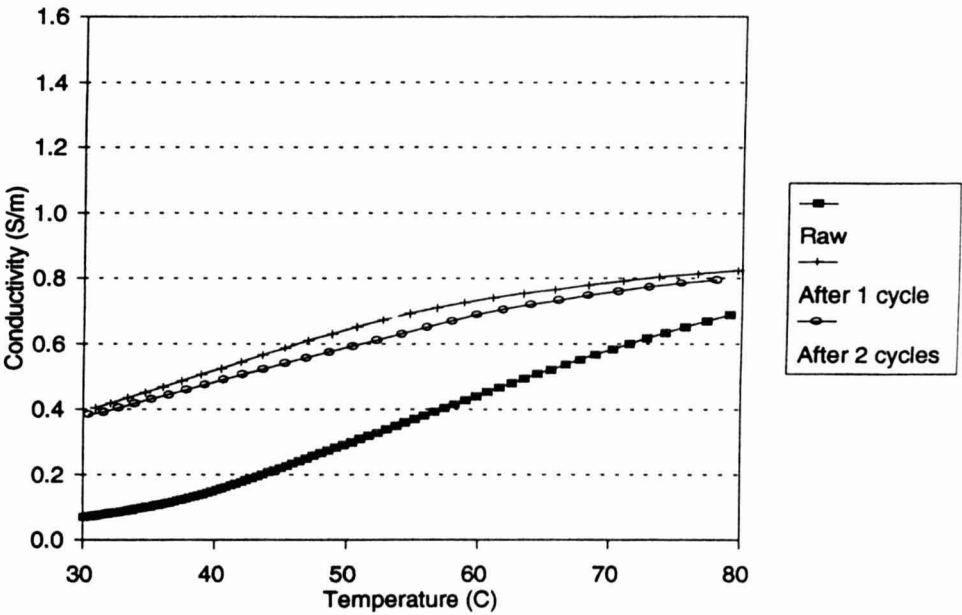
FIG. 6. ELECTRICAL CONDUCTIVITY CURVES IN CYCLIC OHMIC HEATING (YAM)

had higher σ than the raw materials. However, the σ-T curves of samples preheated once and twice almost overlapped for both potato and yam, while a difference was observed for carrot. Using a reference temperature in Eq. (2) as 30C, and parameters σ_{30}, and m, could be obtained, as shown in Table 3. Although the linear σ-T models could be confirmed by the high coefficients of determination ($r^2 \geq 0.96$ in all cases), slope changes were observed for raw materials. Values of σ of raw samples were found to increase quadratically in the low temperature range (30 to 50C), and then curves became linear thereafter. These slope changes might indicate that critical structure changes occurred around 50C during the first cycle of ohmic heating. For samples after one or two cycles of ohmic heating, σ increased linearly; however the slope of conductivity curves decreased when the temperature was higher than 60C (Fig. 4 to 6). This might be due to imperfect contact between the sample and electrodes, resulting from sample shrinkage at high temperature.

TABLE 3.
PARAMETERS σ_{30}, AND m IN CYCLIC OHMIC HEATING

Product	Treatment	σ_{30} (S/m)	m (°C^{-1})	r^2
Carrot	Raw	0.033	0.234	0.97
	After 1 cycle	0.343	0.021	0.99
	After 2 cycles	0.763	0.015	0.96
Potato	Raw	0.080	0.218	0.98
	After 1 cycle	0.576	0.029	0.99
	After 2 cycles	0.623	0.022	0.99
Yam	Raw	0.034	0.395	0.99
	After 1 cycle	0.433	0.021	0.96
	After 2 cycles	0.393	0.023	0.99

Data on moisture content and statistical comparison, from pooled t tests, are shown in Table 4, while the corresponding results for heat capacity are shown in Table 5. The moisture content showed independence of the ohmic heating cycle, based on 99% confidence level (two-tailed test, P-value equals 0.001), while heat capacity was found significantly decreased after one cycle of ohmic heating at the same confidence level (one-tailed test, P-value equals 0.005). The change of heat capacity might explain the significant heating rate differences found between raw and preheated samples.

TABLE 4.
MOISTURE CONTENT OF SAMPLES IN CYCLIC OHMIC HEATING

Product	Treatment	Moisture (% wb)
Carrot	Raw	90.9 ± 0.1^a
	After 1 cycle	90.9 ± 0.3^a
	After 2 cycles	90.7 ± 0.2^a
Potato	Raw	77.4 ± 0.3^b
	After 1 cycle	77.8 ± 0.2^b
	After 2 cycles	77.2 ± 0.2^b
Yam	Raw	86.4 ± 0.2^c
	After 1 cycle	86.3 ± 0.2^c
	After 2 cycles	86.3 ± 0.1^c

[a,b,c] For the same product, mean values followed by the same letter are not significantly different
(two-tailed pooled t test, P=0.01)

TABLE 5.
HEAT CAPACITIES OF SAMPLES IN CYCLIC OHMIC HEATING

Product	Treatment	C_p (kJ/kg°K)
Carrot	Raw	3.23 ± 0.04^a
	After 1 cycle	3.02 ± 0.01^b
	After 2 cycles	2.86 ± 0.01^c
Potato	Raw	2.95 ± 0.01^a
	After 1 cycle	2.87 ± 0.01^b
	After 2 cycles	2.87 ± 0.01^b
Yam	Raw	2.81 ± 0.02^a
	After 1 cycle	2.72 ± 0.02^b
	After 2 cycles	2.73 ± 0.03^b

[a,b,c] For the same product, mean values followed by the same letter are not significantly different
(one-tailed pooled t test, P=0.005)

A clear understanding of the increases of heating rate as well as electrical
conductivity by cyclic ohmic heating can be obtained only if the microstructure
and chemical changes in vegetables during ohmic heating are understood. Studies
on electrical conductivity changes of fruits during growth and ripening have been

done (Bean *et al.* 1960; Sasson and Monselise 1977). Changes occurring in cell walls, membranes and compositions of cell contents were said to be factors influencing σ changes. As vegetable tissue is heated, structure changes like cell wall breakdown, tissue damage and softening occur, affecting σ.

Increase of mobile moisture content caused by structure changes during thermal treatments is also a potential factor. This concept is not new; conventional heating has been employed for denaturation of protoplasm of sugar beet in sugar extraction for some time (Brüniche-Olsen 1962). Thermal processing may enhance the diffusion of solute (sugar) through beet tissue. Thus heating causes more mobile moisture, increasing ionic mobility, which in turn increases electrical conductivity and ohmic heating rate. This might explain why samples in the second and third cycles always had higher electrical conductivities and heating rates than in the first cycle.

For starchy vegetables, gelatinization has to be taken into consideration. Although the gelatinization effect could not be directly observed from heating curves or electrical conductivity data, a typical DSC thermogram of raw potato (Fig. 7) clearly shows the endothermic peak of gelatinization. The gelatinization characteristics obtained in this study are summarized in Table 6. The degree of
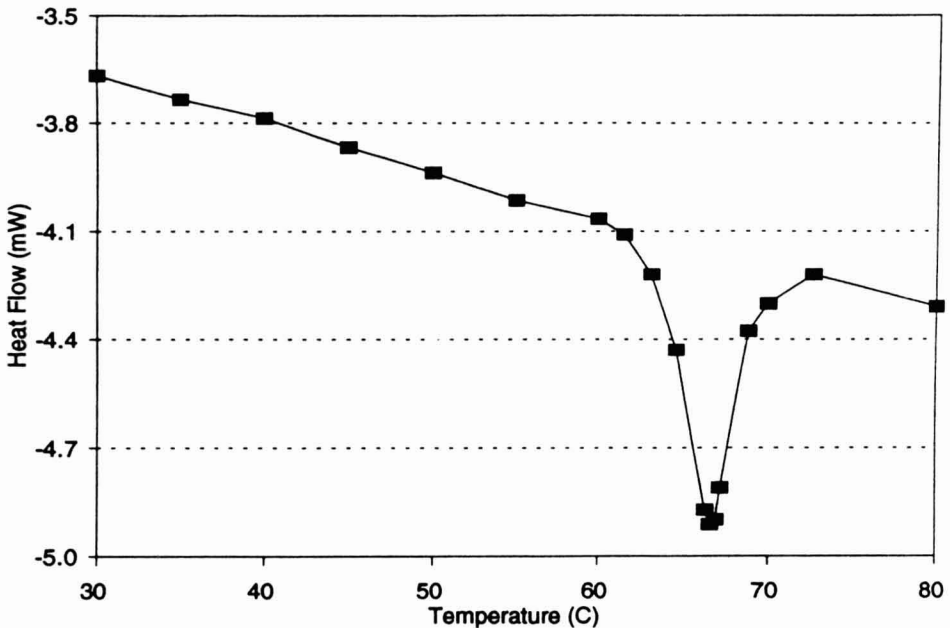
FIG. 7. SAMPLE DSC THERMOGRAM OF POTATO

TABLE 6.
GELATINIZATION OF SAMPLES IN CYCLIC OHMIC HEATING

Product[*]	Treatment	ΔH_G (kJ/kg)
Potato	Raw	2.715 ± 0.058^a
	After 1 cycle	0.111 ± 0.036^b
	After 2 cycles	ND
Yam	Raw	1.470 ± 0.020^a
	After 1 cycle	0.219 ± 0.011^b
	After 2 cycles	ND

[*]   No endothermic peaks of gelatinization occurred in the DSC thermogram of carrot
ND   Not detectable
[a,b]   For the same product, mean values followed by the same letter are not significantly different
      (one-tailed pooled t test, $P = 0.005$)

gelatinization can be quantified by gelatinization energy (ΔH_G); the sample with a higher ΔH_G consists of more "ungelatinized" starch. By performing one-tailed pooled t tests at 99% confidence level (P-value equals 0.005) for ΔH_G, both potato and yam after one cycle of ohmic heating have a smaller ΔH_G, compared to the raw materials (Table 6). However, more work is needed to determine the role of starch gelatinization in ohmic heating.

Ohmic Heating Versus Conventional Heating

Electrical conductivity-temperature curves of preheated (by either ohmic or conventional heating) carrot, potato and yam versus those of raw samples are shown in Fig. 8, 9 and 10, respectively. Table 7 shows the comparison of parameters σ_{30} and m, for all materials, while data on moisture content and the statistical comparison are provided in Table 8. Carrot preheated by ohmic heating showed a higher σ than by conventional heating. However, the σ-T curve of conventionally preheated potato was similar to the sample exposed to two cycles of ohmic heating (shown on Fig. 2). This indicates that the overheated portion of a conventionally preheated potato sample might play an important role in the succeeding ohmic heating. Figure 11 shows both T_c and $\bar{T}$ curves of potato in conventional heating. The center temperature increases slowly by conduction, while the average temperature increased sharply at the initial stage. During the conventional heating, the surface of potato was exposed to long times under gelatinization temperatures, which might translate to a greater succeeding electrical conductivity. Yam samples preheated by conventional and ohmic heating behaved similarly in both heating rate and conductivity. The different curve behavior of vegetable samples might be due to different physical structures and/or chemical compositions.
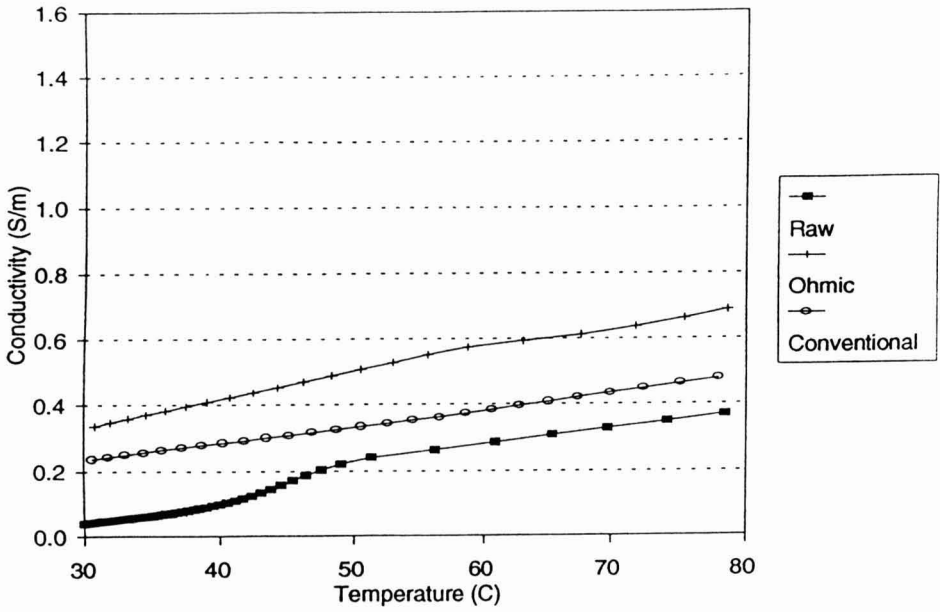
FIG. 8. ELECTRICAL CONDUCTIVITY CURVES OF RAW VS PREHEATED
SAMPLES (CARROT)
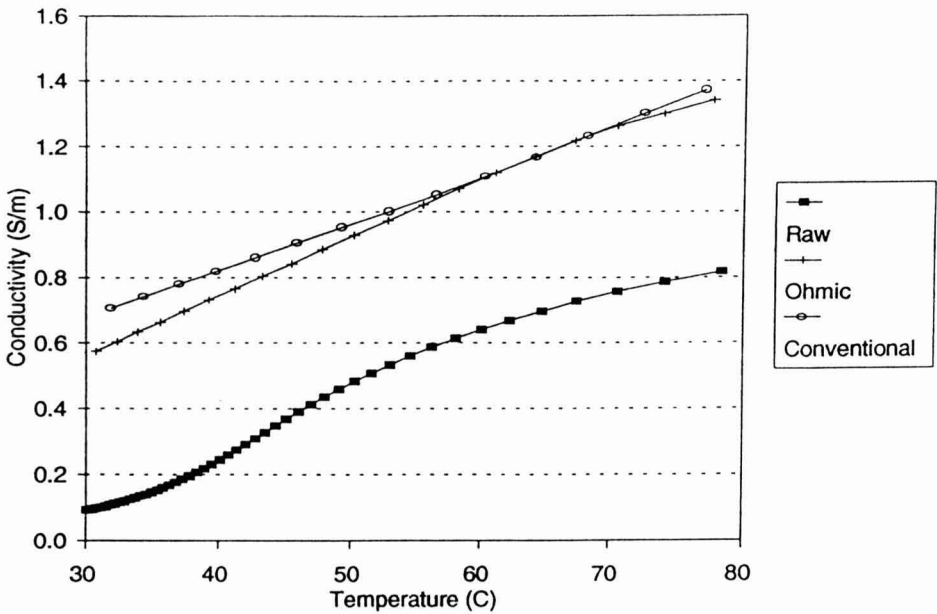
FIG. 9. ELECTRICAL CONDUCTIVITY CURVES OF RAW VS PREHEATED
SAMPLES (POTATO)

W.-C. WANG and S.K. SASTRY
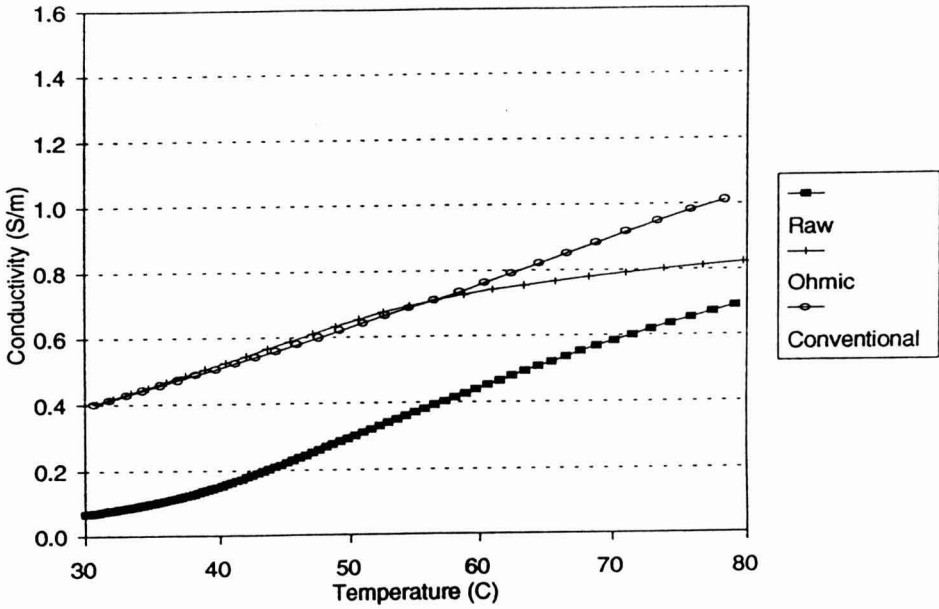
FIG. 10. ELECTRICAL CONDUCTIVITY CURVES OF RAW VS PREHEATED
SAMPLES (YAM)

TABLE 7.

PARAMETERS σ_{30}, AND m OF RAW AND PRETREATED SAMPLES

Product	Treatment	σ_{30} (S/m)	m ($^{\circ}$C^{-1})	r^2
Carrot	Raw	0.033	0.234	0.97
	Ohmic	0.343	0.021	0.99
	Conventional	0.232	0.022	0.99
Potato	Raw	0.080	0.218	0.98
	Ohmic	0.576	0.029	0.99
	Conventional	0.673	0.021	0.99
Yam	Raw	0.034	0.395	0.99
	Ohmic	0.433	0.021	0.96
	Conventional	0.380	0.034	0.99

TABLE 8.
MOISTURE CONTENT OF RAW MATERIALS AND SAMPLES PRETREATED BY
OHMIC AND CONVENTIONAL HEATING

Product	Treatment	Moisture (% wb)
Carrot	Raw	90.9 ± 0.1^a
	Ohmic	90.9 ± 0.3^a
	Conventional	90.2 ± 0.3^a
Potato	Raw	77.4 ± 0.3^b
	Ohmic	77.8 ± 0.2^b
	Conventional	77.1 ± 0.3^b
Yam	Raw	86.4 ± 0.2^c
	Ohmic	86.3 ± 0.2^c
	Conventional	85.9 ± 0.2^c

[a,b,c] For the same product, mean values followed by the same letter are not significantly different
(two-tailed pooled t test, $P=0.01$)
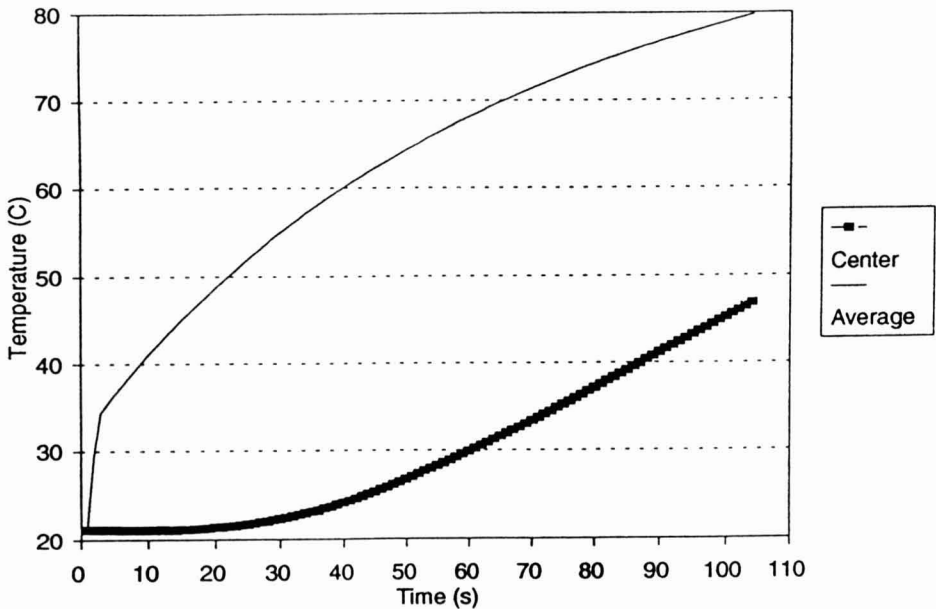
FIG. 11. T_C AND $\bar{T}$ IN CONVENTIONAL HEATING OF POTATO

CONCLUSIONS

The ohmic heating rate was found out to increase by cycles, due to increasing electrical conductivity. Data also showed that moisture content remained constant by cycles, whereas the preheated samples showed lower heat capacity than the raw materials. Vegetable samples preheated by conventional heating also showed an increase in electrical conductivity as well as heating rate; however the thermal effect differences between ohmic and conventional heating were different. The reasons might be due to different physical structures and/or chemical compositions of vegetables. The reasons that preheated vegetable samples have higher electrical conductivities are not clear; factors such as structure changes, increase of moisture mobility and starch gelatinization should be further studied.

NOMENCLATURE

A   cross section area (m^2)
Bi   Biot number
C_p heat capacity (kJ/kg°K)
F_o Fourier number, or dimensionless time ($\alpha t/(L/2)^2$ or $\alpha t/r_o^2$)
h   heat transfer coefficient (w/m²°K)
k   thermal conductivity (w/m°K)
L   length (m)
m   temperature coefficient (in equation (2)) (°C^{-1})
M_n numerical solution of equation (10)
r   radial coordinate
r_o radius of samples (m)
R   resistance (ohm)
R_m numerical solution of equation (11)
t   time (s)
T   temperature (°C)
$\bar{T}$ average temperature (°C)
V   voltage (volt)
z   axial coordinate
α thermal diffusivity (m^2/s)
σ electrical conductivity (S/m)
ρ density (kg/m^3)
$\mathring{u}$ heat-generation rate (W/m^3)
ΔH endothermic enthalpy (kJ/kg)
∇ gradient

Subscript

c   center
G   gelatinization
i   initial
o   onset
p   peak
ref   reference
T   certain temperature
∞   environment

REFERENCES

BALASUBRAMANIAM, V.M. 1993. Liquid-to-particle convective heat transfer in aseptic processing systems. 199 pp. PhD Dissertation, Agric. Engr. Dept., Ohio State Univ., Columbus.

BEAN, E.C., RASOR, J.P. and PORTER, G.C. 1960. Changes in electrical conductivities of avocados during ripening. Year Book of Californian Avocado Soc. *44*, 75–78.

BRÜNICHE-OLSEN, H. 1962. Solid-Liquid Extraction. pp. 178–193, NYT Nordisk Forlag, Arnold Busck, Copenhagen.

CHANDARANA, D.I. and GAVIN III, A. 1989. Establishing thermal processes for heterogeneous foods to be processed aseptically: A theoretical comparison of process development methods. J. Food Sci. *54*, 198–204.

HALDEN, K., DE ALWIS, A.A.P. and FRYER, P.J. 1990. Changes in the electrical conductivity of foods during ohmic heating. Int. J. Food Sci. Technol. *25*, 9–25.

LEE, J.H., SINGH, R.K. and Larkin, J.W. 1990. Determination of lethality and processing time in a continuous sterilization system containing particulates. J. Food Eng. *11*, 67–92.

MURAKAMI, E.G. 1994. Thermal processing affects properties of commercial shrimp and scallops. J. Food Sci. *59*, 237–241.

PALANIAPPAN, S. and SASTRY, S.K. 1991a. Electrical conductivities of selected solid foods during ohmic heating. J. Food Process Engineering *14*, 221–236.

PALANIAPPAN, S. and SASTRY, S.K. 1991b. Electrical conductivity of selected juices: influences of temperature, solids content, applied voltage, and particle size. J. Food Process Engineering *14*, 247–260.

SASSON, A. and MONSELISE, S.P. 1977. Electrical conductivity of 'Shamouti' orange peel during fruit growth and postharvest senescence. J. Amer. Soc. Hort. Sci. *102*, 142–144.

SASTRY, S.K. 1986. Mathematical evaluation of process schedules for aseptic processing of low-acid foods containing discrete particulates. J. Food Sci. *51*, 1323–1328, 1332.

SCHNEIDER, P.J. 1955. *Conduction Heat Transfer*. 395 pp. Addison-Wesley Publishing Co., Reading.

WANG, W.-C. and SASTRY, S.K. 1993. Salt diffusion into vegetable tissue as a pretreatment for ohmic heating: Electrical conductivity profiles and vacuum infusion studies. J. Food Eng. *20* 299–309.

AUTHOR INDEX

SUBJECT INDEX

Baking,
biscuit dough, 389
Blackgram flour-based *papad* dough, 301
Bulk density,
coffee powder, 43

Calcium phosphate removal, 197
Canned biscuit dough, 383
Canned Salmon, 65
Canning of cowpeas, 337
Chicken ball, 19
Coagulation of fish proteins, 285
Coatings on fried foods, 23
Conduction heating in odd shapes, 51
Cooking properties of lentils, 249

Deep-fat frying, 17
De-Nouy ring, 3
Differential Scanning Calorimetry, 32, 253
Dynamic gain matrix approach, 231

Edible film, 17
Egg yolk, 6
Electric field effects in milk chocolate, 77
Emulsifiers, 1
End-over-end rotation of cans, 265
Error analysis,
properties, 45
E. coli in skim milk, 317

Fish mince wash water, 285
Flow modeling,
power-law fluid, 141
Fluid/particulate velocity profile, 165

Fluid-to-particle heat transfer, 269, 453

Headspace volatile analysis, 113
Heat transfer in cans, 265
Hydroxypropyl methylcellulose, 19

Inactivation of *Salmonella dublin*, 367
Infrared Processing,
lentils, 250
Interfacial Tension, 1

Karingda seed, 349
Kinetics of heat coagulation, 289

Least cost formulations,
surimi, 179
Lentils,
micronized, 249
Liquid CO_2 extraction, 110'

Magnetic Resonance Imaging, 165
Mass transfer in osmotic dehydration, 401
Mayonnaise, 4
Microwave baking, 383
Milk cleaning process, 197
Minimizing surface cook, 72
Mirror image method, 77
Modified atmosphere packaging, 231
Modified Fitch Apparatus, 36
Moisture sorption isotherms, 349
Multiple thermal treatments, 499

Noninvasive study,
milk cleaning, 197

JOURNAL OF FOOD PROCESS ENGINEERING
GUIDE FOR AUTHORS

If the manuscript has been produced by a word processor, a disk containing the manuscript would be greatly appreciated. Word Perfect 5.1 is the preferred word processing program. The original and THREE copies of the manuscript should be sent along with the disk to the editorial office. The typing should be double-spaced throughout with one-inch margins on all sides.

Page one should contain: the title, which should be concise and informative; the complete name(s) of the author(s); affiliation of the author(s); a running title of 40 characters or less; and the name and mail address to whom correspondence should be sent.

Page two should contain an abstract of not more than 150 words. This abstract should be intelligible by itself.

The main text should begin on page three and will ordinarily have the following arrangement:

Introduction: This should be brief and state the reason for the work in relation to the field. It should indicate what new contribution is made by the work described.

Materials and Methods: Enough information should be provided to allow other investigators to repeat the work. Avoid repeating the details of procedures that have already been published elsewhere.

Results: The results should be presented as concisely as possible. Do not use tables *and* figures for presentation of the same data.

Discussion: The discussion section should be used for the interpretation of results. The results should not be repeated.

In some cases it might be desirable to combine results and discussion sections.

References: References should be given in the text by the surname of the authors and the year. *Et al.* should be used in the text when there are more than two authors. All authors should be given in the Reference section. In the Reference section the references should be listed alphabetically. See below for style to be used.

RIZVI, S.S.H. 1986. Thermodynamic properties of foods in dehydration. In *Engineering Properties of Foods*, (M.A. Rao and S.S.H. Rizvi, eds.) pp. 133-214, Marcel Dekker, New York.

MICHAELS, S.L. 1989. Crossflow microfilters ins and outs. Chem. Eng. 96, 84-91.

LABUZA, T.P. 1982. *Shelf-Life Dating of Foods*, pp. 66-120, Food & Nutrition Press, Trumbull, CT.

Journal abbreviations should follow those used in Chemical Abstracts. Responsibility for the accuracy of citations rests entirely with the author(s). References to papers in press should indicate the name of the journal and should only be used for papers that have been accepted for publication. Submitted papers should be referred to by such terms as "unpublished observations" or "private communication." However, these last should be used only when absolutely necessary.

Tables should be numbered consecutively with Arabic numerals. The title of the table should appear as below:

TABLE 1.
ACTIVITY OF POTATO ACYL-HYDROLASES ON NEUTRAL LIPIDS, GALACTOLIPIDS AND PHOSPHOLIPIDS

Description of experimental work or explanation of symbols should go below the table proper. Type tables neatly and correctly as tables are considered art and are not typeset. Single-space tables.

Figures should be listed in order in the text using Arabic numbers. Figure legends should be typed on a separate page. Figures and tables should be intelligible without reference to the text. Authors should indicate where the tables and figures should be placed in the text. Photographs must be supplied as glossy black and white prints. Line diagrams should be drawn with black waterproof ink on white paper or board. The lettering should be of such a size that it is easily legible after reduction. Each diagram and photograph should be clearly labeled on the reverse side with the name(s) of author(s), and title of paper. When not obvious, each photograph and diagram should be labeled on the back to show the top of the photograph or diagram.

Acknowledgments: Acknowledgments should be listed on a separate page.

Short notes will be published where the information is deemed sufficiently important to warrant rapid publication. The format for short papers may be similar to that for regular papers but more concisely written. Short notes may be of a less general nature and written principally for specialists in the particular area with which the manuscript is dealing. Manuscripts that do not meet the requirement of importance and necessity for rapid publication will, after notification of the author(s), be treated as regular papers. Regular papers may be very short.

Standard nomenclature as used in the engineering literature should be followed. Avoid laboratory jargon. If abbreviations or trade names are used, define the material or compound the first time that it is mentioned.

EDITORIAL OFFICE: DR. D.R. HELDMAN, COEDITOR, *Journal of Food Process Engineering*, University of Missouri-Columbia, 214 Agricultural Engineering Bldg., Columbia, MO 65211 USA; or DR. R.P. SINGH, COEDITOR, *Journal of Food Process Engineering*, University of California, Davis, Department of Agricultural Engineering, Davis, CA 95616 USA.

CONTENTS